

博士論文

Development of Simplified Numerical Model for Seismic Collapse of RC Frame Structures

(RCフレーム構造物の地震破壊解析のための
簡便型数値解析手法の開発)

by

Shanthanu Rajasekharan Menon
シャンタヌ ラジャセカラン メノン

Meguro Laboratory,
Department of Civil Engineering,
The University of Tokyo.

Abstract

Collapse of buildings due to an earthquake is completely unacceptable. The combination of wide usage of Reinforced Concrete (RC) framed structures for residential buildings in earthquake prone areas and shoddy design and construction practices, exposes the high vulnerability of this type of buildings to a seismic hazard. Collapse of weak buildings has been the main cause of deaths during the past large earthquake disasters in the world, therefore, assessing the collapse capacity of such buildings in advance is very important for disaster reduction.

There are various methods to assess the collapse capacity of buildings but there always seems to be a stand-off between the applicability/ reliability of these methods and the computation effort involved. For practical engineering purposes, the following characteristics are desirable in a collapse simulation, (i) capturing the complete behavior of a structure i.e. from its normal state to a complete collapsed state during an earthquake, (ii) should be accurate and reliable, (iii) computationally efficient (to be performed in conventional personal computers), (iv) easiness in modelling, comprehending and workability, and (v) good visualization of the analysis results.

Considering the above criteria, the Extended Discrete Element Method (EDEM) provides a good platform to meet the requirements. However, the EDEM has some limitations, namely, (i) requirement of a small time step for stability and accuracy, due to the use of an explicit time integration scheme, (ii) no proper theory for spring stiffness derivation, and (iii) inaccuracies due to neglect of Poisson's ratio. These limitations can be overcome by the assembly of a global stiffness matrix, for the discretized system, which contains theoretically derived spring stiffness that implicitly considers the Poisson's ratio effect. The Lattice Models or Spring Networks consists of an assembly of interconnected springs. When an appropriate spring network is chosen, a model similar to the assembly of joint-springs in the EDEM can be obtained, the difference being the effect of the contact-springs i.e. inter-element interaction at the surface.

By combining this property of both the models, an effective two-phase numerical collapse simulation of structures can be performed, which can predict the initial behavior of structures (elastic/nonlinear/crack initiation/ stiffness degradation/ maximum load capacity) through a spring network (implicit numerical integration) and predict the final behavior of structures (geometric non-linearity, instability, separation, and collision) through the EDEM (explicit numerical integration).

The first part of the research involves the development of a linear elastic spring network. A finite element mapping scheme is used to derive the spring stiffness for two kinds of spring network discretization, namely, the CST (Constant Strain Triangle) spring network and the Quad spring network. The validity of the mapping scheme, which was earlier used for an infinite domain, is checked for the finite domain of an RC structure. The global finite element matrix and a corresponding spring network global stiffness are assembled. The spring stiffness are derived and were observed to be equal to the theoretical spring stiffness from past literature. To adopt in the EDEM, the domain was discretized by linear quadrilateral elements/constant strain triangle elements and the corresponding spring stiffness were obtained. There were three kinds of springs for the Quad spring network, namely, (i) inner edge (ii) inner diagonal (iii) boundary springs. There were two kinds of spring for the CST spring network, namely (i) inner spring (ii) boundary spring. The inner edge and diagonal springs were mutually orthogonal, whereas the boundary springs were orthogonal along the Eigen direction. In order to obtain this there is a Poisson ratio's limit of ($0.03 < \nu < 0.47$). Once the spring network, with these derived spring stiffness, are assembled, the same finite element global matrix is obtained. A simple cantilever analysis is performed to check for accuracy. In a special case in the CST network when Poisson's ratio = $1/3$, the spring network reduced to a network of 1D springs.

Since the global stiffness matrix of the assembled spring network is the same as the finite element stiffness matrix it showed (i) good accuracy (ii) convergence in energy (iii) ability to model the Poisson's ratio. The assumption of lumping of mass at nodes was verified through modal analysis, and good results were obtained. This implies the spring network can accurately perform linear dynamic analysis also.

The second part of the research involves the simulation of concrete non-linearity. The spring were divided based on their physical location as (i) Reinforced concrete spring (ii) Plain concrete spring (iii) Steel spring. Spatially averaged material models were used for concrete and steel. Spring networks are known to suffer from mesh dependency.

A secant stiffness based formulation is used for the nonlinear analysis of RC. To cater for this effect, the softening curve of the tension model is varied based on the element size, in order to maintain constant fracture energy. A size effect analysis is performed of a concrete cube under tension. It was observed that the mesh density dependency effect had reduced.

Using the simple CST spring network, and only concrete compression/tension model, numerical validation of the spring network was performed for a series experiments on RC beams. Good correlation between the experimental data and numerical simulation was obtained. Numerical validation of an RC frame using the CST spring network with varying element sizes was performed. Good agreement was observed between experimental and analytical data even when the element size is increased. Crack pattern matched the experimentally observed cracks in an averaged sense.

In order to incorporate a shear model into the spring network, a quad spring network with shear models are used. Numerical simulation of a series of concrete panel experiments were performed. It was observed that the spring network could model the cases where reinforcement were isotopically arranged. The shear transfer post-cracking due to aggregate interlock must be appropriately considered.

Once the structure has been subjected to significant damage, the analysis shifts to the EDEM phase. The cracked springs represent the ruptured joint springs. Simplified linear material models are adopted, whose stiffness has been reduced based on the softening of material models from Phase I. The RC frame validated earlier is used for analysis. The joint spring stability is checked under gravity load for the undamaged frame and damaged frame as well. The damaged and undamaged frame reached a stable state under gravity loading. Once stable the frame is subjected to displacement based loading. The model could follow the collapse of the frame. A 12 storey RC frame is subject to damage, and is subjected to input displacement loading. The EDEM phase could follow the collapse of the 12 storey RC frame effectively.

Through this two-phase analysis method, a new, relatively simple method is proposed which can, (i) model elastic behavior of structures accurately, (ii) follow the initial non-linear behavior of RC buildings, (iii) given the initial cracking and propagation of cracks, (iv) perform large deformation analysis, (v) model separation, collision and collapse, (vi) due to its simplicity, computation time for collapse of buildings has been drastically reduced, and (vii) can be used for research that requires analysis of a large building stock or probabilistic analysis which involves a large number of analysis.

Acknowledgements

Foremost, I would like to express my sincere gratitude to my academic supervisor, Professor Kimiro Meguro. Performing research under his supervision has been a wonderful journey, which has been technically and philosophically fulfilling. He has been a pillar of strength right through my doctoral course, helping me realise my own potential, while honing my skills and shaping up my views on the importance of research, especially in the field of Disaster Mitigation.

I am deeply grateful to Lecturer Dr. Muneyoshi Numada for his support during my research life, and also for his technical support as my one of my supervisors.

I am deeply indebted to my supervising committee members, Professor Yoshiaki Nakano, Associate Professor Tsuyoshi Ichimura and Associate Professor Kohei Nagai, for their valuable discussions and critical reviews of my research. I am also grateful to Professor Koichi Maekawa and Associate Professor Lalith Wijerathne, for their valuable suggestions.

I would like to sincerely thank Assistant Professor Hideomi Gokon, for providing support during the final and important phase of my research. I am deeply thankful to Ms. Sakai, Ms. Minemoto, Ms. Ogawa, Ms. Ohno, Ms. Nakajo, Ms. Ashita, Ms. Masumi, Ms. Aoyama and Ms. Izumi for their kind support through my life at the Meguro Laboratory, Department of Civil Engineering, The University of Tokyo.

I am grateful to the Japan Ministry of Education, Science, Sports and Culture for providing me financial support during my doctoral course.

I thank my friends Chaitanya, Etri, Yash, Ramesh ji, Fan Zeipei, Mehrdad, Mahendra, Adnan ji, Umair ji, Jothi and Supun for the support they provided to my research. I would like to thank Takanori Sawara for his immense support and being my first friend in Japan. I would also like to thank my lab mates Nao, Yamamoto, Joe, Niwat, Matsushita san, Fujiu san, Ikenaga, Tanaka, Ayaka, Murakami, Mera for making me fall in love with Japan.

As the famous Sanskrit saying goes “*Mata, Pita, Guru, Deivam*”, which translates to Mom, Dad, Teacher and God. This doctoral work is dedicated to my parents, for their endless love, support and encouragement. My teachers at every level of my life have been my role models and I am thankful to them for their motivation. I would like to thank my sister Sangeetha, my close family and friends for their continuous love and support.

This thesis is only the beginning to the new route in the journey called life. I am looking forward to the rest of the journey with zeal and zest.

Shanthanu Rajasekharan Menon

August, 2015

List of Publications

1. Shanthanu RAJASEKHARAN, Muneyoshi NUMADA, Kimiro MEGURO:
Simplified Collapse Analysis of Structures using the Extended Distinct Element Method and Finite Element Mapped Spring Network, *Proceedings of the Third International Conference on Urban Disaster Reduction*, Earthquake Engineering Research Institute, Boulder, CO, USA, Track 3: Breakout #3, September 29th, 2014.
2. Shanthanu RAJASEKHARAN, Muneyoshi NUMADA, Kimiro MEGURO:
Application of Finite Element Mapped Spring Network System in the Extended Distinct Element Method, *Proceedings of the 14th Japan Earthquake Engineering Symposium*, Chiba, Japan, OS13-Thu-AM-8, pp.128-136, December 4th 2014.
3. Shanthanu RAJASEKHARAN, Muneyoshi NUMADA, Kimiro MEGURO:
Application of Finite Element Mapped Spring Network System in the Extended Distinct Element Method, *Journal of Earthquake and Tsunami*, 2015 (accepted)

Table of Contents

Abstract	iii
Acknowledgements	vii
List of Publications	ix
Table of Contents	xi
List of Figures	xiii
List of Tables	xvii
Chapter 1 Introduction	1
1.1 Discrete modelling of structures	3
1.1.1 Characteristics of a discrete element method	3
1.1.2 Existing methods to analyse RC structures	5
1.2 Problem Statement	8
1.3 Objectives	11
1.4 Organization of this Thesis	12
Chapter 2 Two-Phase Analysis Scheme	15
2.1 Spring Network models	15
2.2 Finite Element Mapped Spring Network	16
2.3 The Extended Distinct Element Method (EDEM)	17
2.4 Two Phase Analysis	18
2.5 Spring Network requirements	20
Chapter 3 Phase I: Linear Static Analysis	23
3.1 Spring Stiffness derivation	23
3.1.1 Constant Strain Triangle discretization	25
3.1.2 Bilinear quadrilateral discretization	28
3.2 Linear Analysis	30
3.2.1 Poisson's Ratio	34
3.2.2 Modal Analysis	35
3.3 Conclusion	36
Chapter 4 Reinforced Concrete Analysis	39

4.1	Spring Classification	39
4.2	Reinforced Concrete Material Models	40
4.2.1	Concrete compression model	41
4.2.2	Concrete Tension model	43
4.2.3	Concrete Shear model	45
4.2.4	Reinforcement model	48
4.3	Iterative Secant Stiffness Formulation	49
4.3.1	Simple cube compression	49
4.3.2	Mesh objectivity of results	51
4.4	Experimental validation	53
4.4.1	RC Beam	53
4.4.2	RC Frame	59
4.4.3	Concrete Shear Panel	62
4.5	Conclusion	66
Chapter 5	EDEM Phase	69
5.1	Transition	69
5.1.1	Contact springs	69
5.1.2	Joint springs	72
5.1.3	Element details	72
5.1.4	Time step	72
5.1.5	Damping	73
5.2	1-storey frame analysis	73
5.3	11-storey frame analysis	78
5.4	Conclusion	87
Chapter 6	Conclusion	89
6.1	Linear Analysis	89
6.2	Non-Linear RC Analysis	89
6.3	EDEM phase	90
6.4	Future Work	90
6.5	Overall Conclusion	91
	References	93

List of Figures

Figure 1.1– EDEM simulation of RC frame collapse due to dynamic loading (Meguro, 1993)	5
Figure 1.2– Existing discrete element methods and their classification	7
Figure 1.3– Preferable properties for simplified collapse simulation	9
Figure 1.4– Characteristics required from the proposed scheme	9
Figure 2.1– Finite element mapping of spring network	16
Figure 2.2– EDEM modelling of concrete (Meguro and Hakuno 1989)	17
Figure 2.3– Analysis flow of the EDEM	18
Figure 2.4– Overall Analysis Method	19
Figure 2.5– Domain discretization in EDEM and spring network	19
Figure 2.6– Simple discretization pattern and their corresponding finite element	21
Figure 3.1– Elemental Stiffness matrix in Finite Element Method and Spring Network	23
Figure 3.2– Global stiffness matrix and its translational invariance property	24
Figure 3.3– Domain for deriving spring stiffness and the basic elements	25
Figure 3.4– Quadrilateral elements: Domain discretization	28
Figure 3.5– Properties of the cantilever used for linear analysis	30
Figure 3.6– Quad Spring Network: Variation of energy, displacement error with increase in no. of elements	32
Figure 3.7– CST Spring Network: Variation of energy, displacement error with increase in no. of elements	32
Figure 3.8– Poisson’s ratio verification	33
Figure 3.9– Comparison between calculated and analytical Poisson’s ratios	34
Figure 3.10– Effect on the orientation of springs with varying Poisson’s ratio.	35
Figure 3.11– Mode shapes obtained from the spring network system	35
Figure 3.12– Errors in fundamental frequencies of different mode shapes	36
Figure 4.1– Classification of springs for RC modelling	40
Figure 4.2– Concrete compression model	41
Figure 4.3– Reduction of compressive strength of springs present in cracked concrete zone	42
Figure 4.4– Concrete tension model and zonation of springs	44
Figure 4.5– Concrete shear model	46

Figure 4.6– Steel material model	49
Figure 4.7– Flow Chart of the analysis procedure	50
Figure 4.8– Concrete cube compression	50
Figure 4.9– Concrete cube tension loading and size dependant tension model.....	52
Figure 4.10– Mesh size sensitivity.....	52
Figure 4.11– Experimental setup: Various dimensions, loading and boundary condition	54
Figure 4.12– Cross sectional details of the beams	55
Figure 4.13– Spring network model of the beams	56
Figure 4.14– Force-deformation relationship of the beams-I	57
Figure 4.15– Force-deformation relationship of the beams-II.....	58
Figure 4.16– Cracked spring pattern obtained during analysis.....	59
Figure 4.17– RC frame details	60
Figure 4.18– Three kinds of spring network discretization used for spring network analysis	60
Figure 4.19– Load- Displacement curve comparison between experimental and analysis	61
Figure 4.20– Cracked springs pattern observed.....	61
Figure 4.21– Concrete Panel: Experimental setup and its spring network model	62
Figure 4.22– Comparison of experimental and analytical results for concrete panel specimens I	64
Figure 4.23– Comparison of experimental and analytical results for concrete panel specimens II.....	65
Figure 5.1– Transition between the two phases.....	70
Figure 5.2– EDEM model of the RC Frame	74
Figure 5.3– Damped deformation profile of undamaged frame under gravity loading.....	74
Figure 5.4– Damping of element under gravity loading with varying damping ratios.....	75
Figure 5.5– Z displacement time history under gravity loading.....	75
Figure 5.6– Fundamental Mode Shape of the Frame.....	76
Figure 5.7– Input motion time history	76
Figure 5.8– Displacement time history of undamaged frame under input motion	77
Figure 5.9– Damage induced in the frame due to lateral loading.....	77
Figure 5.10– Stable (Damped) deformation profile of damaged frame under gravity loading	78
Figure 5.11– Collapse of 1 storey frame.....	79
Figure 5.12– Details of the 11 storey frame	80
Figure 5.13– Fundamental mode shape of the 11 storey building	81
Figure 5.14– Deformation profile of the (a) undamaged and (b) damaged frame under gravity loading (c) Failed spring in the damaged model.....	82
Figure 5.15– Input Ground Motion.....	82
Figure 5.16–X direction Displacement time history along its height	83
Figure 5.17–Z direction Displacement time history along its height.....	83

Figure 5.18–X direction Velocity time history along its height	84
Figure 5.19–Z direction velocity time history along its height.....	84
Figure 5.20– Collapse of 11-storey frame I	85
Figure 5.21– Collapse of 12-storey frame II.....	86

List of Tables

Table 3.1 – Spring stiffness and local spring orientation for CST elements (Plane Strain)	27
Table 3.2 – Spring stiffness and local spring orientation for Plane Stress CST elements (Poisson’s ratio = 1/3)	28
Table 3.3 – Spring stiffness and local spring orientation for quadrilateral finite elements	29
Table 3.4 – Spring stiffness and local spring orientation for quadrilateral finite elements	31
Table 4.1 – Various element mesh densities and corresponding values of parameter “ c ”	51
Table 4.2 – Dimensions of the experimented beam	53
Table 4.3 – Dimensions of the beams used in numerical analysis	54
Table 4.4 – Reinforcement bar details	56
Table 4.5 – Properties of the Concrete panels	63
Table 5.1 – Dimensions of the beams used in numerical analysis	70
Table 5.2 – 1-storey frame EDEM input parameters	73
Table 5.3 – 11-storey frame EDEM input parameters	80

Chapter 1 **Introduction**

Collapse of building structures due to the onset of an earthquake is completely unacceptable. Having densely populated urban sprawls, in seismically active regions, living in relatively weak buildings, especially in developing countries, points towards an impending unavoidable large scale disaster. The combination of, wide usage of Reinforced Concrete (RC) framed structures for residential buildings, in earthquake prone areas of both industrialised and developing countries (Murty et al. 2006), and, shoddy design and construction practices, exposes the high vulnerability of this type of buildings to a seismic hazard.

Collapse of weak buildings has been the main cause of deaths during the past large scale earthquake disasters (Coburn and Spence 2002), therefore, assessing the collapse capacity of such buildings in advance is important in disaster mitigation. “Collapse” of a building structure, from an engineering viewpoint, can be defined as, the inability of the structural elements of a part (partial collapse) or the whole building (complete collapse), to resist the gravity loads acting on it, when subjected to earthquake forces. Assessing the collapse capacity of existing structures is not a straight forward task (Villaverde 2007), as it involves many factors, and, it is difficult to accurately consider all these factors. This task becomes further complicated when it comes to assessing the seismic vulnerability of RC buildings in developing countries due to additional factors like (i) lack of structural data (material properties, geometric properties, reinforcement detailing etc.), (ii) non-compliance of seismic design codes, (iii) poor construction practices, (iv) inadequate strong motion data, and, (v) socio-economic issues.

There exists various methods to assess the collapse capacity of buildings (Villaverde 2007; Zareian et al. 2010), but, there always seems to be a stand-off between the applicability/reliability of these methods and the computation effort involved. Although simplified methods like the nonlinear static pushover analysis provides a good assessment of the seismic demand on the structure, it must be cautiously used, as in certain cases, the pushover predictions will

be inadequate or even misleading (Krawinkler and Seneviratna 1998). Numerical simulation of collapse, like for example, using methods based on finite element models, has a wider applicability and also gives valuable insights into the collapse mechanism of a building. Using a detailed numerical model, to model accurately the various phenomena involved in the simulation of a building collapse, is a computationally demanding process. Moreover, for better reliability, a large number of inputs of ground motions have to be considered (Krawinkler et al. 2003), and also, to compensate for the epistemic / aleatoric uncertainties (Vamvatsikos and Fragiadakis 2010), a large number of simulations have to be performed, further increasing the computation effort required, sometimes, rendering these methods impractical.

For practical engineering purposes, the following characteristics are desirable in a collapse simulation, (i) capturing the complete behaviour of a structure i.e. from its normal state to a complete collapsed state during an earthquake, (ii) should be accurate and reliable, (iii) computationally efficient (to be performed in conventional personal computers), (iv) easiness in modelling, comprehending and workability, and, (v) good visualization of the analysis results.

There exists various analytical tools to model the transient dynamic response of a RC structure subjected to seismic loading, but they can be broadly classified based on the discretization of the material being analysed, namely the *continuum based* methods and the *discontinuum based* methods. There also exists hybrid formulations that bridge the gap between these two kinds of methods. The collapse simulation of RC structures usually involves modelling of fracture of concrete, material degradation, geometric nonlinearities, instabilities, element separation, collision and collapse. The approach of discretizing the structure into an assemblage of discrete elements (discrete element methods) interacting with each other, is highly preferable due to its ability to capture element separation (crack initiation and propagation), with ease of modelling and lesser computational requirement, as compared to continuum based collapse analysis techniques (Isobe and Tsuda 2003; Lu et al. 2013; Sasani and Kropelnicki 2008; Sivaselvan and Reinhorn 2002).

1.1 Discrete modelling of structures

The discrete modelling of materials was initially introduced in rock mechanics, as a method to simulate a system of semi-rigid blocks (Cundall 1971). Since then, the discrete element methods have been used in various fields of research and numerous variations of the method have been introduced depending on the requirement. Discrete modelling involves discretising the domain into a discontinuous medium, which is characterised by the existence of contacts or interfaces between the discrete bodies. The discrete element methods are characterised by finite displacement / rotation of discrete bodies, complete detachment of elements, and, automatic contact detection (Cundall and Hart 1992).

1.1.1 Characteristics of a discrete element method

The discrete element methods encompasses a wide range of methods which usually differ in the way they handle the following characteristics:-

1.1.1.1 *Contact*

Based on the treatment of interaction between elements at the interface, the contact between the elements can be divided into the *soft contact approach* and *hard contact approach*. In the soft contact approach, interpenetration of elements are allowed, and the contact forces are calculated based on the level of this interpenetration, usually through contact springs. In the *hard contact approach*, this interpenetration is considered to be non-physical, and the condition of non-penetration is maintained through numerical iterations. The *soft contact approach* provides a simpler approach to the handling of contacts.

1.1.1.2 *Element Deformability*

The elements could either be rigid or deformable. Deformable elements give a more accurate representation of the physical condition. Deformability can be handled by further discretizing the elements using finite elements. Rigid elements on the other hand, provides a more simplified and computationally less demanding representation of the material.

1.1.1.3 *Element Shape*

The geometric shapes of the elements used can vary, for example, spherical, ellipsoidal, cube etc. There are two issues regarding the element shape, the contact detection and packing of elements. Usage of spherical elements (circular in 2-D) is preferable because contact detection is relatively simple in this case, as only the radius of the particles is required for the definition of its geometry and inter-particle contact detection. But spherical particles will lead to geometric porosity (voids created due to the geometric shape of element) which might change the response of the system. In the case of polygon elements, although there is no geometric porosity, the contact detection becomes more complex and computationally more demanding.

1.1.1.4 *Solution Scheme*

The governing equations of motions of the particles can be numerically solved using either an *explicit numerical scheme* or *implicit numerical scheme*. *Explicit numerical schemes* are suitable for large and extremely complex systems, but are usually conditionally stable, i.e. there is a restriction on the temporal discretization to ensure numerical stability. On the other hand, *implicit numerical schemes* essentially involves the solution of simultaneous equations, and are usually unconditionally stable, hence larger time increments can be used. Implicit schemes are preferred when the scale of analysis is not very large.

1.1.1.5 *Analysis Type*

Usually most discrete models are capable of modelling the dynamic response of structures, however, some discrete models, like the *Rigid Body Spring Model* (RBSM), are sometimes specifically used only for determining the static behaviour of structures. Discrete methods which are capable of performing only explicit numerical integration, have to be numerically damped in order to simulate the static behaviour of structures.

1.1.2 Existing methods to analyse RC structures

There exists many methods that can be categorised as a discrete element method, and are being used (or have the capacity to be used) for collapse simulation of RC structures. They are as follows:-

1.1.2.1 *Distinct Element Method (DEM)*

The formulation of the discrete element models had started with the Distinct Element Method (DEM) (Cundall 1971), which was initially introduced to model highly discontinuous and granular media. The domain was discretized into an assembly of rigid elements with springs at the point of contact. The DEM efficiently models granular (Cundall and Strack 1979) and highly discontinuous media (Cundall and Hart 1992), and is popular in the modelling soil rock mechanics. Various shapes of the rigid elements have been used depending on the requirement (Donzé et al. 2008). The DEM can also capture the behaviour of a continuous heterogeneous media like concrete (Hentz et al. 2004) and rock (Camborde et al. 2000).

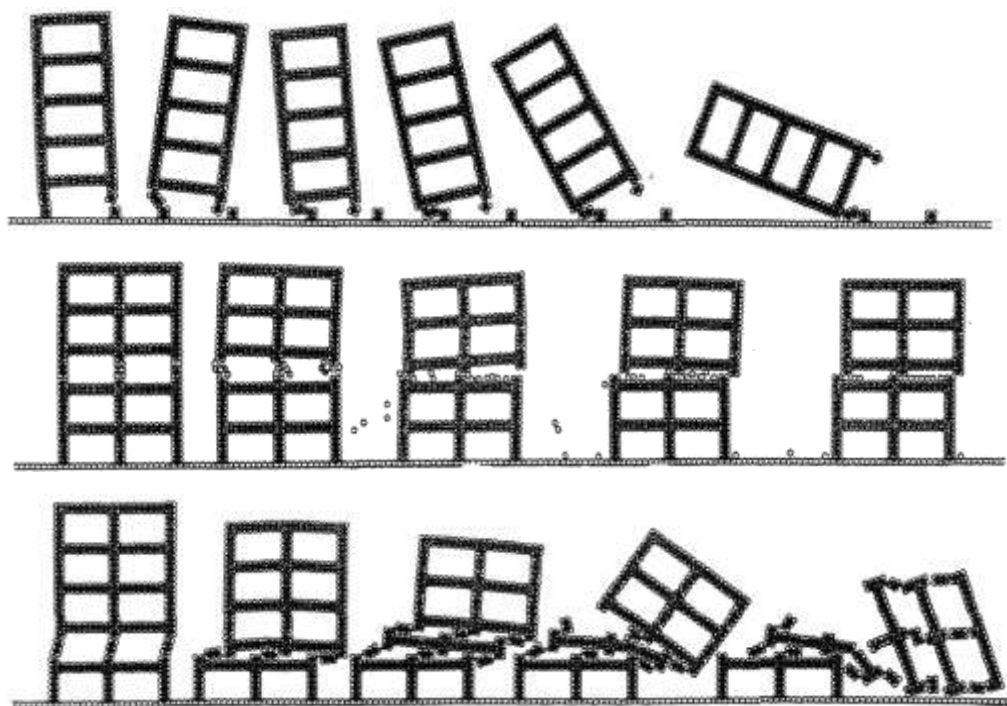


Figure 1.1– EDEM simulation of RC frame collapse due to dynamic loading (Meguro, 1993)

The explicit time marching scheme used in the DEM is useful to model materials under high strain loading, hence, concrete structures subjected to impact loading were analysed using the DEM (Liu et al. 2004; Sawamoto et al. 1998).

1.1.2.2 Extended Distinct Element Method (EDEM)

The aforementioned methods only consider the interaction at the surface of contacts (contact springs), although suitable for discontinuous granular material like soil, in order to capture the behaviour of a continuous heterogeneous media like concrete, it is easier to have connectivity between two adjacent discrete elements. The *Extended Discrete Element Method* (EDEM) introduces a pair of joint-spring (or pore-spring), in addition to the contact springs, in order to simulate the behaviour of a continua, thus the complete material behaviour, from continuous, to fracture and collapsed states can be simulated. The EDEM has previously been used to simulate concrete fracture (Meguro and Hakuno 1989), dynamic cliff collapse (Iwashita and Hakuno 1990), and collapse of concrete (Meguro and Hakuno 1994) and masonry structures (Nakagawa et al. 2012). The EDEM provides a simple and effective way to model large deformations, element separation and collapse of RC structures (Figure 1.1). However, the EDEM has some limitations namely, (i) requirement of a small time step for stability and accuracy (Hakuno and Meguro 1993), due to the use of an explicit time integration scheme, (ii) no proper mechanics theory for spring stiffness derivation, and (iii) inaccuracies due to neglect of Poisson's ratio.

1.1.2.3 Discontinuous Deformation Analysis (DDA)

Initially introduced as a back-analysis scheme for rock mechanics, the *Discontinuous Deformation Analysis* (DDA) (Shi and Goodman 1985), provides an implicit discrete element model with a hard contact approach, which offers some advantages over other explicit discrete models (Jing 1998). The DDA, although widely used in rock engineering, it is also applicable to model concrete fracture (Pearce et al. 2000). Similar formulations to the DDA, named the Discrete Finite Element Method (DFEM) (Barbosa and Ghaboussi 1990) was also developed, which can perform dynamic large deformation analysis of multiple interacting deformable bodies.

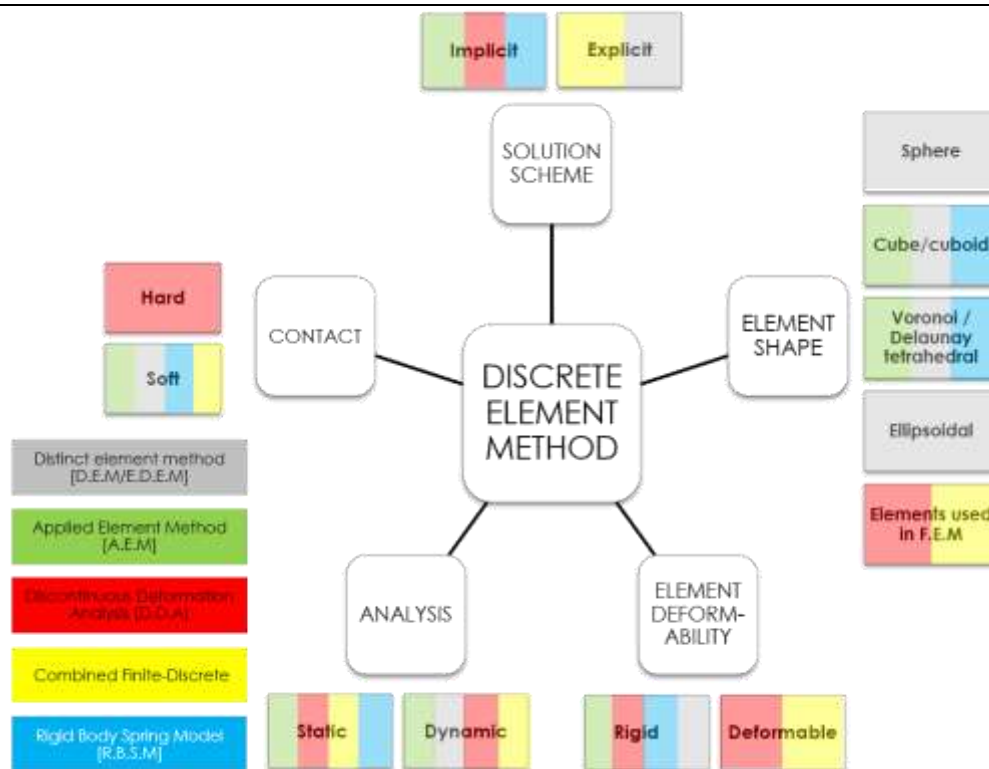


Figure 1.2– Existing discrete element methods and their classification

1.1.2.4 Rigid Body Spring Model (RBSM)

The *Rigid Body Spring Model* (RBSM) (Kawai 1977), comprises of rigid elements of variable shapes, with six degrees of freedom, suitable for static small deformation analysis of structures. They are preferable to model three-dimensional fracture mechanics, while using relatively less number of degrees of freedom (Kikuchi et al. 1992). This method is very effective in the modelling of reinforced concrete (Bolander and Saito 1998), and also, mesoscopic analysis of concrete (Nagai et al. 2004). Although, large geometric nonlinearities have been modelled through the RBSM with relatively simple elements (Ren et al. 1999), collapse analysis of structures, which requires a dynamic contact detection algorithm, has yet not been implemented into the RBSM.

1.1.2.5 Combined Finite-Discrete Element Method

The *Combined Finite-Discrete method* (Munjiza 2004) is applicable to problems involving fracturing, fragmentation and collapse. It aims at combining the Finite Element Method and the Discrete Element Method to analyses structures, using an explicit time

marching scheme, whilst taking advantage of the modern computing performance. Each element is capable of deforming and also fragmenting into smaller components. Analysis of a large structure usually starts with a very large number of elements and ends with an even larger number of elements.

1.1.2.6 Applied Element Method (AEM)

The *Applied Element Method* (AEM) (Tagel-Din 1998) introduces a simple and numerically efficient method to analyse RC structures till collapse. The structure is modelled as an assembly of distinct elements made by dividing the structural elements virtually, interconnected through a number of normal and tangential springs. The presence of these numerous springs enables the usage of simpler concrete material models and also effectively follow crack initiation and propagation, but, this presents a limitation on the size of the elements used, in order to obtain accurate results.

An overview of the existing methods and their corresponding characteristics can be observed in the figure below (Figure 1.2). There exists other discrete element methods which find their applicability in soil mechanics (Donzé et al. 2008) and modelling of masonry (Lemos 2007), but, are not discussed here.

1.2 Problem Statement

The aim of this research is to create a numerical scheme which can be used for practical collapse simulation of RC structures. As mentioned earlier there are few desirable characteristics of the analysis method for this purpose. Overlaying these characteristics with the properties of a discrete element method (Figure 1.3), the required properties of a proposed scheme can be established (Figure 1.4).

The shape of the element used plays a vital role in the computation effort required. In discrete analysis, a majority of the computation time is spent on contact detection (Williams and O'Connor 1999), hence, the usage of spherical elements drastically reduces the computation effort required for collapse analysis.

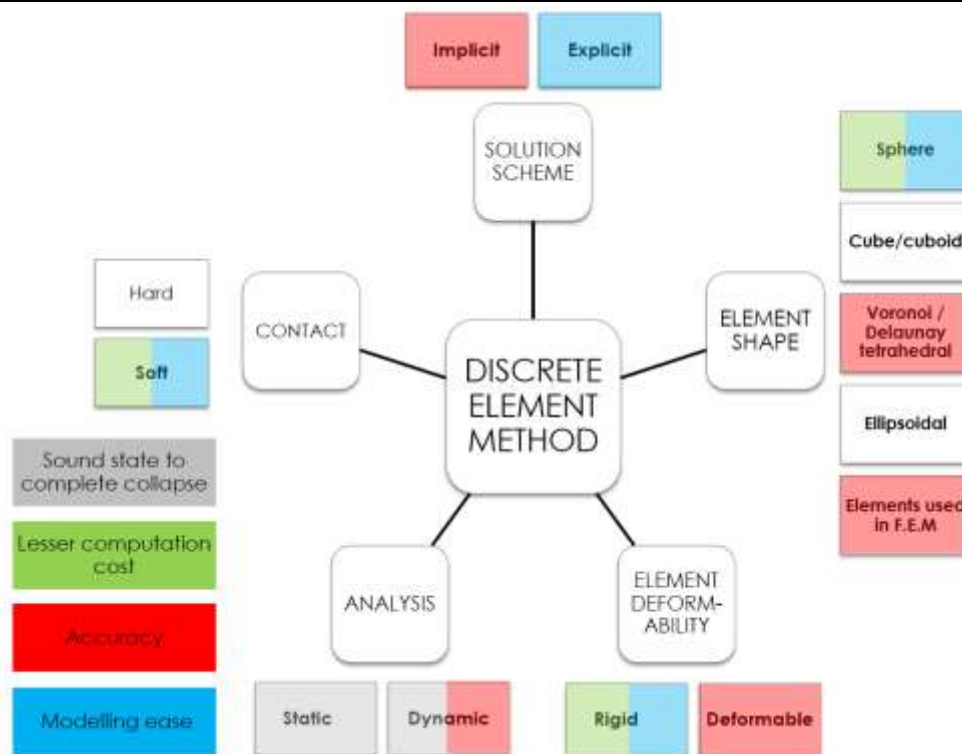


Figure 1.3– Preferable properties for simplified collapse simulation

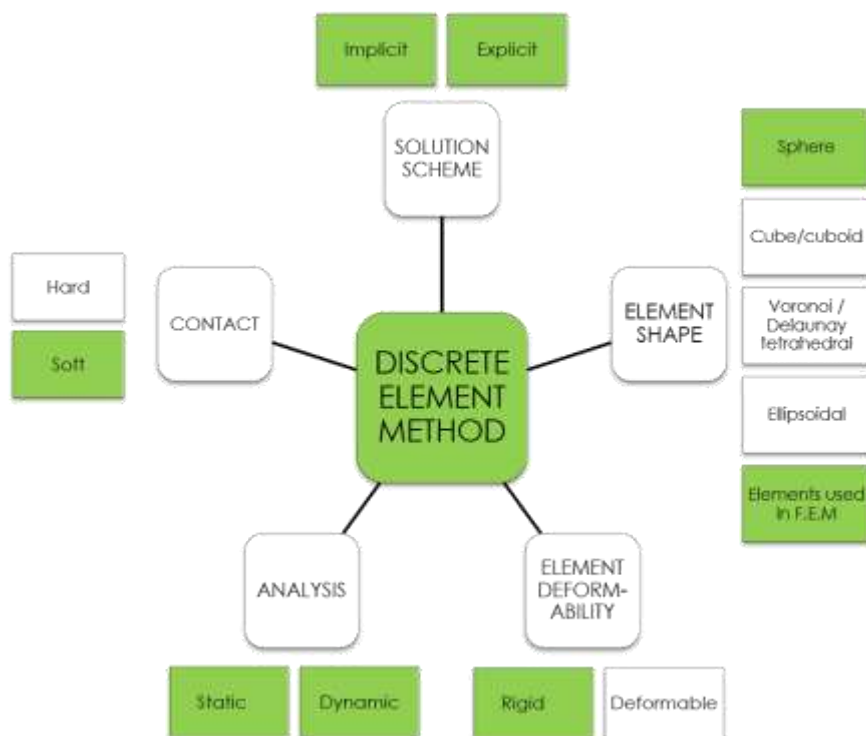


Figure 1.4– Characteristics required from the proposed scheme

Following a soft contact approach while using rigid elements, contributes to the simplicity of the model and the numerical effort required. The model should also have the capability to readily switch between implicit and explicit numerical methods.

Considering the above criteria, the Extended Discrete Element Method (EDEM) provides a good platform to meet the requirements, but EDEM suffers from few disadvantages as mentioned above. These limitations can be overcome by the assembly of a global stiffness matrix, for the discretised system, which contains theoretically derived spring stiffness that implicitly considers the Poisson's ratio effect. Using the EDEM also presents an advantage that it can be easily integrated with the Distinct Element Method, which offers a wide potential of applicability for future research.

The Lattice Models or Spring Networks, consists of an assembly of interconnected springs, which have shown their applicability in modelling micromechanics of a continua (Ostoja-Starzewski 2002). When an appropriate spring network is chosen, a model similar to the assembly of joint springs in the EDEM can be obtained, the difference being the effect of the contact springs i.e. inter-element interaction at the surface. By combining this property of both the models, an effective *two-phase* numerical collapse simulation of structures can be performed, which can predict the initial behaviour of structures (elastic/nonlinear/crack initiation/ stiffness degradation/ maximum load capacity) through a spring network (implicit numerical integration) and predict the final behaviour of structures (geometric non-linearity, instability, separation, collision, and collision) through the EDEM (explicit numerical integration).

The spring network model should include a method to derive these spring stiffness theoretically, which gives accurate results for any kind of media and any kind of particle discretization. A Finite Element Mapping scheme (Gusev 2004) was proposed for spring stiffness derivation for an infinite elastic continuum. Through this mapping, the global matrix of the assembled spring network is the same as that of the Finite Element discretization, which offers many advantages. But, the applicability of this scheme for the analysis a finite domain has to be verified.

Spring networks are very effective in modelling concrete at a small scale (micro / mesoscopic analysis), through simple material models. But, to model actual structures, this scale of analysis will involve a large number of nodes and springs, which is impractical. Therefore, in order to perform macroscopic analysis of concrete, concrete models meant for a larger scale of analysis have to be used. The smeared crack method for concrete analysis, provides a macroscopic approach to analyse concrete structures and has been successfully used to analyse RC structures using the Finite Element Method (Maekawa et al. 2003). The models can be used for a wide range of element size, therefore reducing the total number of elements required to perform RC analysis. But, the validity of using these spatially averaged models in spring network model has to be examined with a numerically stable algorithm that can analyse the material nonlinearity. The spring network should be able to perform transient dynamic analysis of the structure subjected to earthquake loading. When the structure is subjected to extreme loading, after experiencing significant damage, the analysis must automatically switch to the EDEM, to model separation, collision and collapse.

The transition between Spring Network Model and the EDEM for the second phase of analysis also raises up issues that have to be solved like, deciding when to changeover to the EDEM, the (simpler) concrete models that have to be adopted, the material models for the contact springs, optimizing the required time increment, exploring possibilities of having a combined implicit-explicit scheme etc.

1.3 Objectives

The objectives of the current study, considering the problems above, firstly, can be summarised as developing a spring network with the following characteristics:-

1. Compatible with the EDEM's joint spring network.
2. Having a general method of derivation for the spring stiffness for any kind of discretization of spring network (periodic/ disordered topology), and to obtain a global stiffness matrix.
3. Performing linear static analysis accurately, considering the Poisson ratio's effect.

4. Capable of modelling RC structures through well-established concrete and reinforcement models.
5. Using generalized material models that enable the usage of wide range of element sizes, so that large structures can be analysed with minimum number of elements, while not compromising on accuracy.
6. Having the ability to perform dynamic analysis of RC structures, through an implicit time integration method.

The above mentioned spring network should be combined with the EDEM for the second phase of analysis, to model large deformations, collision and collapse. In addition to the above objectives, the analysis method must be validated with experimental data at every step, to check the reliability of the proposed method. The current research is restricted to analysis of the RC framed buildings, which is the most common RC building type, and also, the most vulnerable to earthquakes. The final objective is to perform the overall collapse simulation of an RC structure using the proposed analysis method.

Through this two-phase analysis method, a new, relatively simple method is proposed which can, (i) model elastic behavior of structures accurately, (ii) follow the initial non-linear behavior of RC buildings, (iii) given the initial cracking and propagation of cracks, (iv) perform large deformation analysis, (v) model separation, collision and collapse, (vi) due to its simplicity, computation time for collapse of buildings has been drastically reduced, and (vii) can be used for research that requires analysis of a large building stock or probabilistic analysis which involves a large number of analysis.

1.4 Organization of this Thesis

This chapter gives an overview of the collapse analysis of buildings, existing discrete element methods to model collapse, the problem statement, research gaps and the objectives of the study.

Chapter 2 discusses the two models used in the analysis, namely the spring network model and, the Extended Distinct Element model. Various kinds of spring network (lattice) models available from literature and their application in modelling mechanics of materials are discussed. The EDEM and its formulations are introduced. The overall proposed two-phase analysis scheme, namely, the spring network phase and the EDEM phase, is introduced. The required properties of the spring network in order to be compatible with the EDEM are discussed.

Chapter 3 introduces the Finite Element Mapping scheme, and the spring constant derivation for two kinds of discretization, namely, the linear triangular elements and serendipity quadrilateral elements, are performed as an example. The issues with modelling finite domains with these derived spring constants are discussed.

The applicability of the assembled network is verified with simple linear static analysis of the bending of a cantilever beam. The ability to model the Poisson's ratio effect and the assumption of mass lumping at the nodes are verified.

Chapter 4 introduces the existing lattice models capable of modelling concrete. The various existing concrete models are discussed. The smeared crack models used in the spring network are discussed. The secant stiffness formulation used, is introduced, and, its algorithm is discussed. Experimental validation of RC concrete panels, beam and frame under monotonic loading is performed, to check the reliability of the models.

Chapter 5 discusses the transition to the second phase of analysis. The transition criteria required to switch between the two phases are discussed. A 1-storey and 12-storey RC frame structure are analysed. The structures are damaged and their collapse is simulated.

Chapter 6 presents an overview of all the results obtained in this study. The important aspects of the analysis method are explained. The scope of future work and research direction are discussed.

Chapter 2 **Two-Phase Analysis Scheme**

The proposed analysis scheme involves the combination of two methods of analysis, the spring network model, and, the Extended Distinct Element Method (EDEM). The two methods are briefly introduced below.

2.1 Spring Network models

At the initial stages of research, it was observed that complex elastic continua problems could be solved by dividing it into an assemblage of simple structural elements, whose mechanical properties were well understood (Hrennikoff 1941). With similar formulations, the Lattice (or Spring Network) model, which are based on the atomic lattice model of materials, have been found to have the potential for usage in micromechanics (Ostoja-Starzewski 2002). The model consists of nodes that are interconnect with springs, or in a more general case, with rheological elements. There are various kinds of lattice models depending on the kind of connecting element used. They are practically an algebraic equivalent of the Finite Element Method, but, are usually useful in modelling complex heterogeneous systems with a large number of degrees of freedom (Ostoja-Starzewski et al. 1996).

The spring network model is highly preferable to model fracture at a small material scale (micro/mesoscopic) with simple material models. The initial spring stiffness are determined by equating the energy stored by the network, to the energy of the equivalent continuum it represents. Once loaded externally, the springs rupture based on an element breaking rule (Jagota and Bennison 1999) and, once ruptured, the spring is removed and its force is redistributed in the spring network, thereby effectively simulating crack initiation and propagation.

While modelling with spring networks, the issue that has to be addressed is that any arbitrarily discretized spring network should have the ability (Jagota and Bennison 1994) to (a) model uniform strain field i.e. when subjected to uniform strain, its distribution should be homogenous among the network (b) model crack propagation in an isotropic material without mesh-bias/mesh dependency.

2.2 Finite Element Mapped Spring Network

The Finite Element mapping scheme for spring network representation of mechanics of solids (Gusev 2004), presented a rigorous method for spring stiffness derivation for any anisotropic infinite media. The spring stiffness of the spring network is derived by invoking the property of translation invariance, to equate the off-diagonal blocks of both the global stiffness matrices, derived by finite element technique, and, from assembly of a spring network respectively (Figure 2.1).

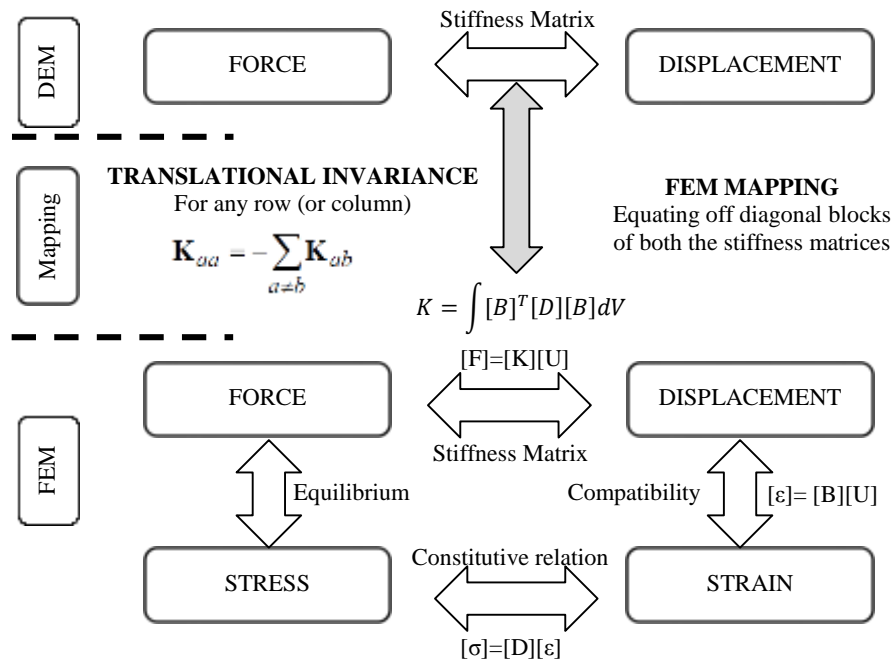


Figure 2.1– Finite element mapping of spring network

The spring stiffness was derived for an infinite elastic media, discretized into an assemblage of constant strain triangular finite elements. The assembled spring network with the derived spring stiffness leads to the same global stiffness matrix as that of the finite element system.

2.3 The Extended Distinct Element Method (EDEM)

As mentioned in the previous chapter, the EDEM modified the Distinct Element Method by adding joint (or pore) springs, in addition to the contact springs, between two elements (Figure 2.2). Viscous dash pots are placed in parallel to the springs to model the damping of the structure. Each element has three degrees of freedom in 2D (two translation and rotation). Simple linear concrete models were used in normal and shear directions. A critical tensile strain value was used to decide the rupture of tension springs. A Mohr-Coulomb failure criteria was used to determine the failure of shear springs. A relatively simple explicit numerical method was used for the simulation (Figure 2.3), hence there is no requirement of assembling a global stiffness matrix. Although, this enables the EDEM to effectively follow geometric nonlinearity, instability, separation, collision and collapse, there is a restriction on the time increment. As the central difference method is only conditionally stable (Courant et al. 1967), a very small time increment (order of 10^{-4} to 10^{-6} sec) is required to ensure numerical stability.

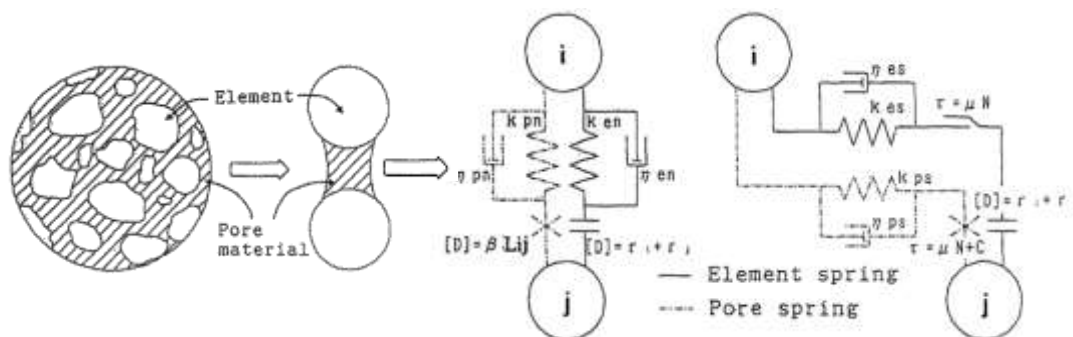


Figure 2.2– EDEM modelling of concrete (Meguro and Hakuno 1989)

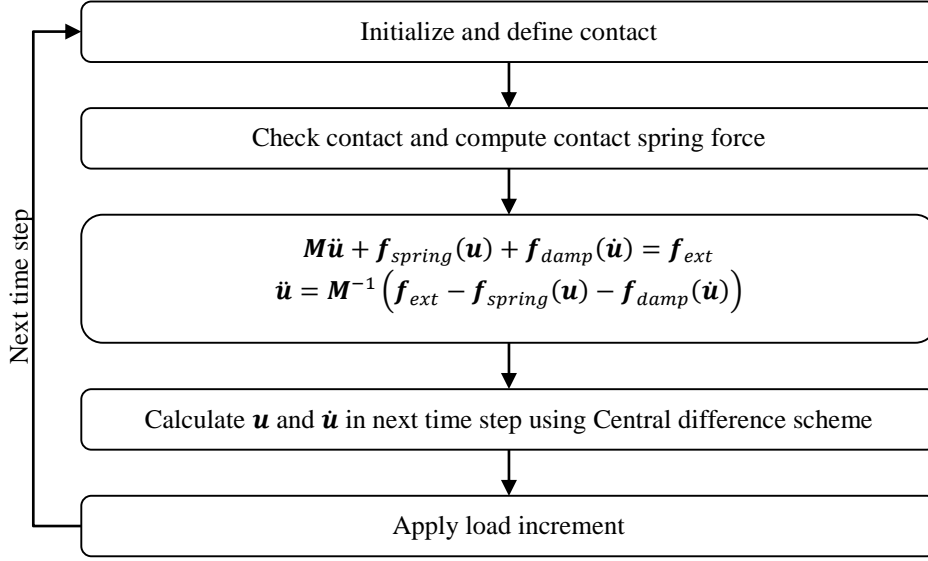


Figure 2.3– Analysis flow of the EDEM

If the mapped spring network is adopted into the EDEM's joint spring network, the following advantages are obtained ; (i) Due to global stiffness matrix assembly, an implicit time integration numerical scheme can be used, thereby increasing the critical time required for stable analysis, (ii) Accurate spring constants derivation, hence accuracy in the initial phase is high, (iii) The spring constants for any arbitrary discretization can be derived, making the method have a wider applicability (iv) The spring network is capable of modelling uniform strain ,even with disordered topology, if they are mapped to a good finite element meshing, as they usually pass the patch test (modelling uniform strain) (v) The meshing can be made in random direction with random sizes of elements, hence, can reduce mesh-bias in cracking (vi) Poisson's ratio is implicitly included, and (vii) Mass matrix is diagonal, which makes its inversion during dynamic analysis trivial.

2.4 Two Phase Analysis

The analysis of the structure comprises of two phases: (i) *Finite Element Mapped Spring Network Phase*, (ii) *Extended Distinct Element Method Phase*. The overall behaviour of the building from normal state to complete collapse state can be captured by these two phases (Figure 2.4).

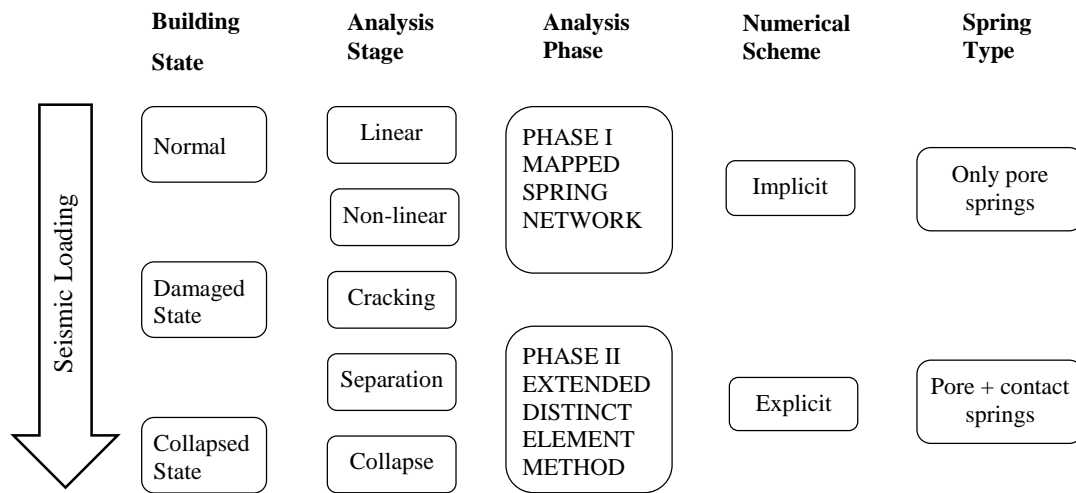


Figure 2.4– Overall Analysis Method

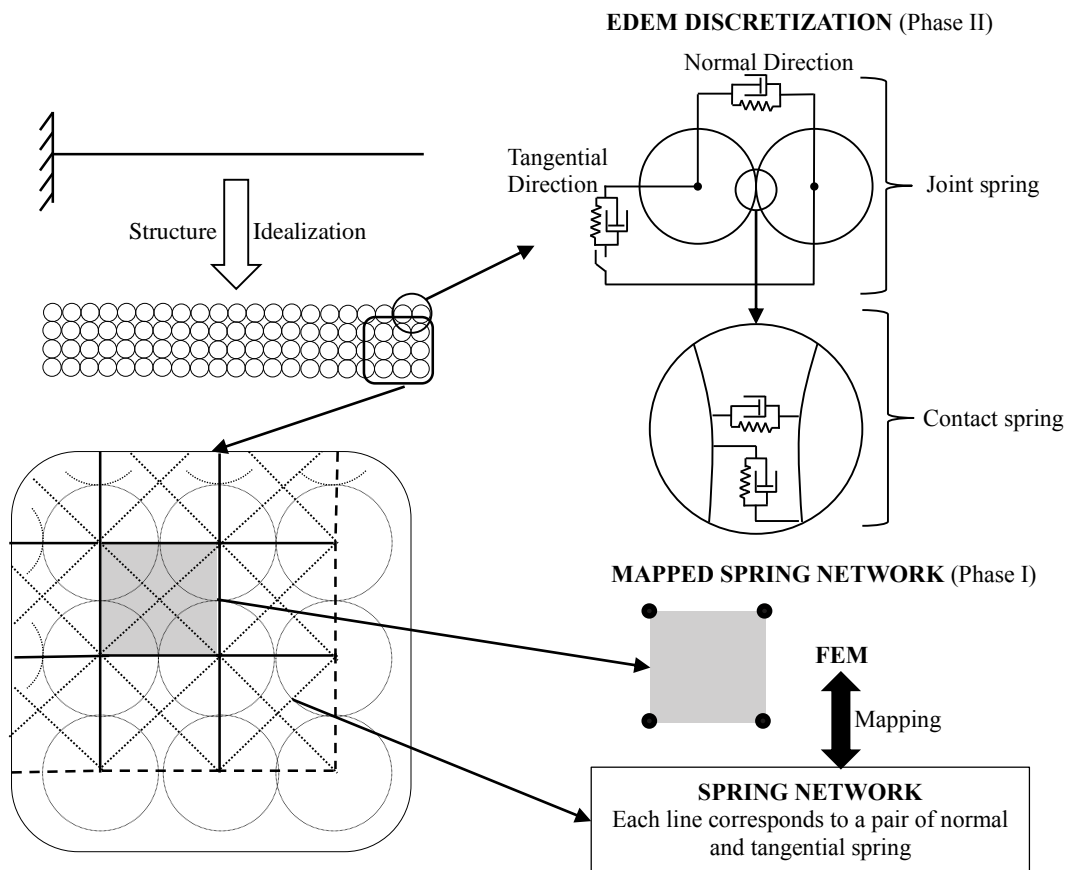


Figure 2.5– Domain discretization in EDEM and spring network

The domain is initially discretized into a spring network as shown above (Figure 2.5). The spring stiffness is derived from an equivalent finite element discretization. The element shape and contact springs, do not have a meaning in this phase. The mass is assumed to be concentrated at the nodes. The global stiffness matrix assembly is performed at each step of computation and this matrix is used at each time step to obtain the deformation. A sufficiently large time increment is used in dynamic analysis using an unconditionally stable, implicit numerical integration method. Once the deformations are considerable, the analysis switches to the conventional EDEM phase. The contact springs and the pore springs work at tandem, and the element shapes now have a physical meaning, for contact detection and force computation. A small time increment is used for an explicit, step-by-step time marching scheme for the dynamic analysis.

2.5 Spring Network requirements

Analytical derivation of the spring stiffness of a connected DEM domain, has been previously done (Griffiths and Mustoe 2001; Liu et al. 2004; Sawamoto et al. 1998) with the same intent of modelling fragmentation and collapse, using a grillage of structural elements, consisting of cylindrical elements in a closed hexagonal packing. However, its applicability for complex domains and large deformation analysis is not yet verified and also, there is a restriction to the kind of basic unit of discretization used. Simple lattice models, comprising of an assemblage of 1-D truss elements have been used along with EDEM to simulate collapse of RC bridges (Sun et al. 2003). However, it has been observed that shear springs have to be incorporated into the lattice spring model, in order to allow the full range of the Poisson's ratio of the solid to be modelled (Zhao et al. 2010).

The nodes in EDEM have three degrees of freedom and have to be initially spaced more than the sum of the radii of two adjacent elements. Keeping this in mind, while choosing the parent finite element, that the spring network has to be mapped from, the simplest elements that can be chosen are the Constant Strain Triangle (CST) and the bilinear quadrilateral element, which can be mapped to obtain, a triangular and quadrilateral element packing pattern respectively (Figure 2.6).

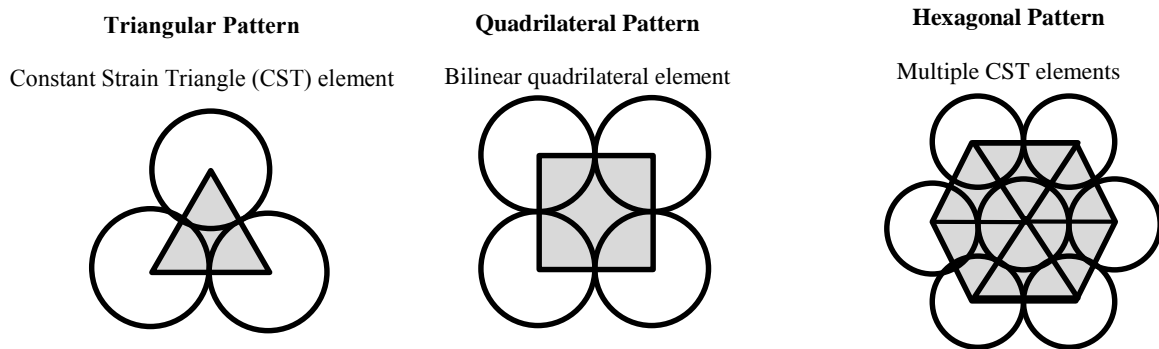


Figure 2.6— Simple discretization pattern and their corresponding finite element

The hexagonal pattern offers very less geometric porosity and can be obtained by combining multiple triangular elements. Higher order elements can be used to improve the accuracy of spring network. Random meshing with variable element size can also be performed, which has to be correspondingly mapped to a random finite element meshing. In order, to maintain simplicity of model, currently the bilinear quadrilateral element is considered, to create a periodic/ordered quadrilateral element arrangement, as they can be used to easily mesh the RC frame domain.

The spring network obtained from the finite element mapping using the aforesaid elements, has only, one central two-body interaction (normal spring) and one non-central two-body interaction (tangential spring), limiting the rotational degree of freedom at the nodes. This spring network is similar to the *Born Lattice Model* (Jagota and Bennison 1994; Yan et al. 2007), and is a simple and effective model, but, this model is not rotationally invariant (Keating 1966). This problem can be solved by (a) considering rotational degree of freedom in parent finite element (beam element) (b) using a local strain based deformation measurement (Zhao et al. 2010). But, since the finite elements stiffness are derived based on infinitesimal strain theory, and, for small deformations, the effect of this invariance is unimportant, and hence can be neglected (Hassold and Srolovitz 1989). The change in length of spring is used during computation to detect rigid body rotation, and if excessive rigid body movement is present (due to yielding/excessive cracking), the analysis shifts to the EDEM phase, which considers the elemental rotation in its computation.

Chapter 3 Phase I: Linear Static Analysis

The spring stiffness is derived using the finite element mapping. And the spring network with derived spring stiffness are verified for linear elastic analysis.

3.1 Spring Stiffness derivation

The stiffness matrix for a simple domain using the Finite Element Method can be found in various Finite element literature (Zienkiewicz and Taylor 2000). As seen below (Figure 3.1) for a simple domain the element stiffness matrix can be derived by assuming a continuous distribution of displacement across the element, through appropriate shape functions.

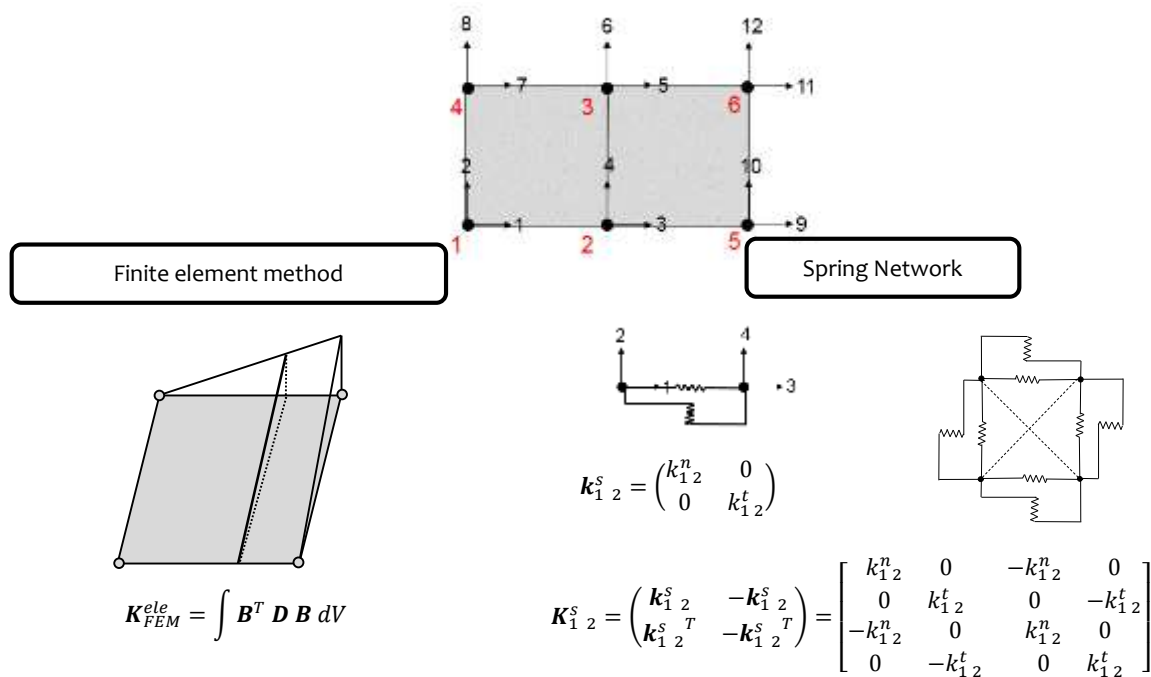


Figure 3.1– Elemental Stiffness matrix in Finite Element Method and Spring Network

The elemental stiffness is calculated through the deformation matrix (**B**) and the constitutive matrix (**D**). The spring network for the same domain consists of two perpendicular springs connecting two adjacent nodes. And the element stiffness between two nodes, are expressed in terms of their normal and tangential stiffness.

The naming convention of the spring network, which connects nodes l and m is as follows; k_{lm}^n and k_{lm}^t are the spring stiffness in the normal and tangential directions respectively, \mathbf{k}_{lm}^s is the 2x2 spring stiffness matrix when the other end is fixed, \mathbf{K}_{lm}^s is the 4x4 matrix corresponding to the global stiffness matrix in local coordinate system, \mathbf{K}_{lm}^G is the same matrix in global coordinate system.

The simple domain shown above (Figure 3.1), has 12 degrees of freedom (dof) and when assembled, will result in a 12 X 12 global stiffness matrix. This global matrix can be subdivided into 6 X 6 blocks (Figure 3.2). Each off-diagonal 2 X 2 block corresponds to the connection between two nodes. The global matrix, which is usually a sparse matrix, consists many zero blocks, (shown by white dots) which represents unconnected nodes. For example, in the given domain node 2 is connected to all other nodes, therefore all its off-diagonal blocks are non-zero (shown by black dots).

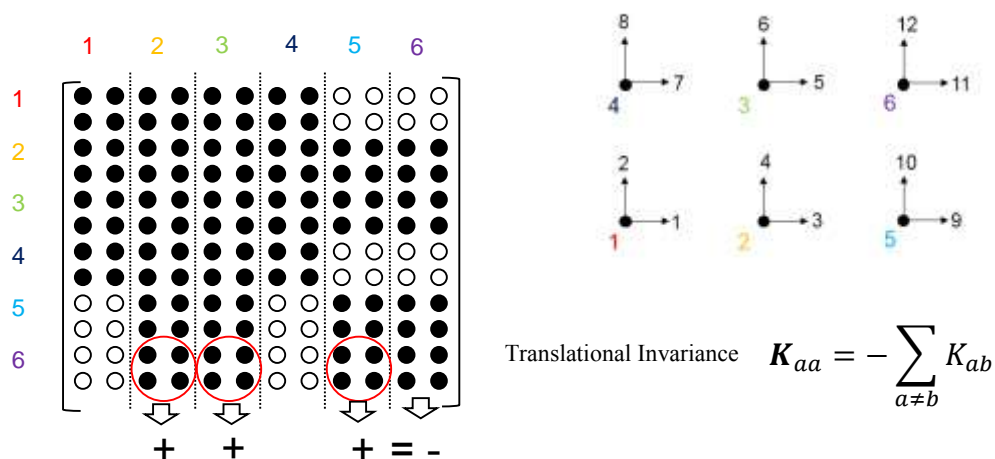


Figure 3.2– Global stiffness matrix and its translational invariance property

The translational invariance of the global stiffness matrix essentially means that the sum of all the off-diagonal block will be equal to the diagonal block, with a negative sign. While comparing the global assembled matrix of the finite element matrix and the spring network, the off-diagonal blocks of both the matrices are made equal. Spring stiffness are derived in order to make the off-diagonal blocks equal. By doing so, equal stiffness matrices are obtained from the finite element and spring network discretization.

3.1.1 Constant Strain Triangle discretization

The simplest element used in finite element discretization is the constant strain triangle (CST) element. Plane strain condition is assumed. A simple domain consisting of two equilateral plane strain CST elements is assumed (Figure 3.3). The equivalent spring network for the same domain consists of 5 springs connecting the 4 nodes. The finite element global stiffness matrix was derived for the domain (Eqn. 3.1). The blocks and their corresponding 2 X 2 blocks are marked in the equation. A sample spring stiffness derivation is given below. As an example, the spring stiffness for the spring connecting nodes 2 and 4 will be derived. The corresponding off-diagonal of nodes 2 and 4 are shaded grey in the equation.

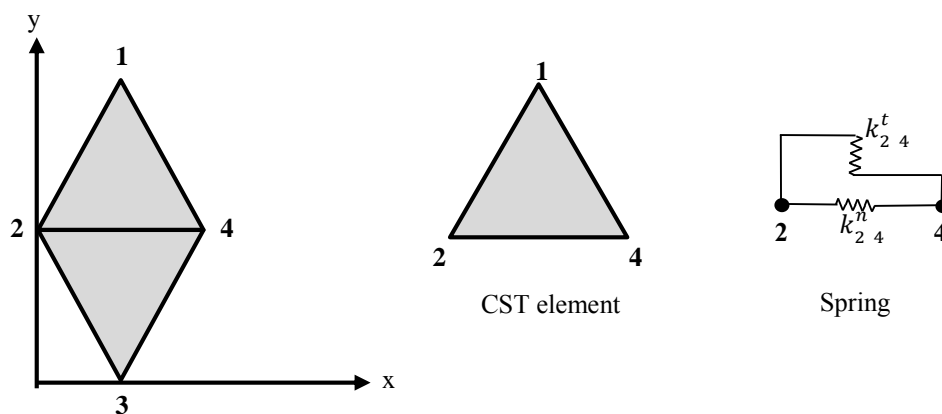


Figure 3.3– Domain for deriving spring stiffness and the basic elements

$$K_{FEM}^G = \begin{pmatrix} \begin{matrix} \text{Node 1} \\ \frac{\mu}{\sqrt{3}} & 0 \\ 0 & \frac{\lambda + 2\mu}{\sqrt{3}} \end{matrix} & \begin{matrix} \text{Node 2} \\ -\frac{\mu}{2\sqrt{3}} & -\frac{\mu}{2} \\ -\frac{\lambda}{2} & -\frac{\lambda + 2\mu}{2\sqrt{3}} \end{matrix} & \begin{matrix} \text{Node 3} \\ 0 & 0 \\ 0 & 0 \end{matrix} & \begin{matrix} \text{Node 4} \\ -\frac{\mu}{2\sqrt{3}} & \frac{\mu}{2} \\ \frac{\lambda}{2} & -\frac{\lambda + 2\mu}{2\sqrt{3}} \end{matrix} \\ \begin{matrix} \text{Node 1} \end{matrix} & & & \\ \begin{matrix} \text{Node 2} \\ -\frac{\mu}{2\sqrt{3}} & -\frac{\lambda}{2} \\ -\frac{\mu}{2} & -\frac{\lambda + 2\mu}{2\sqrt{3}} \end{matrix} & \begin{matrix} \begin{matrix} \text{Node 2} \\ 3\lambda + 7\mu \\ 2\sqrt{3} & 0 \end{matrix} \\ \begin{matrix} \text{Node 3} \\ \frac{\lambda + 5\mu}{2\sqrt{3}} \end{matrix} \end{matrix} & \begin{matrix} \begin{matrix} \text{Node 2} \\ -\frac{\mu}{2\sqrt{3}} & \frac{\lambda}{2} \\ \frac{\mu}{2} & -\frac{\lambda + 2\mu}{2\sqrt{3}} \end{matrix} \\ \begin{matrix} \text{Node 3} \\ \frac{\mu}{\sqrt{3}} & 0 \\ 0 & \frac{\lambda + 2\mu}{\sqrt{3}} \end{matrix} \end{matrix} & \begin{matrix} \begin{matrix} \text{Node 4} \\ -\frac{3\lambda + 5\mu}{2\sqrt{3}} & 0 \\ 0 & \frac{\lambda - \mu}{2\sqrt{3}} \end{matrix} \\ \begin{matrix} \text{Node 3} \\ -\frac{\mu}{2\sqrt{3}} & -\frac{\mu}{2} \\ -\frac{\lambda}{2} & -\frac{\lambda + 2\mu}{2\sqrt{3}} \end{matrix} \end{matrix} \\ \begin{matrix} \text{Node 2} \end{matrix} & & & \\ \begin{matrix} \text{Node 3} \\ 0 & 0 \\ 0 & 0 \end{matrix} & \begin{matrix} \begin{matrix} \text{Node 2} \\ -\frac{\mu}{2\sqrt{3}} & \frac{\mu}{2} \\ \frac{\lambda}{2} & -\frac{\lambda + 2\mu}{2\sqrt{3}} \end{matrix} \\ \begin{matrix} \text{Node 3} \\ \frac{\mu}{\sqrt{3}} & 0 \\ 0 & \frac{\lambda + 2\mu}{\sqrt{3}} \end{matrix} \end{matrix} & \begin{matrix} \begin{matrix} \text{Node 2} \\ -\frac{\mu}{2\sqrt{3}} & \frac{\lambda}{2} \\ \frac{\mu}{2} & -\frac{\lambda + 2\mu}{2\sqrt{3}} \end{matrix} \\ \begin{matrix} \text{Node 3} \\ \frac{\mu}{\sqrt{3}} & 0 \\ 0 & \frac{\lambda + 2\mu}{\sqrt{3}} \end{matrix} \end{matrix} & \begin{matrix} \begin{matrix} \text{Node 4} \\ -\frac{\mu}{2\sqrt{3}} & -\frac{\mu}{2} \\ -\frac{\lambda}{2} & -\frac{\lambda + 2\mu}{2\sqrt{3}} \end{matrix} \\ \begin{matrix} \text{Node 3} \\ -\frac{\mu}{2\sqrt{3}} & -\frac{\mu}{2} \\ -\frac{\lambda}{2} & -\frac{\lambda + 2\mu}{2\sqrt{3}} \end{matrix} \end{matrix} \\ \begin{matrix} \text{Node 3} \end{matrix} & & & \\ \begin{matrix} \text{Node 4} \\ -\frac{\mu}{2\sqrt{3}} & \frac{\lambda}{2} \\ \frac{\mu}{2} & -\frac{\lambda + 2\mu}{2\sqrt{3}} \end{matrix} & \begin{matrix} \begin{matrix} \text{Node 2} \\ -\frac{3\lambda + 5\mu}{2\sqrt{3}} & 0 \\ 0 & \frac{\lambda - \mu}{2\sqrt{3}} \end{matrix} \\ \begin{matrix} \text{Node 3} \\ -\frac{\mu}{2\sqrt{3}} & -\frac{\lambda}{2} \\ -\frac{\mu}{2} & -\frac{\lambda + 2\mu}{2\sqrt{3}} \end{matrix} \end{matrix} & \begin{matrix} \begin{matrix} \text{Node 2} \\ -\frac{\mu}{2\sqrt{3}} & \frac{\lambda}{2} \\ \frac{\mu}{2} & -\frac{\lambda + 2\mu}{2\sqrt{3}} \end{matrix} \\ \begin{matrix} \text{Node 3} \\ -\frac{\mu}{2\sqrt{3}} & -\frac{\lambda}{2} \\ -\frac{\mu}{2} & -\frac{\lambda + 2\mu}{2\sqrt{3}} \end{matrix} \end{matrix} & \begin{matrix} \begin{matrix} \text{Node 4} \\ \frac{3\lambda + 7\mu}{2\sqrt{3}} & 0 \\ 0 & \frac{\lambda + 5\mu}{2\sqrt{3}} \end{matrix} \\ \begin{matrix} \text{Node 3} \\ -\frac{\mu}{2\sqrt{3}} & -\frac{\lambda}{2} \\ -\frac{\mu}{2} & -\frac{\lambda + 2\mu}{2\sqrt{3}} \end{matrix} \end{matrix} \\ \begin{matrix} \text{Node 4} \end{matrix} & & & \end{pmatrix} \quad (3.1)$$

λ and μ are the Lamé's parameters. If $k_{2\ 4}^n$ and $k_{2\ 4}^t$ are the normal and tangential spring stiffness between nodes 2 and 4. The local spring stiffness matrix is,

$$k_{2\ 4}^s = \begin{bmatrix} k_{2\ 4}^n & 0 \\ 0 & k_{2\ 4}^t \end{bmatrix} \quad \text{.....(3.2)}$$

In global coordinates

$$K_{l\ m}^G = R \cdot k_{l\ m}^s \cdot R^T \quad \text{.....(3.3)}$$

where the transformation matrix,

$$R = \begin{pmatrix} \cos\theta & \sin\theta \\ -\sin\theta & \cos\theta \end{pmatrix} \quad \text{.....(3.4)}$$

In the case of nodes 2 and 4, angle of inclination of spring with horizontal, $\theta=0^\circ$. There by equating Eq. 3.3 and its corresponding off-diagonal block from Eq. 3.1,

$$K_{2\ 4}^G = \begin{bmatrix} \cos\theta & \sin\theta \\ -\sin\theta & \cos\theta \end{bmatrix} \cdot \begin{bmatrix} k_{2\ 4}^n & 0 \\ 0 & k_{2\ 4}^t \end{bmatrix} \cdot \begin{bmatrix} \cos\theta & \sin\theta \\ -\sin\theta & \cos\theta \end{bmatrix}^T = \begin{bmatrix} \frac{3\lambda + 5\mu}{2\sqrt{3}} & 0 \\ 0 & \frac{\mu - \lambda}{2\sqrt{3}} \end{bmatrix} \quad \text{.....(3.5)}$$

Solving the above equation we obtain,

$$\begin{bmatrix} k_{2\ 4}^n & 0 \\ 0 & k_{2\ 4}^t \end{bmatrix} = \begin{bmatrix} \frac{3\lambda + 5\mu}{2\sqrt{3}} & 0 \\ 0 & \frac{\mu - \lambda}{2\sqrt{3}} \end{bmatrix} \quad \dots\dots(3.6)$$

The above spring stiffness can also be obtained by finding the eigenvalues of the off-diagonal block. The eigenvalues correspond to the spring stiffness and the eigenvectors correspond to the orientation of the springs. Once the stiffness of all springs were derived, it was observed that there were two kinds of springs for this kind of discretization (Table 3.1). The *inner springs*, which are mutually orthogonal to each other. A special case, when $\lambda=\mu$, then the tangential stiffness becomes zero and the spring network for an infinite domain (no boundary springs), becomes a network of one directional Hook's law springs, with spring stiffness $k = \frac{4}{\sqrt{3}}\lambda = \frac{4}{\sqrt{3}}\mu$, which has been observed earlier in literature (Ashurst and Hoover 1976). The *boundary springs* are not mutually perpendicular to each other, but are oriented along the eigenvector direction given below (Table 3.1). In the case of plane stress formulation, when Poisson's ratio is 1/3 it lead to a simplified 1-D spring system (Table 3.2).

Table 3.1 – Spring stiffness and local spring orientation for CST elements (Plane Strain)

Spring Type		Spring stiffness (Eigen Value)	Spring direction (Eigen direction)
Inner	normal	$\frac{3\lambda + 5\mu}{2\sqrt{3}}$	$\begin{pmatrix} 1 & 0 \\ 0 & 1 \end{pmatrix}$ (Orthogonal)
	tangential	$\frac{-\lambda + \mu}{2\sqrt{3}}$	
Boundary	normal	$\frac{\lambda + 3\mu + A}{4\sqrt{3}}$	$\begin{pmatrix} \frac{2\lambda + 2\mu + A}{\sqrt{3}(\lambda - \mu)} & \frac{2\lambda + 2\mu - A}{\sqrt{3}(\lambda - \mu)} \\ 1 & 1 \end{pmatrix}$ where, $A = \sqrt{\lambda^2 + 14\lambda\mu + \mu^2}$
	tangential	$\frac{\lambda + 3\mu - A}{4\sqrt{3}}$	

Table 3.2 – Spring stiffness and local spring orientation for Plane Stress CST elements (Poisson's ratio = 1/3)

Spring Type		Spring stiffness	Spring direction
Inner	normal	$\frac{\sqrt{3} E}{2}$	$\begin{pmatrix} 1 & 0 \\ 0 & 1 \end{pmatrix}$ (Orthogonal)
	tangential	0	
Boundary	normal	$\frac{\sqrt{3} E}{4}$	$\begin{pmatrix} 1 & 0 \\ 0 & 1 \end{pmatrix}$ (Orthogonal)
	tangential	0	

3.1.2 Bilinear quadrilateral discretization

The current study involves simple structural elements therefore, the simple bilinear quadrilateral (square) finite element is also preferable for discretization (Figure 3.4).

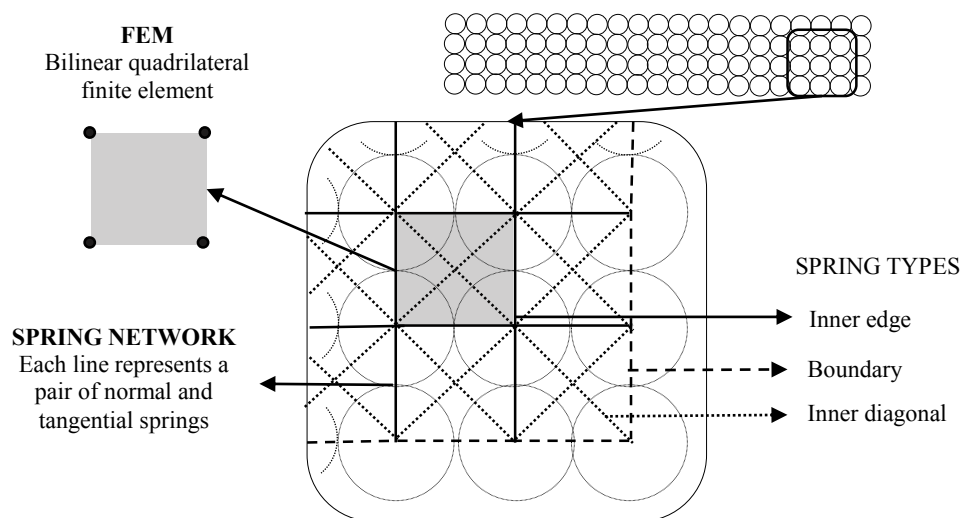


Figure 3.4– Quadrilateral elements: Domain discretization

Table 3.3 – Spring stiffness and local spring orientation for quadrilateral finite elements

Spring type			Spring stiffness (Eigen Value)	Spring direction (Eigen direction)
Inner	Edge	normal	$\frac{E(3 + \nu)}{6(1 - \nu^2)}$	$\begin{pmatrix} 1 & 0 \\ 0 & 1 \end{pmatrix}$ (Orthogonal)
		tangential	$\frac{E \cdot \nu}{3(-1 + \nu^2)}$	
	Diagonal	normal	$\frac{E(9 + \nu)}{24(1 - \nu^2)}$	$\begin{pmatrix} 1 & 0 \\ 0 & 1 \end{pmatrix}$ (Orthogonal)
		tangential	$\frac{E(-3 + 5\nu)}{24(-1 + \nu^2)}$	
Boundary		normal	$\frac{E \left(-3 + \nu + 6\sqrt{2}\sqrt{(\nu - \nu^2)} \right)}{24(-1 + \nu^2)}$	$\left(\begin{array}{cc} \frac{1 + \nu - 2\sqrt{2}\sqrt{(\nu - \nu^2)}}{-1 + 3\nu} & \frac{1 + \nu + 2\sqrt{2}\sqrt{(\nu - \nu^2)}}{-1 + 3\nu} \\ 1 & 1 \end{array} \right)$
		tangential	$\frac{E \left(-3 + \nu - 6\sqrt{2}\sqrt{(\nu - \nu^2)} \right)}{24(-1 + \nu^2)}$	

For a domain discretized by bilinear quadrilateral finite elements, it was observed that there were three different kinds of springs in the corresponding mapped spring network, namely, *inner edge*, *inner diagonal* and *boundary springs* (Table 3.2). In the case of *inner springs*, orthogonal springs were obtained as seen from the table. For certain values of Poisson's ratio (ν), the spring stiffness of the internal diagonal spring ceases to be positive-definite, which seems physically unreasonable (Nukala and Šimunović 2006) and may lead to adverse stability issues. However, the negative stiffness is important to maintain rotational invariance of the whole system and at the global level, the assembled stiffness matrix is always positive definite (Gusev 2006).

While deriving the spring stiffness for the *boundary springs*, it was observed that the springs were not orthogonal to each other. However, a diagonal spring matrix can be obtained, if the springs are oriented along the eigenvector direction.

Distinct diagonal spring stiffness for the boundary springs along the eigenvector direction can be obtained when the Poisson's ratio (ν) varies between $0.25 - \frac{5\sqrt{2}}{32} < \nu < 0.25 + \frac{5\sqrt{2}}{32}$ ($\sim 0.03 < \nu < 0.47$) (Wei et al. 2006). As most conventional construction materials like steel and concrete lie within this range of Poisson's ratio, it can be assumed that distinct eigenvalues are always obtained while deriving the spring stiffness.

The numbering of the boundary springs are important. Since local nodal numbering of finite elements are usually counter-clockwise. If the spring being mapped is numbered clockwise (against the local numbering of the finite element), the spring stiffness must be mapped to the transpose of the corresponding off diagonal block.

3.2 Linear Analysis

In order to check the accuracy of the assembled spring network, a simple linear analysis of bending of a cantilever beam was performed. The details of the cantilever are given below (Figure 3.5). The cantilever is discretized using the spring network derived from the two fore mentioned finite element discretization viz. Quad spring network and CST spring network respectively (Table 3.4). With the increase in number of rows of elements, its influence on energy and error in deflection are observed.

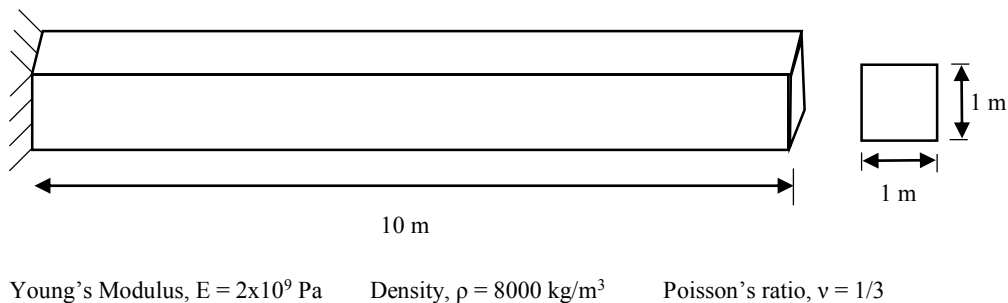
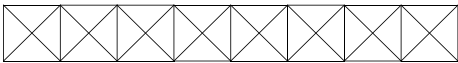
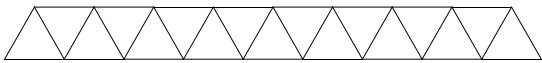
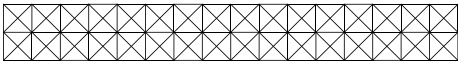
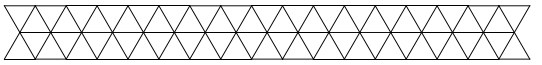
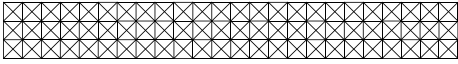
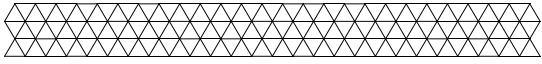
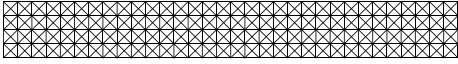
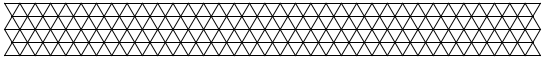
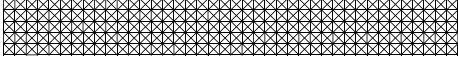

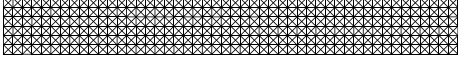






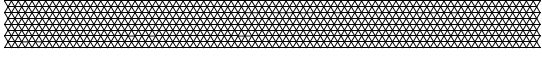


Figure 3.5– Properties of the cantilever used for linear analysis

Table 3.4 – Spring stiffness and local spring orientation for quadrilateral finite elements

No. of element rows	Quad Spring network	CST Spring network
2		
3		
4		
5		
6		
7		
8		
9		
10		

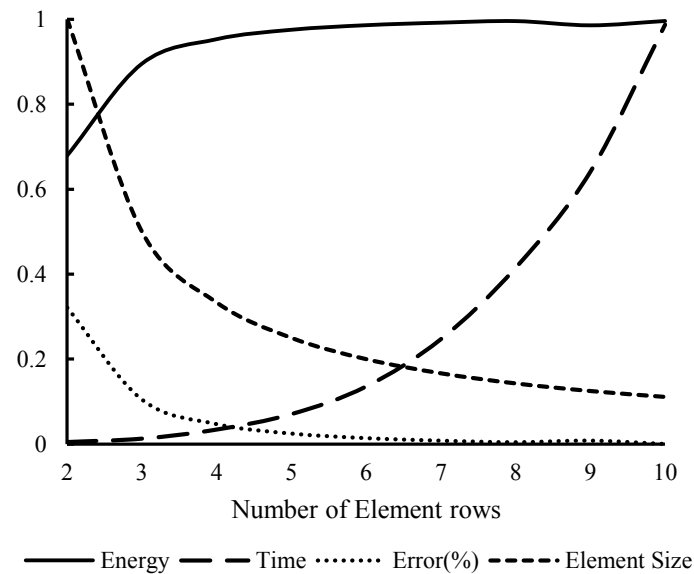


Figure 3.6– Quad Spring Network: Variation of energy, displacement error with increase in no. of elements

A normalized plot is shown for the Quad spring network (Figure 3.6.) and CST spring network (Figure 3.7). The energy, size of element, time are normalized with their respective maximum values. The global stiffness matrix is exactly the same as the finite element stiffness matrix, hence it exhibits the same properties of that of the finite element system, like energy convergence and error reduction with finer meshing.

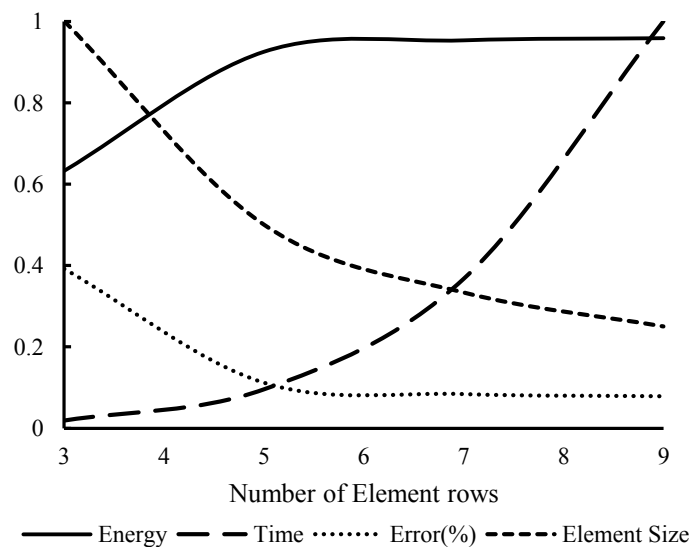
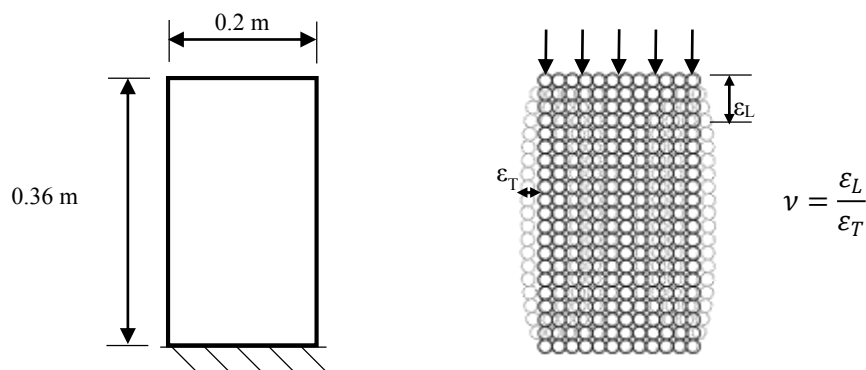
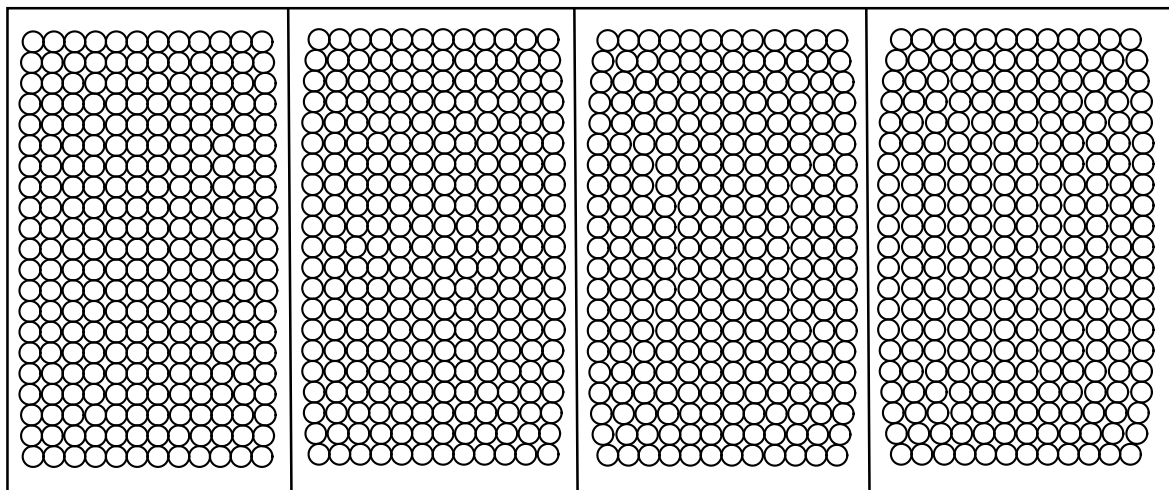


Figure 3.7– CST Spring Network: Variation of energy, displacement error with increase in no. of elements

It is observed that 2 rows of elements (element size = 0.5m) leads to erroneous results (>30%) and has to be avoided. Between 4 and 5 rows of elements, an optimum balance between accuracy and computation time was observed. From these results, it was observed that the spring system leads to good results in the elastic range and the accuracy also depends on the kind of finite element used for derivation and also the meshing used. If this spring system is used in EDEM, it will essentially lead to a system which is accurate in its elastic phase.



(a) Dimensions of the analyzed plate (b) EDEM discretization



(c) Deformation profile with increasing Poisson's ratios (illustration scale factor is 100)

Figure 3.8– Poisson's ratio verification

3.2.1 Poisson's Ratio

The Poisson's ratio is considered in the element constitutive relation while deriving the stiffness relations, during the finite element global stiffness matrix derivation. As the assembled stiffness matrices are the same, the spring constants implicitly model the Poisson's ratio effect. In order to demonstrate the capability of the spring network system to capture Poisson's ratio, a simple rectangular elastic plate of unit thickness, subjected to compression is considered (Figure 3.8(a)). Constant strain is applied to the top row of elements and the elongation at the mid-level of the specimen is used to calculate the transverse strain for Poisson's ratio computation.

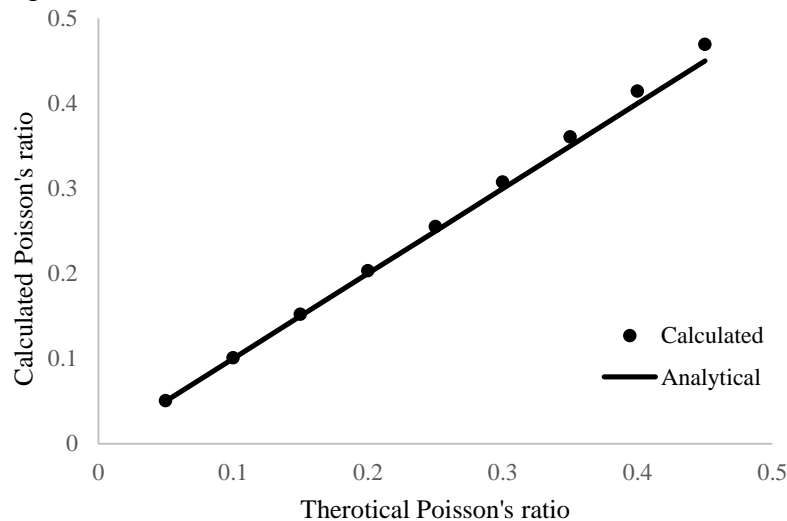


Figure 3.9– Comparison between calculated and analytical Poisson's ratios

The Poisson's ratio value is varied from 0.05 to 0.45, as mentioned earlier, there is a limit for the Poisson's ratio in order to diagonalise the boundary springs. The deformation profiles (illustration scale factor of 100 in transverse direction) show the effect of increase in transverse strain due to increase in Poisson's ratio (Figure 3.8(c)). When comparing the calculated and analytical Poisson's ratios (Figure 3.9), it can be seen the calculated values are very close to analytical values.

As seen above the direction of the boundary springs depends on the Poisson's ratio (Table 3.1). The variation of the orientation of the normal and tangential spring with varying Poisson's ratio can be seen below (Figure 3.10).

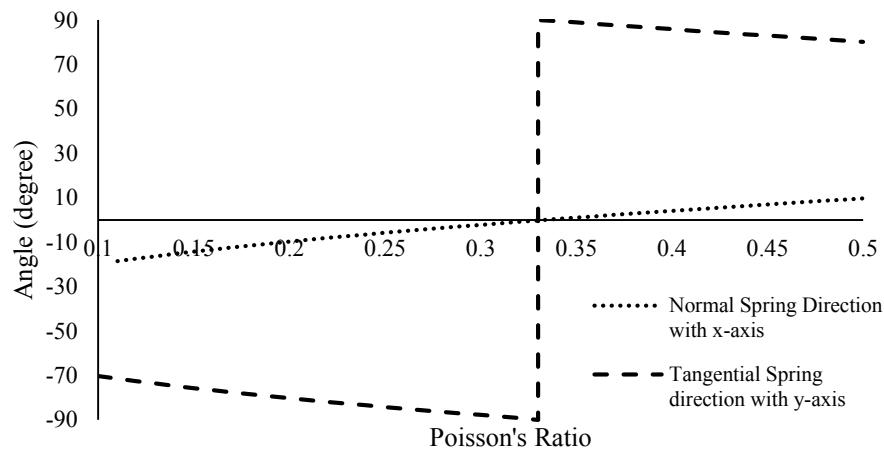


Figure 3.10– Effect on the orientation of springs with varying Poisson's ratio.

The Poisson's ratio decides whether the tangential spring is positive or not. When there are negative spring stiffness, necessary modifications need to be made while performing non-linear analysis. It can be observed that when Poisson's ratio is equal to $1/3$ the boundary springs are mutually orthogonal to each other.

3.2.2 Modal Analysis

The mass of each circular element in EDEM is similar to the lumping of mass at the nodes. In order to check this assumption and its effects on dynamic analysis, modal analysis of the spring network is performed. Shifted vector iteration scheme (Chopra 2007) is used to obtain the mode shapes and their corresponding circular natural frequencies.

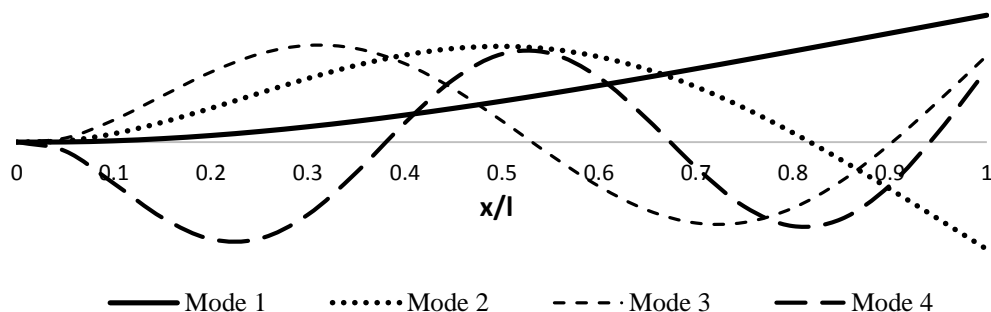


Figure 3.11– Mode shapes obtained from the spring network system

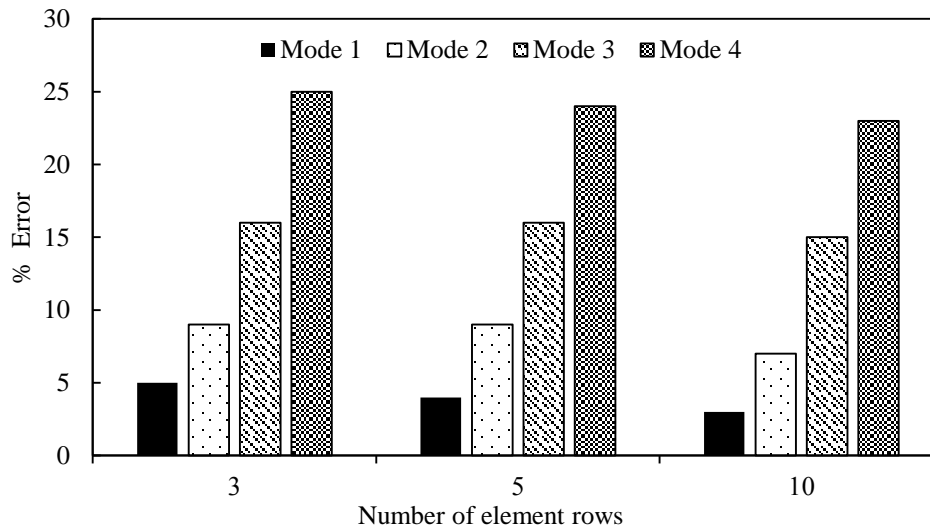


Figure 3.12– Errors in fundamental frequencies of different mode shapes

The values are verified with analytical values of un-damped cantilever beam vibration. The mode shapes obtained are similar to the analytical mode shapes (Figure 3.10). The error in fundamental frequency can be observed in Figure 3.11. It is observed the error reduces with the increase in number of rows of elements and it increases at higher modes. The increase in error can be attributed to the assumption of neglecting shear deformation in the analytical solution. The results obtained from the modal analysis verify the lumped mass assumption. Due to the lumping of mass, the global mass matrix is a diagonal matrix which makes its inversion during dynamic analysis, trivial. This helps in both implicit and explicit numerical time integrations, as it drastically reduces the computation time required.

3.3 Conclusion

The spring network which is derived from 2-D continuum elements, has only two translational degree of freedom at each node. This makes the system rotationally variant, because of the fictitious energy that is generated during rigid body rotation. As mentioned earlier there also exists negative springs (springs with negative stiffness), at a certain range of Poisson's ratio. Although, this has little effect in linear analysis, the presence of these negative springs during nonlinear analysis causes a global increase in stiffness, every time the spring stiffness is reduced due to loading. Proper modifications have to be incorporated to account for this change in global stiffness.

In conclusion, a spring network model is proposed, which has advantages such as:-

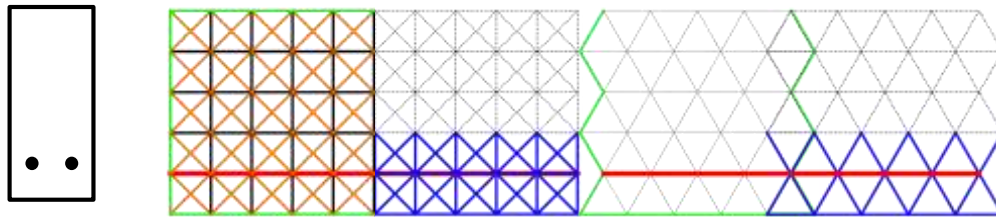
- Be used in tandem with circular discrete elements
- Has good accuracy in the elastic range
- Models Poisson's ratio
- Has a generalised spring stiffness derivation
- Has a diagonal mass matrix

Chapter 4 **Reinforced Concrete Analysis**

4.1 Spring Classification

For modelling the material models in the spring network, the springs are first classified based on their physical location and material location. As mentioned earlier, for the quadrilateral discretization there are three kinds of springs based on physical location, namely (i) boundary spring (ii) inner edge spring (iii) inner diagonal spring. And in the case of CST discretization, there are two kinds of spring, namely (i) inner spring and (ii) boundary spring. Based on the material location the springs are classified into (i) steel spring (ii) concrete spring in plain concrete zone (PC zone) and (iii) concrete spring in reinforced concrete zone (RC zone) (Figure 4.1). The springs that are connected to the nodes with reinforcing bars exhibit tension stiffening effect and these springs are assumed to be in the RC zone while the other springs are in the plain concrete zone (which exhibits tension softening). In the Quad spring network, steel springs are placed in parallel to concrete springs, at the location of the reinforcing bars. For the CST spring network, the steel springs connect the nodes that are present at the reinforcement bar location (not necessarily parallel to the concrete springs). Usually in RC frames, steel reinforcements are orthogonally arranged, hence it's convenient to define the steel springs in the Quad spring network.

Though inconvenient to discretize, the CST spring network is simpler to define and in the special case, when Poisson's ratio is assumed to be $1/3$, it greatly simplifies the spring network to 1-D springs (Table 3.2). For the non-linear analysis of RC structural members two kinds of discretization are used (i) Simplified CST spring network with 1-D springs using only concrete compression and tension model (ii) Quad spring network with 2-D springs which incorporates the concrete shear model also.



	Quad Spring Network	CST Spring Network
Based on location	<ul style="list-style-type: none"> • Inner diagonal • Inner edge • Boundary spring 	<ul style="list-style-type: none"> • Inner spring • Boundary spring
Based on material	<ul style="list-style-type: none"> • Steel • Concrete in PC Zone • Concrete in RC Zone 	

Figure 4.1– Classification of springs for RC modelling

4.2 Reinforced Concrete Material Models

A smeared crack approach for RC, consisting of spatially averaged constitutive models for concrete and reinforcing steel (Maekawa et al. 2003), is adopted for the springs. Finite element analysis with these material models have shown to accurately model the nonlinear response of RC. In finite element analysis, the nonlinearity is introduced through the nonlinear constitutive relations at the Gauss integration points. The failure (crack) criteria is based on the principal stresses, and once failed, the smeared crack is assumed to be oriented along the critical principal stress direction. At every load step, the strains are transformed along the cracking direction and the stresses are computed based on the cracking direction.

The spring network model is analogous to the fixed smeared crack approach with the active crack assumed to be propagating along the direction of the springs. The failure criteria is the stresses computed along the direction of the springs. This puts a restriction on the direction of the propagating smeared crack i.e. the crack is assumed to be propagating perpendicular to the cracked springs.

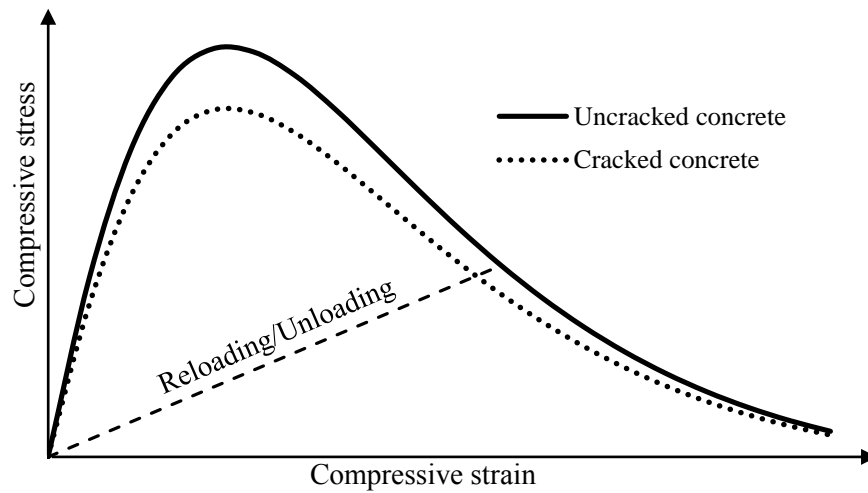


Figure 4.2– Concrete compression model

The current study involves the implementation of these models in a spring network system. As stress transformation are not possible, few modifications are made to the original models, including a Mohr-Coulomb failure criteria for the shear springs.

4.2.1 Concrete compression model

A compressive material model (Figure 4.2) based on the Elasto-Plasto Fracture (EPF) model (Okamura and Maekawa 1991) is used. The advantage of using these models is that they are based on uniaxial constitutive relations, using parameters which are obtained from simple experiments, for example the uniaxial compressive strength (f_c). Once cracking occurs, there is a reduction of compressive strength along the direction of the crack and it is dependent on the lateral tensile strain. The cracking of springs is initiated when the tensile springs reach the maximum tensile stress. Once a spring cracks, the compressive strength of all the springs connected to the nodes of the cracked spring are reduced based on their lateral strain (tangential spring strain). This can be visualized as a zone created around the cracked spring with reduced compressive material model (Figure 4.3).

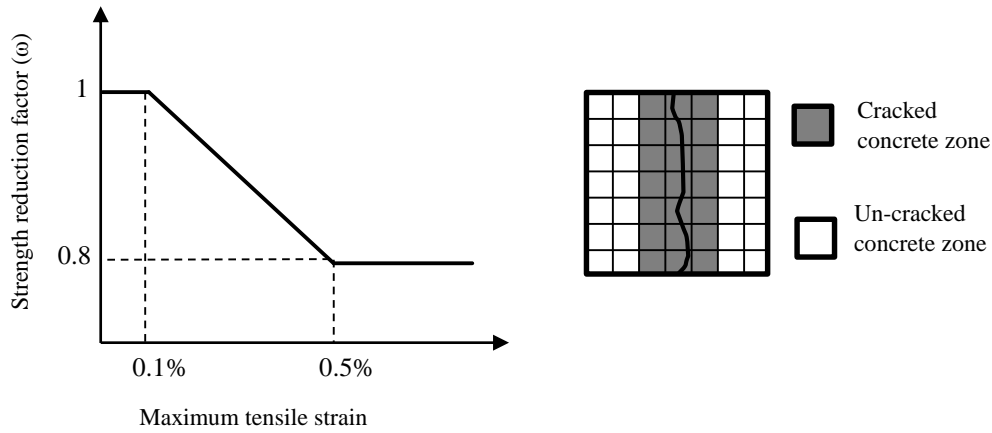


Figure 4.3– Reduction of compressive strength of springs present in cracked concrete zone

4.2.1.1 Equation of curve

(a) Loading condition $\varepsilon \geq \varepsilon_{c \max}$

$$\sigma_{cc} = \omega K_0 E_{c0} (\varepsilon - \varepsilon_p) \quad \text{.....(4.1)}$$

$$K_0 = \exp\left(-0.73 \frac{\varepsilon}{\varepsilon_c} \left(1 - \exp\left(-1.25 \frac{\varepsilon}{\varepsilon_c}\right)\right)\right) \quad \text{.....(4.2)}$$

$$\varepsilon_p = \beta \left(\frac{\varepsilon}{\varepsilon_c} - \frac{20}{7} \left(1 - \exp\left(-0.35 \frac{\varepsilon}{\varepsilon_c}\right)\right) \right) \varepsilon_c \quad \text{.....(4.3)}$$

$$E_{c0} = E_0 \frac{f_c}{\varepsilon_c} \quad \text{.....(4.4)}$$

(b) Unloading/ Reloading condition $\varepsilon < \varepsilon_{c \max}$

$$\sigma_{cc} = \left(\frac{\sigma_{c \max}}{\varepsilon_{c \max}} \right) \varepsilon \quad \text{.....(4.5)}$$

where,

ε	: current input strain (-ve)	σ_{cc}	: compressive stress
$\varepsilon_{c \max}$: maximum compressive strain	$\sigma_{c \max}$: maximum compressive strain
ε_p	: plastic strain	f_c	: compressive strength (MPa)
ε_c	: strain at f_c	K_0	: fracture parameter
ω	: strength reduction factor	E_0	: 2
β	: strain rate factor = 1 (for dynamic) = 2 (for static)		

4.2.2 Concrete Tension model

The elastic modulus of the tension model before cracking reduces based on the fracture parameter (K_0). Cracking criteria is a function of the tensile strength (f_t) and K_0 . Post cracking the tensile spring exhibits softening and the slope of the softening curve depends on the element size, and also, the concrete zone it exists. The parameter c varies the slope of the softening curve. For concrete springs in RC zone, the value of c remains constant regardless of the size of the element. In the RC zone, the slope of the softening curve is small, which represents the tension stiffening effect of the concrete in the vicinity of the reinforcement. For concrete springs in PC zone the value of c varied depending on the size of the element, in order to maintain a constant fracture energy released per unit area.

4.2.2.1 Equation of curve

(a) Failure criteria

$$f_{tt} = K_0^3 f_t \quad \text{.....(4.6)}$$

$$\varepsilon_t = \frac{f_{tt}}{K_0 E_{c0}} \quad \text{.....(4.7)}$$

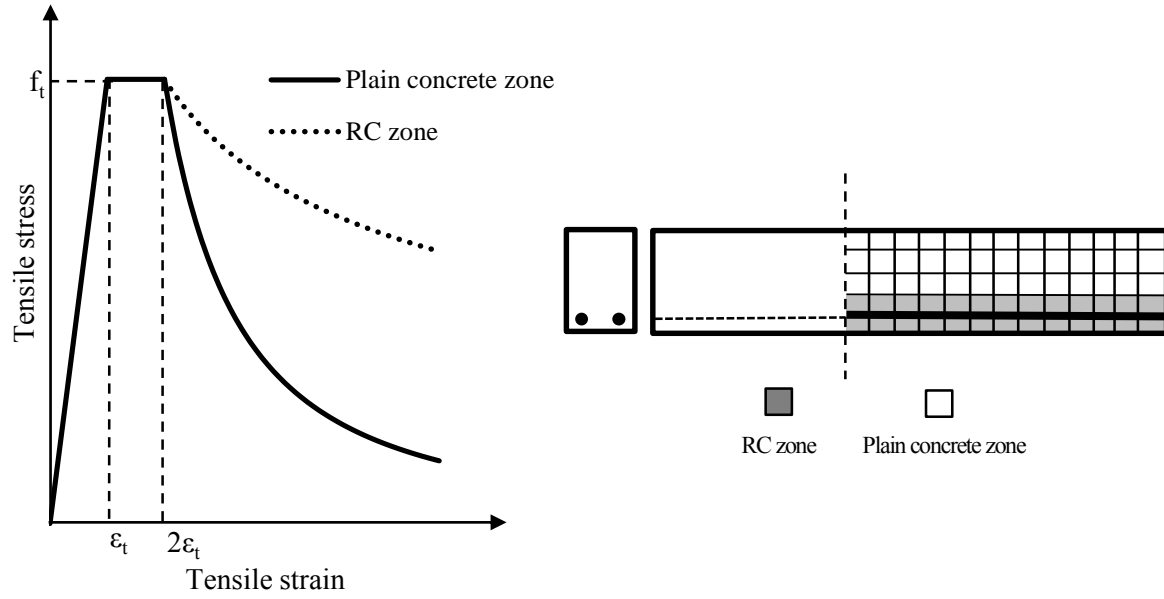


Figure 4.4– Concrete tension model and zonation of springs

(b) Loading condition $\varepsilon \leq \varepsilon_{t \max}$

(i) $\varepsilon \leq \varepsilon_t$

$$\sigma_{cb} = K_0 \varepsilon \quad \dots\dots(4.8)$$

(ii) $\varepsilon > \varepsilon_t$ and $\varepsilon \leq 2\varepsilon_t$

$$\sigma_{cb} = f_{tt} \quad \dots\dots(4.9)$$

(iii) $\varepsilon > 2\varepsilon_t$

$$\sigma_{cb} = f_{tt} \left(\frac{2\varepsilon_t}{\varepsilon} \right)^c \quad \dots\dots(4.10)$$

(c) Unloading/ Reloading condition $\varepsilon > \varepsilon_{t \max}$

$$\sigma_{cb} = \left(\frac{\sigma_{t \max}}{\varepsilon_{t \max}} \right) \varepsilon \quad \dots\dots(4.11)$$

where,

σ_{cb} : tensile stress	ε : current input strain (+ve)
f_t : tensile strength of concrete (MPa)	f_{tt} : failure stress
ε_t : failure strain	c : stiffening/softening parameter
$\varepsilon_{t \max}$: maximum tensile strain	$\sigma_{t \max}$: maximum tensile strain

4.2.3 Concrete Shear model

In the case of FEM analysis, the transformation of stress are possible, therefore an explicit shear failure criteria and a pre-cracking shear model are not required. In the case of the spring network, stress transformation is not straightforward, and tensile failure is checked only along the orientation of the springs. In the case of quadrilateral elements, tensile failure is checked along three directions (horizontal, vertical and diagonal directions), which might lead to mesh orientation bias. This problem can be solved using a randomly generated mesh or by increasing the mesh density.

To simplify the shear behaviour, a linear shear model is assumed up to a failure criteria which is governed by the Mohr-Coulomb failure model. Post failure, a softening relationship exactly similar to the tension model is assumed. The Mohr-Coulomb parameters which were previously used for discrete RC analysis is used (Kawai et al. 1986) . The initiation of the shear softening depends on whether the spring is present in RC zone or PC zone.

Once a springs fails in tension, the shear stress transferred is calculated based on the contact density idealization (Xuehui et al. 1998), which gives the shear stress as a function of the shear strain and lateral tensile strain. Shear strain is the tangential spring strain and lateral tensile strain is the normal spring strain.

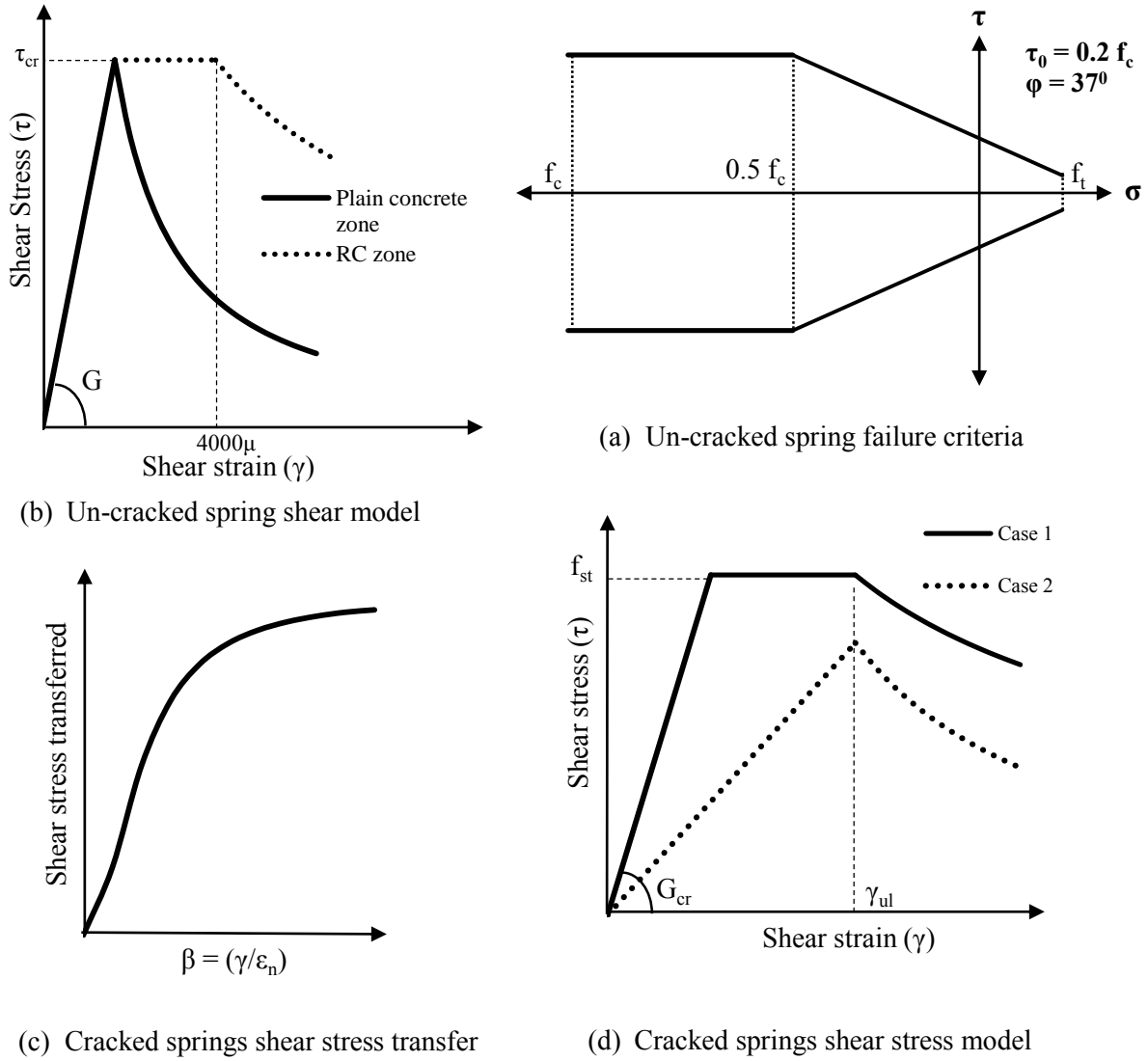


Figure 4.5– Concrete shear model

4.2.3.1 Equation of curve

(a) For un-cracked shear spring (normal spring yet to fail in tension)

i. $\gamma \leq \tau_{cr} G$

$$\tau = G \gamma \quad \text{.....(4.12)}$$

ii. $\gamma > \tau_{cr} G$ and spring in plain concrete zone

$$\tau = \tau_{cr} \left(\frac{\tau_{cr} G}{\gamma} \right)^c \quad \text{.....(4.13)}$$

- iii. $\gamma > \tau_{cr} G$ and $\gamma \leq \gamma_{ul}$ and spring in RC zone

$$\tau = \tau_{cr} \quad \text{.....(4.14)}$$

- iv. $\gamma > \gamma_{ul}$ and spring in RC zone

$$\tau = \tau_{cr} \left(\frac{\gamma_{ul}}{\gamma} \right)^c \quad \text{.....(4.15)}$$

(b) Shear failure criteria

- i. Normal spring in compression ($\sigma_{cc} < 0$)

$$\tau_{cr} = \tau_0 - \sigma_{cc} \tan \phi \quad \text{.....(4.16)}$$

- ii. Normal spring in tension ($\sigma_{cb} > 0$)

$$\tau_{cr} = \tau_0 - \sigma_{cb} \tan \phi \quad \text{.....(4.17)}$$

(c) For cracked shear spring (normal spring failed in tension)

- i. Shear stress transferred through cracks

$$\tau_{st} = f_{st} \frac{\beta^2}{1 + \beta^2} \quad \text{.....(4.18)}$$

$$\beta = \frac{\gamma}{\varepsilon_n} \quad \text{.....(4.19)}$$

$$f_{st} = 3.8 f_c^{1/3} \text{ (MPa)} \quad \text{.....(4.20)}$$

- ii. Shear modulus across cracked springs

$$G_{st} = \frac{\tau_{st}}{\gamma} \quad \text{.....(4.21)}$$

$$G_{cr} = \left(\frac{1}{G_{st}} + \frac{1}{G} \right)^{-1} \quad \text{.....(4.22)}$$

$$\text{iii.} \quad \gamma \leq \gamma_{ul} \text{ and } \gamma < \frac{G_{cr}}{f_{st}}$$

$$\tau = G_{cr} \gamma \quad \text{.....(4.12)}$$

$$\text{iv.} \quad G_{cr} \gamma > f_{st} \text{ and } \gamma \leq \gamma_{ul} \text{ (Case 1)}$$

$$\tau = f_{st} \quad \dots\dots(4.14)$$

$$\text{v. } G_{cr} \gamma > f_{st} \text{ and } \gamma > \gamma_{ul} \text{ (Case 1)}$$

$$\tau = f_{st} \left(\frac{\gamma_{ul}}{\gamma} \right)^c \dots\dots(4.15)$$

$$\text{vi.} \quad G_{cr} \gamma < f_{st} \text{ and } \gamma > \gamma_{ul} \text{ (Case 2)}$$

$$\tau = \left(\frac{G_{cr}}{\gamma_{ul}} \right) \left(\frac{\gamma_{ul}}{\gamma} \right)^c \dots\dots(4.17)$$

γ	: current shear strain	τ	: corresponding shear strain
τ_{cr}	: failure stress by Mohr-Coulomb	f_{st}	: shear transfer strength
τ_0 & φ	: Mohr-Coulomb parameters	ϵ_n	: normal strain
G_{st}	: shear transfer modulus		
G	: shear modulus of uncracked concrete = $E / 2(1+\nu)$		
γ_{ul}	: ultimate shear strain = 4000μ (RC zone) = 400μ (PC zone)		

A simple bi-linear stress-strain model (Figure 4.6) is used to model the reinforcement. A very small modulus of elasticity (1/100) is assumed after yield. Currently, the shear resistance of reinforcement bars (dowel action) and the bond-slip of reinforcement bars are not considered.

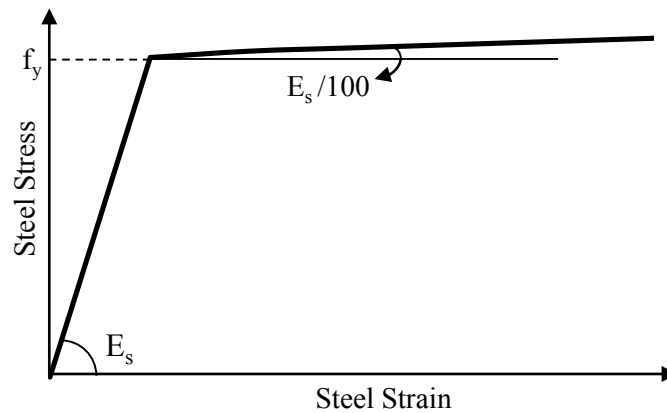


Figure 4.6– Steel material model

4.3 Iterative Secant Stiffness Formulation

An iterative secant stiffness based formulation is used for computation, as it is numerically stable while handling complex material models (Vecchio 1989) and post peak response of structures. At every iterative step, secant modulus value of the total stress-strain relationship of the springs are updated till convergence. The flow of the program can be found below (Figure 4.7). It was observed that good convergence was obtained in around 20 iterations. One of the advantages of this method is that good accuracy can be obtained even with the use of relative simple finite elements.

4.3.1 Simple cube compression

To check the applicability of the formulation a simple concrete cube (300 mm x 300 mm x 300 mm) subjected to compression is modelled and the analysis results is compared to compression equation given by JSCE (Japan Society of Civil Engineers 2007). The results (Figure 4.8) shows the capability of the model to follow the nonlinear behaviour of concrete up till the peak load.

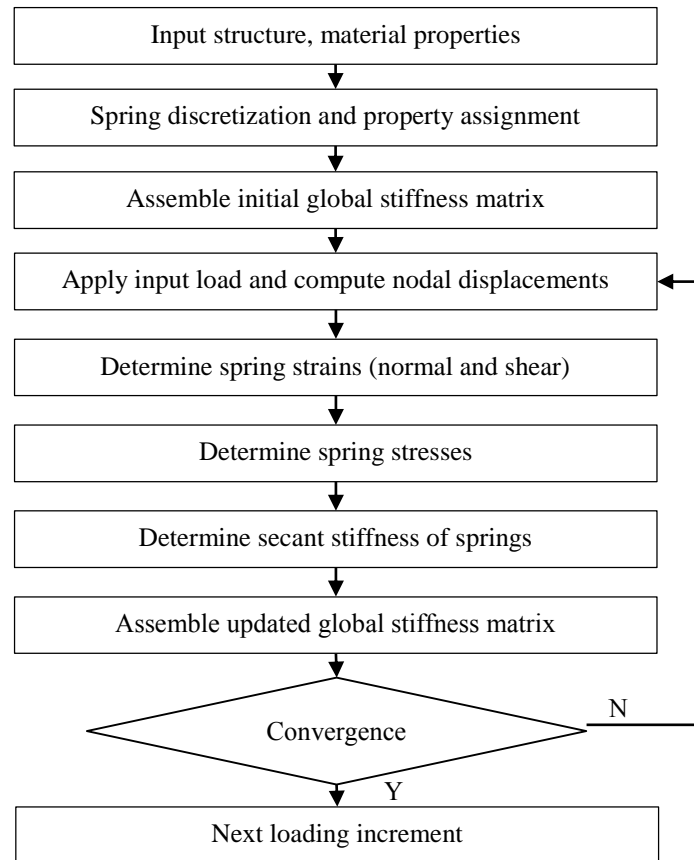


Figure 4.7– Flow Chart of the analysis procedure

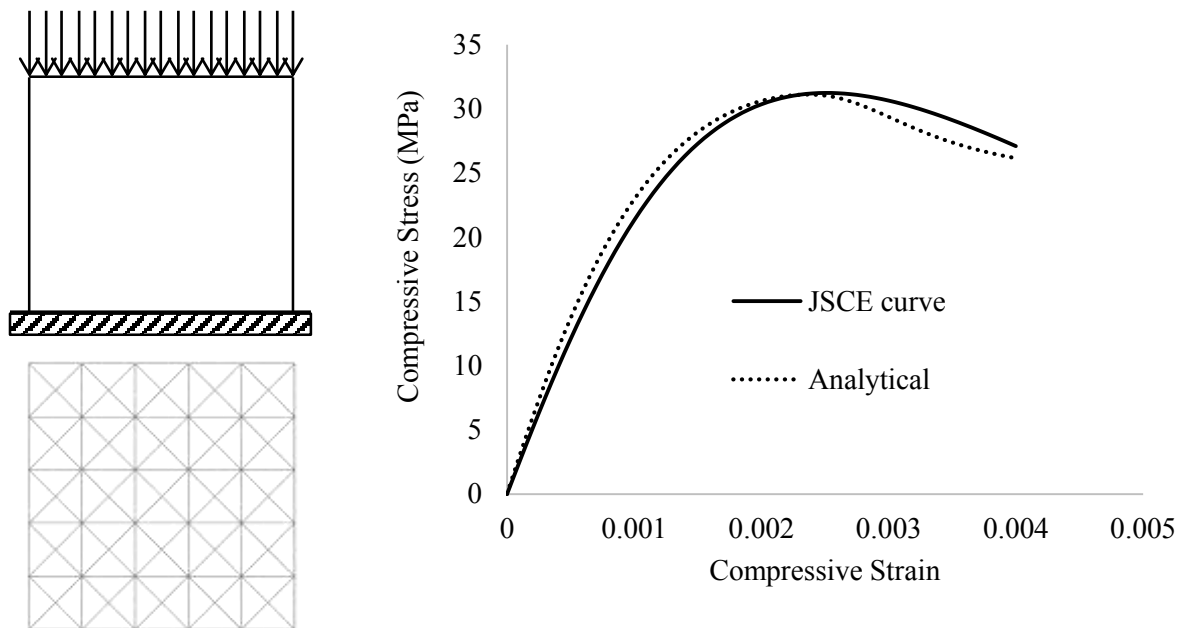


Figure 4.8– Concrete cube compression

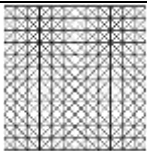
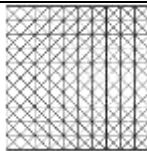
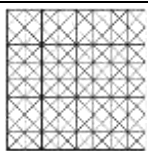
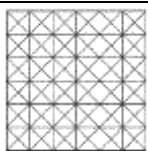
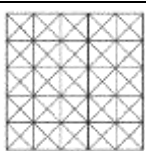
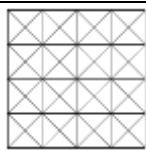
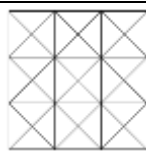
4.3.2 Mesh objectivity of results

Spring networks are known to suffer from mesh dependency. The results obtained from the spring networks are dependent on the mesh orientation and the mesh density. The dependency on the mesh orientation can be solved by having a random orientation of mesh. The dependency on to the density of mesh can be heuristically solved by ensuring that the fracture energy release per unit area remains constant. This fracture energy is obtained by computing the area under the stress vs crack width curve of the material. Based on the Crack Band Theory (Bazant and Oh 1983), the constant fracture energy release is achieved by appropriately reducing the softening curve of the tension model. By this theory, it is assumed that cracking is represented as a propagating blunt crack, whose fracture process zone is approximately equal to the width of the element. This poses a limit on the element size that can be used. The limitation is from around $3d_{agg}$ to $15 d_{agg}$, where d_{agg} is the maximum aggregate size. The fracture energy is related to the stress strain diagram by

$$\int \sigma_t d\varepsilon_t = \frac{G_f}{l_r} \quad \text{.....(4.11)}$$

Where, G_f is the fracture energy and is a constant value for concrete and l_r is the length of the element. In the current model, the softening curve slope is varied by varying the parameter c (Mackawa et al. 2003).

Table 4.1 – Various element mesh densities and corresponding values of parameter “ c ”

Size (mm)	100	120	150	200	240	300	400
Elements	13x13	11x11	9x9	7x7	6x6	5x5	4x4
c	0.7719	1.0079	1.3619	1.9519	2.4239	3.1319	4.3119
Image							

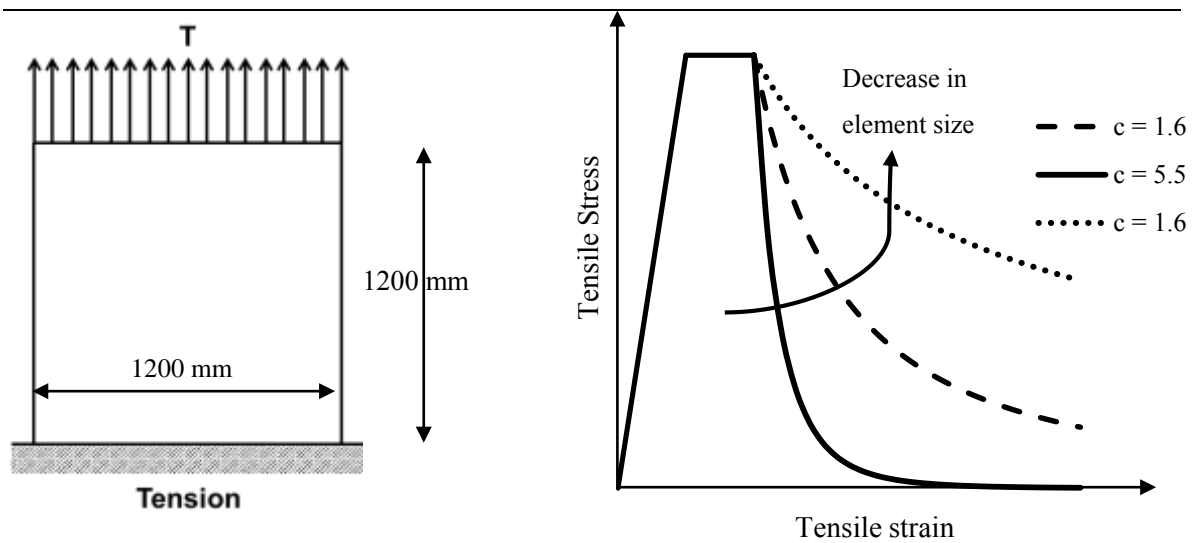
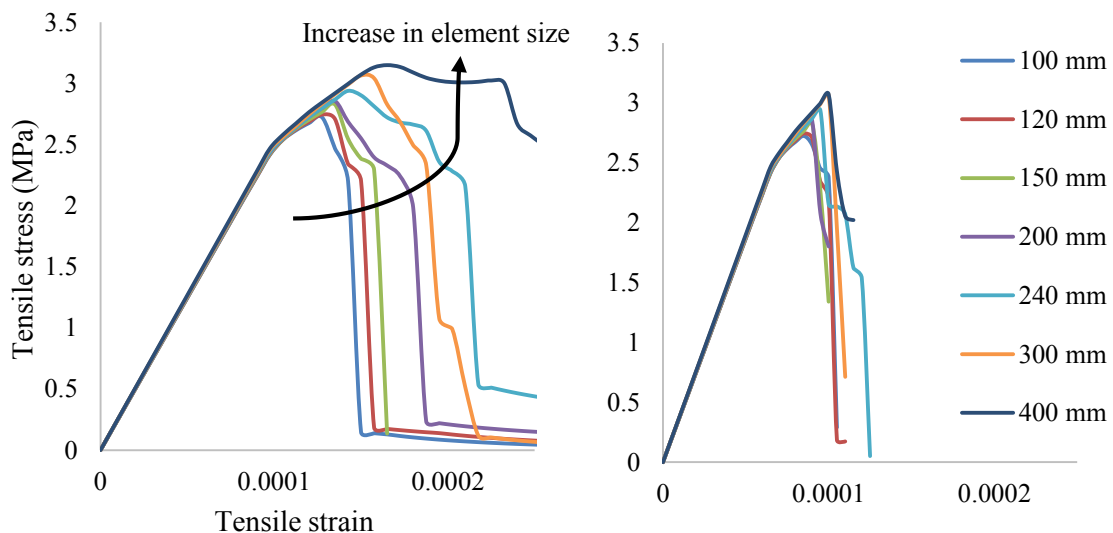


Figure 4.9– Concrete cube tension loading and size dependant tension model

To check the validity of the model, a simple concrete cube of dimension 1200mm x 1200mm x 1200mm is subjected to tensile loading. The cube mesh size is varied as given in Table 4.1. When the value of c is kept constant, the mesh sensitivity can be observed (Figure 4.10 (a)). When the value of c is varied according to the element size, similar results were observed for varying element sizes (Figure 4.10 (b)). The results show that the loss in mesh density dependency through the variation in tension softening model.



(a) Constant value of c

(b) c value modified based on element size

Figure 4.10– Mesh size sensitivity

4.4 Experimental validation

To check the validity of the spring network, numerical simulation of experimental testing of various structural elements are performed. The validity of the simple CST spring network to model simple RC beam and RC frame are checked. To check the capability of the specimens to model shear dominated RC members, the Quad spring network with shear models are used to validate a series of experimentally testes RC shear panels.

4.4.1 RC Beam

A series of testing was performed on 12 beam specimens with varying length, breadth and reinforcing ratio (Bresler and Scordelis 1963). The actual dimension of the beams used for experimentation can be found below (Table 4.2). The length and breadth of the specimens were varied accordingly in order to induce various kinds of damage modes.

Table 4.2 – Dimensions of the experimented beam

Beam	Breadth 'b' (mm)	Height 'h' (mm)	Depth 'd' (mm)	Length 'L' (mm)	Span Length 'l' (mm)
OA1	310	556	461	4100	3660
OA2	305	561	466	5010	4570
OA3	307	556	462	6840	6400
A1	307	561	466	4100	3660
A2	305	559	464	5010	4570
A3	307	561	466	6840	6400
B1	231	556	461	4100	3660
B2	229	561	466	5010	4570
B3	229	556	461	6840	6400
C1	155	559	464	4100	3660
C2	152	559	464	5010	4570
C3	155	554	459	6840	6400

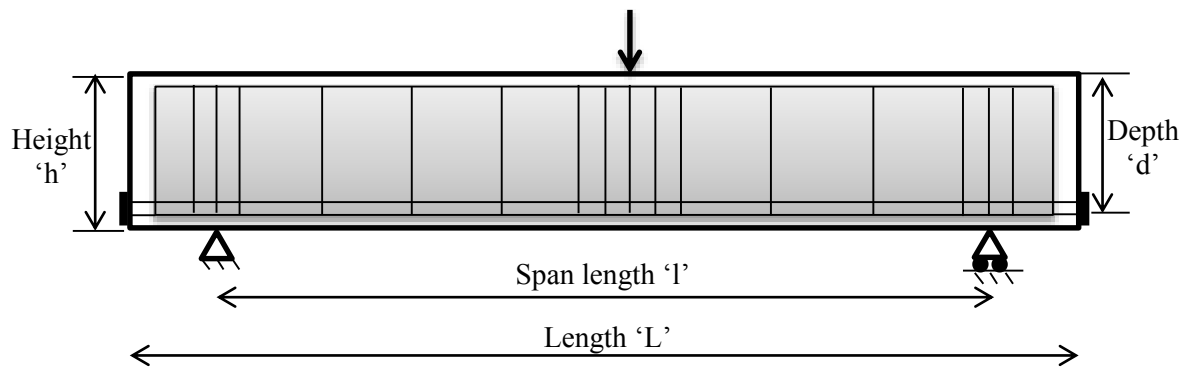


Figure 4.11– Experimental setup: Various dimensions, loading and boundary condition

Table 4.3 – Dimensions of the beams used in numerical analysis

Analysis Beam no.	Spring length (mm) “2r”	Depth d (mm)	Length L (mm)	Span (mm)	Reinforcement			Concrete properties	
					#9 bar	#4 bar	#2 bar Spacing (mm)	f_c (MPa)	f_t (MPa)
OA1_1	110	$6\sqrt{3} r$	76 r	68 r	4	-	-	22.6	1.75
OA2_1	110	$6\sqrt{3} r$	92 r	84 r	5	-	-	23.7	2
OA3_1	110	$6\sqrt{3} r$	126 r	118 r	6	-	-	37.6	2
A1_1	110	$6\sqrt{3} r$	76 r	68 r	4	2	210	24.1	2.5
A2_1	110	$6\sqrt{3} r$	92 r	84 r	5	2	210	24.3	2.5
A3_1	110	$6\sqrt{3} r$	126 r	118 r	6	2	210	35.1	2.5
B1_1	110	$6\sqrt{3} r$	76 r	68 r	4	2	190	24.8	3
B2_1	110	$6\sqrt{3} r$	92 r	84 r	4	2	190	23.2	3
B3_1	110	$6\sqrt{3} r$	126 r	118 r	5	2	190	38.8	3
C1_1	110	$6\sqrt{3} r$	76 r	68 r	2	2	210	29.6	3
C2_1	110	$6\sqrt{3} r$	92 r	84 r	4	2	210	23.8	4.5
C3_1	110	$6\sqrt{3} r$	126 r	118 r	4	2	210	35.1	4

The dimensions used for numerical analysis varies slightly due to the triangular shape of discretization used. The dimensions had to be multiples of the spring length, which corresponds to the element diameter in the EDEM phase. The steel reinforcement provided in the beams are also varied (Figure 4.12). There were three kinds of reinforcement used for the two longitudinal and transverse arrangement of reinforcement respectively (Table 4.4).

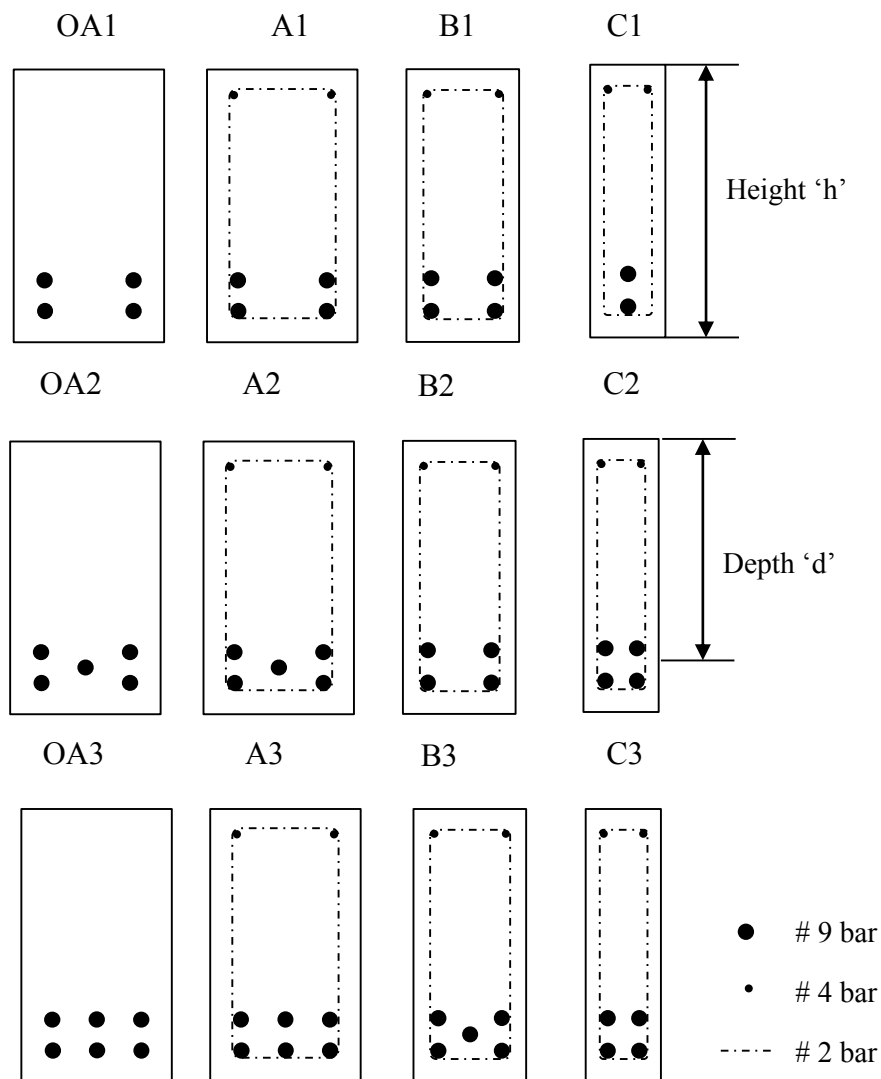


Figure 4.12– Cross sectional details of the beams

Table 4.4 – Reinforcement bar details

Bar no.	Diameter (mm)	Area (mm ²)	f_y (MPa)	f_u (MPa)	E_s (MPa)
# 9 bar	6.4	32.2	325	430	190,000
# 4 bar	12.7	127	345	542	201,000
# 2 bar	28.7	645	555	933	218,000

The spring network discretization of the beams can be seen below (Figure 4.13). In the case of transverse reinforcement, the steel springs are not parallel to the concrete springs. The steel springs are provided at the appropriate steel nodes and the steel stiffness is appropriately added to the global stiffness matrix.

4.4.1.1 Results and Discussion

The specimen is subjected to central loading and the mid span deflection is measured. The load-deflection curves obtained during experimentation are compared with the results obtained through numerical analysis (Figure 4.14 and Figure 4.15). Good agreement was observed in most specimens between the experimental and analysis data.

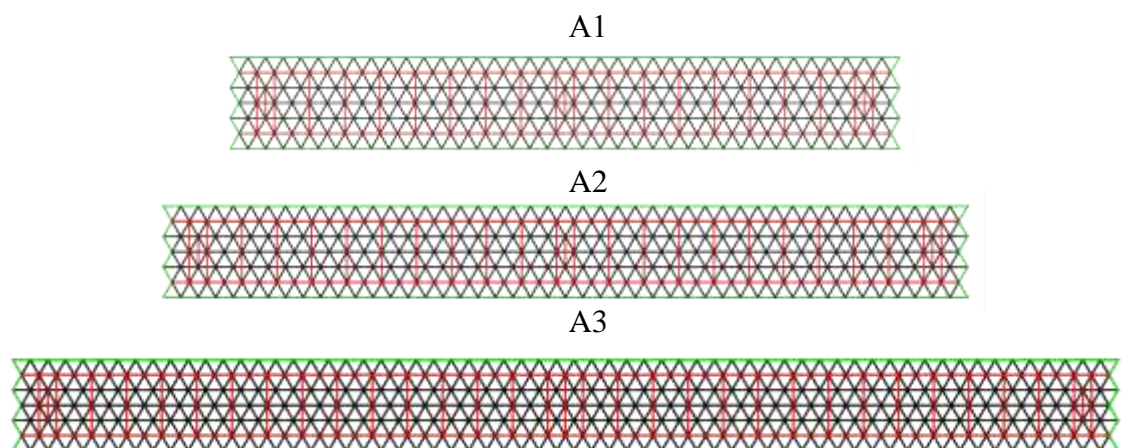


Figure 4.13– Spring network model of the beams

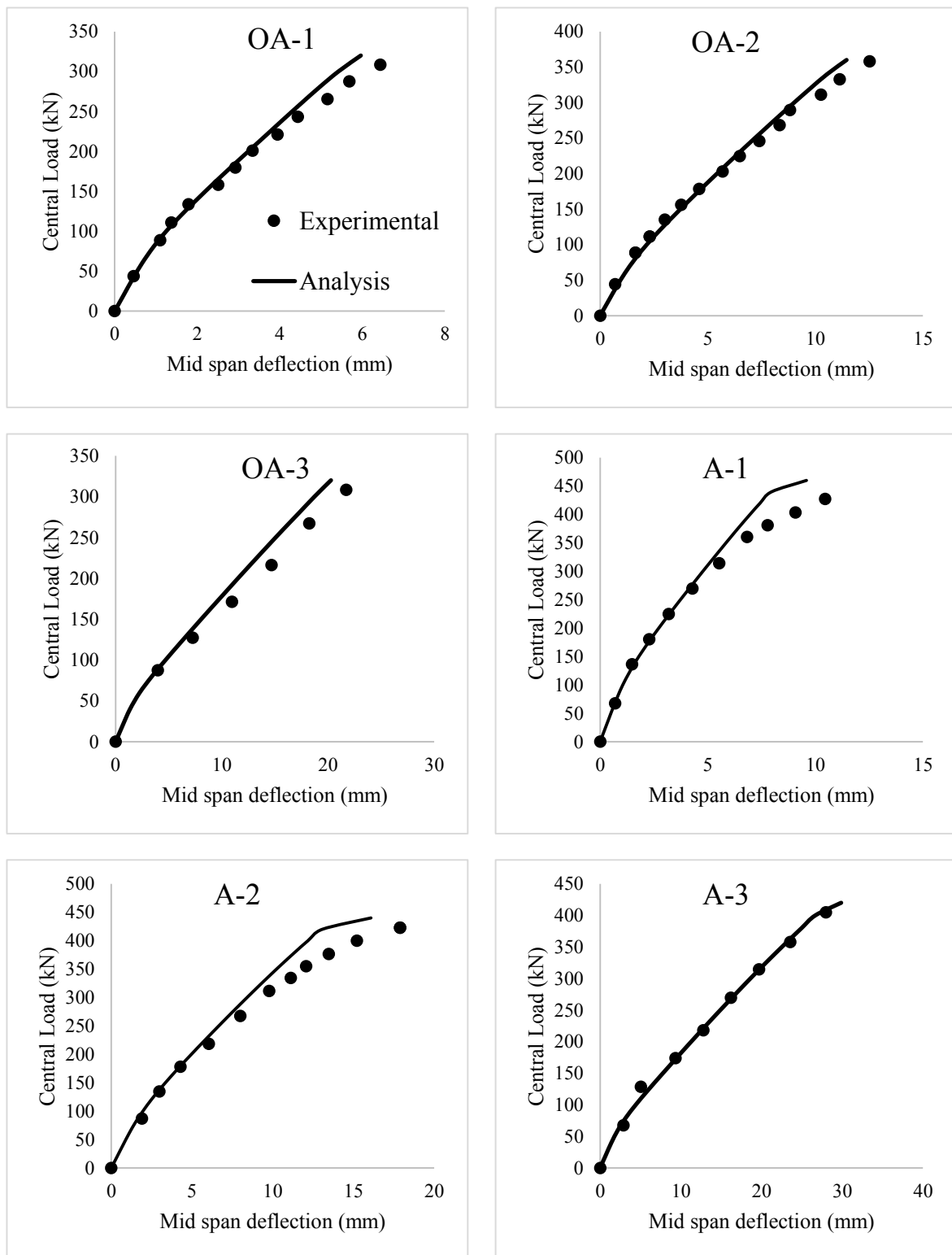


Figure 4.14– Force-deformation relationship of the beams-I

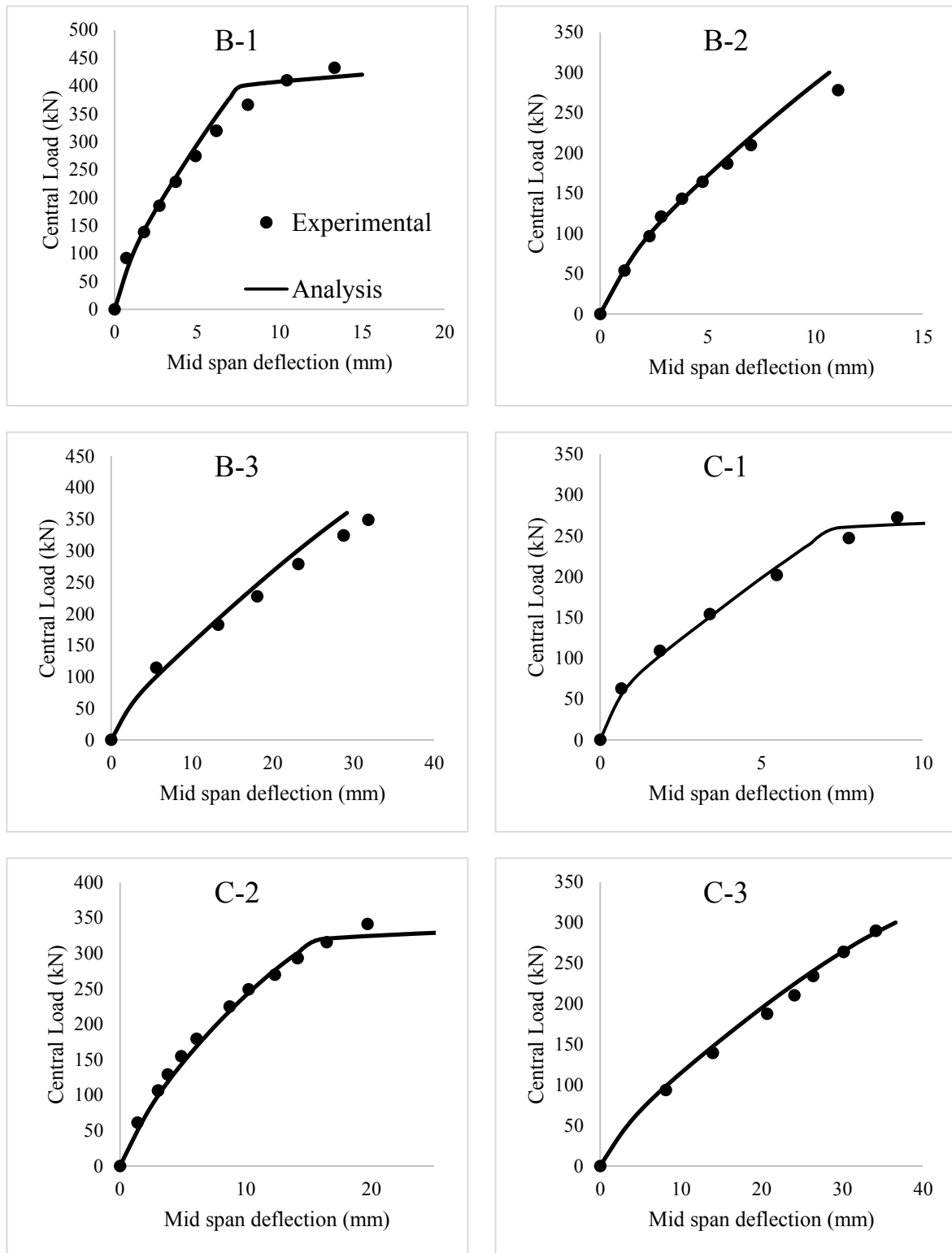


Figure 4.15– Force-deformation relationship of the beams-II

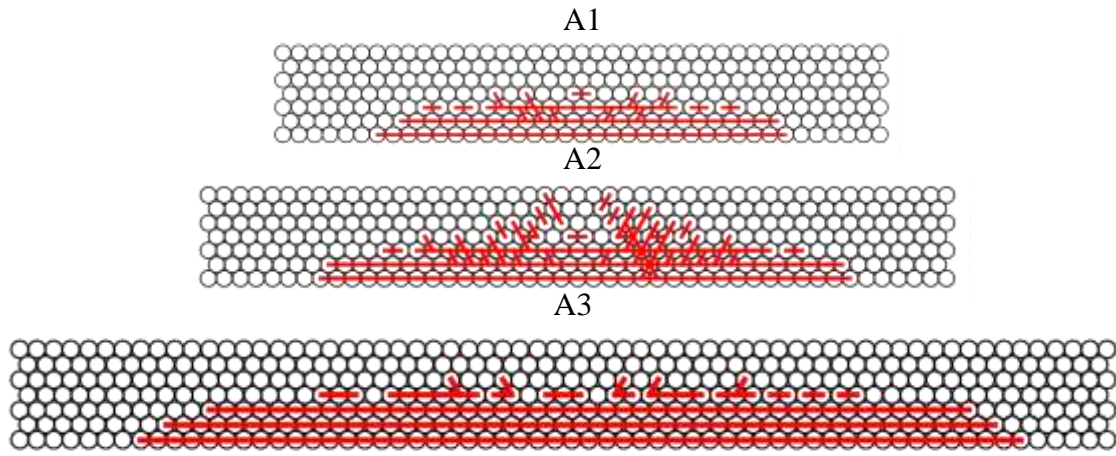


Figure 4.16– Cracked spring pattern obtained during analysis

The experimentally obtained values of concrete compressive strength (f_c) and steel material properties were used for the analysis. The crack springs obtained from the analysis (Figure 4.16) correspond to the crack pattern obtained from experimentation. The concrete tensile strength (f_t) which was not provided, was approximately assumed to be equal to $0.2f_c^{2/3}$ (MPa) (Okamura and Maekawa 1991). In specimens with a low depth-to-span (d/l) ratio, where shear behaviour is more significant, the tensile concrete strength was lesser due to the prominence of shear failure. The comparison of results show the capability of the CST spring network to predict the non-linear behaviour of RC beams using simple 1D material models. The Figure 4.16 shows not only the failed springs, but also the corresponding circular elements, which will be used during the EDEM phase.

4.4.2 RC Frame

The results obtained from the lateral loading experimentation on a RC frame (Muto 1965) are used to check the capability of the spring network. The details of the frame are given below. (Figure 4.17). The material properties are as follows:-

- Concrete compressive strength $f_c = 18$ MPa
- Steel Yield Strength $f_y = 450$ MPa
- Concrete tensile strength $f_t = 1.5$ Mpa

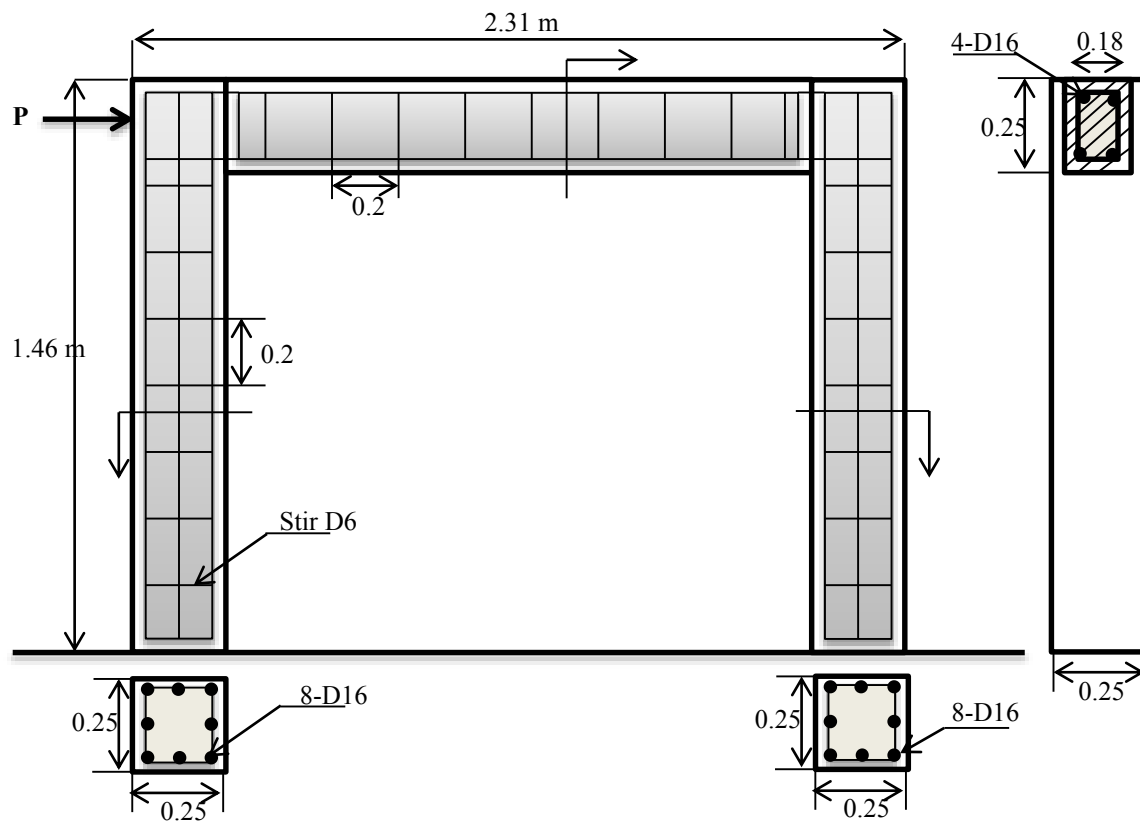


Figure 4.17– RC frame details

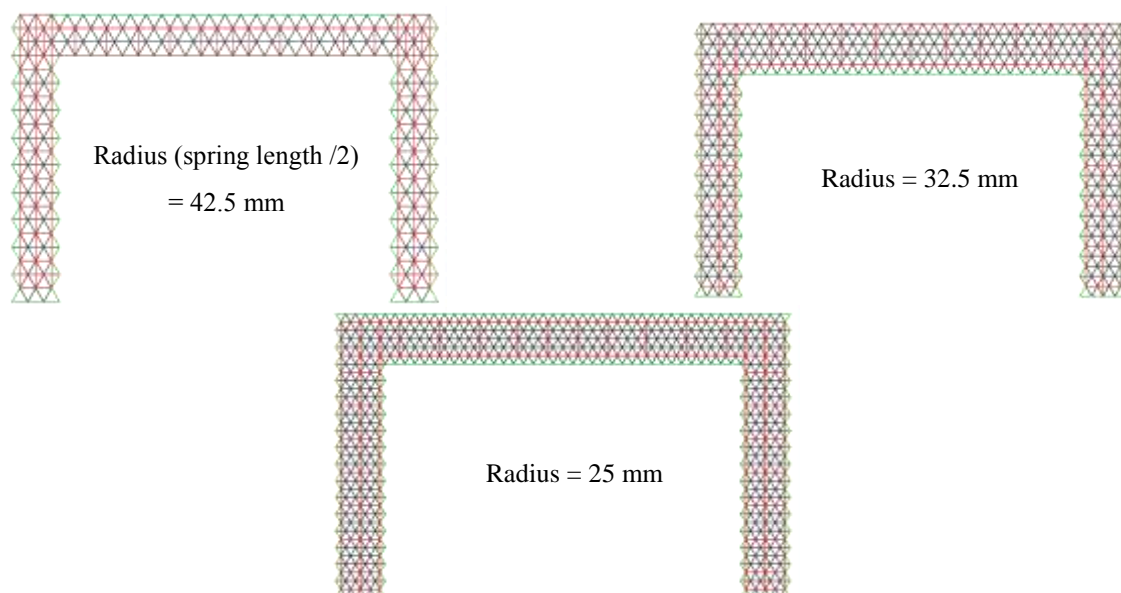


Figure 4.18– Three kinds of spring network discretization used for spring network analysis

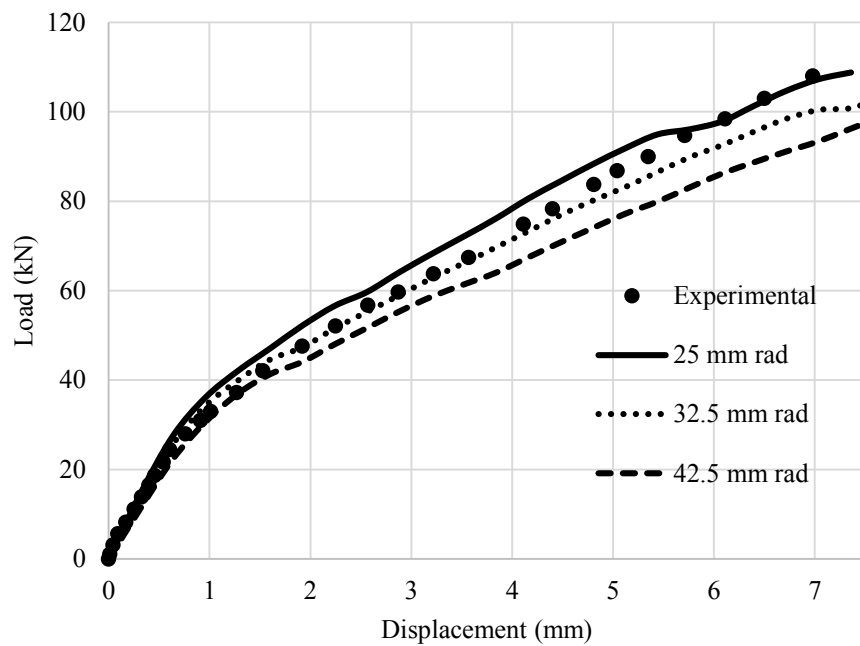


Figure 4.19– Load- Displacement curve comparison between experimental and analysis

The analysis is performed with three kinds of discretization with varying element sizes radius viz. 25 mm, 32.5 mm and 42.5 mm (Figure 4.18). The lateral load-displacement curve obtained through numerical analysis can be seen above.

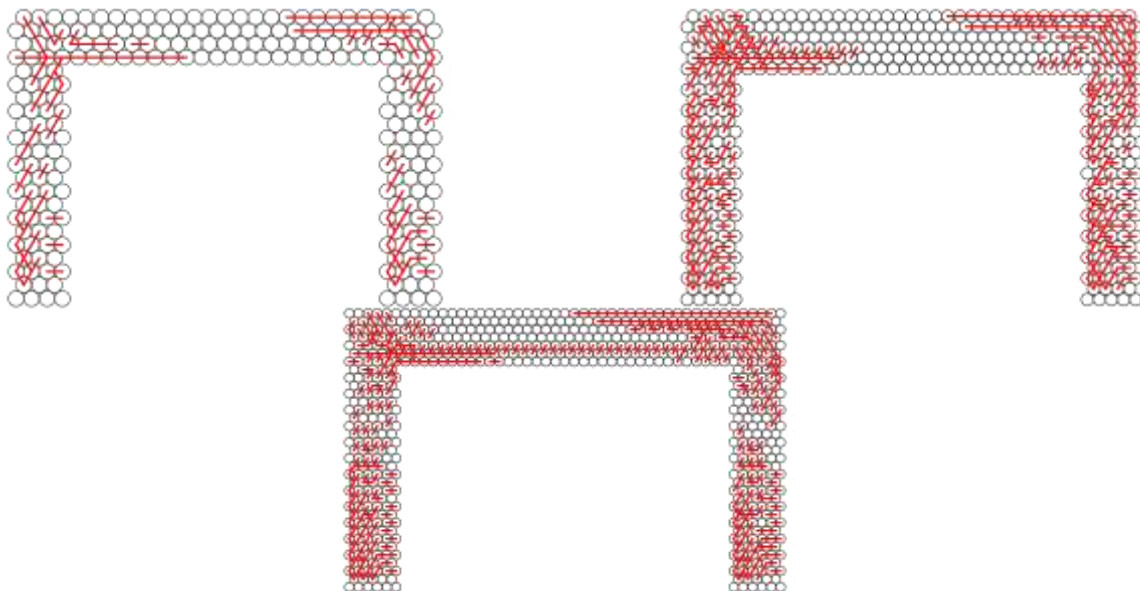


Figure 4.20– Cracked springs pattern observed

When the element size increases, there is an issue with the definition of nodes for the steel reinforcement. There are some approximations made in the reinforcement arrangement. And also in some cases, the size of concrete volume in compression reduces due to the approximation of dimensions. The variation of the results can be observed with increased stiffness when the element size reduces, because of the better consideration on concrete in compression and the reinforcement spacing. Good results were obtained when the element size was kept small. Even while using of larger elements (85mm dia), fairly good results were obtained. The results show the capability of the simplified spring network to predict the nonlinear behaviour of a RC frame.

4.4.3 Concrete Shear Panel

The nonlinear analysis performed up till now used only compression and tension model for concrete. As seen before, in cases where shear is dominant, the failure behaviour is not accurately captured. To check the applicability of modelling shear, the shear model (Section 4.2.3) is incorporated in to Quad spring network. The PV series of experiments on RC panels (Vecchio and Collins 1982), are modelled to check the material models under monotonic shear loading conditions.

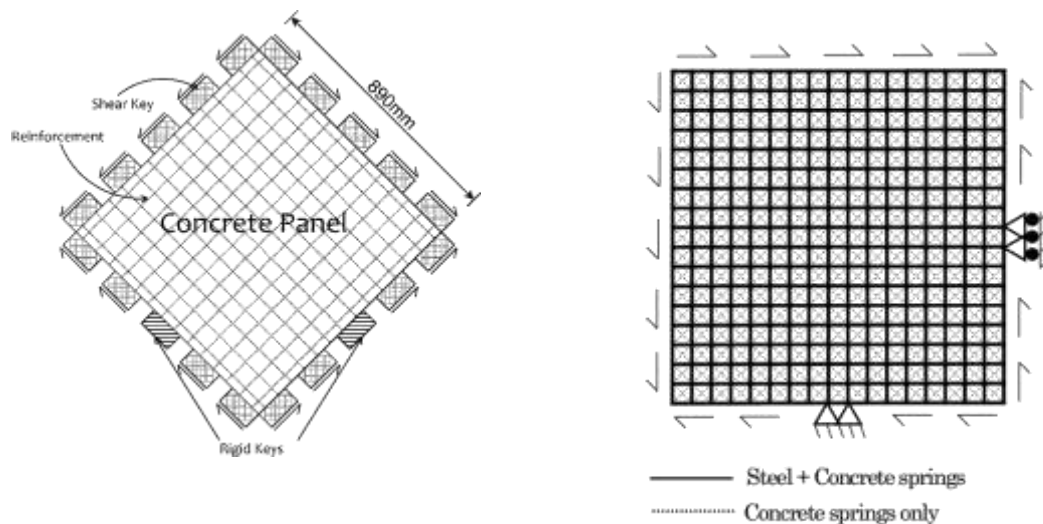


Figure 4.21– Concrete Panel: Experimental setup and its spring network model

The series of experiments consists of tests conducted on 30 RC panels (890mm x 890mm x 70mm) with varying loading conditions, reinforcement ratios and failure patterns. 12 RC panels with the properties given below (Table 4.5) were analysed using the given model and the results were compared with experimental data. In order to model the experiments, a spring network as shown above (Figure 4.21) is used. The constant shear stress is applied through forces applied at the boundary nodes. Average shear strain is obtained by taking the average of the strain on the left edge and the right edge of the concrete panel. The results obtained from the analysis are given below.

Table 4.5 – Properties of the Concrete panels

Panel	Loading ratio	Longitudinal steel		Transverse Steel		Concrete		
		ρ_x	f_y	ρ_y	f_y	ϵ_c	f_c	f_t
PV3	1:0:0	0.0048	662	0.0048	662	0.0023	26.6	1.7
PV4	1:0:0	0.0106	242	0.0106	242	0.0025	26.6	1.9
PV10	1:0:0	0.0179	276	0.01	276	0.0027	14.5	1.3
PV11	1:0:0	0.0179	235	0.0131	235	0.0026	15.6	1.4
PV16	1:0:0	0.0074	255	0.0074	255	0.0020	21.7	1.8
PV19	1:0:0	0.0179	458	0.0071	299	0.0022	19	1.9
PV20	1:0:0	0.0179	460	0.0089	297	0.0018	19.6	2.0
PV21	1:0:0	0.0179	458	0.0130	302	0.0018	19.5	2.2
PV22	1:0:0	0.0179	458	0.0152	420	0.0020	19.6	2.3
PV23	1: -.39: -.39	0.0179	518	0.0179	518	0.002	20.5	2.3
PV27	1:0:0	0.0179	442	0.0179	442	0.0019	20.5	2.9
PV28	1: .32: .32	0.0179	483	0.0179	483	0.0019	19	2.4

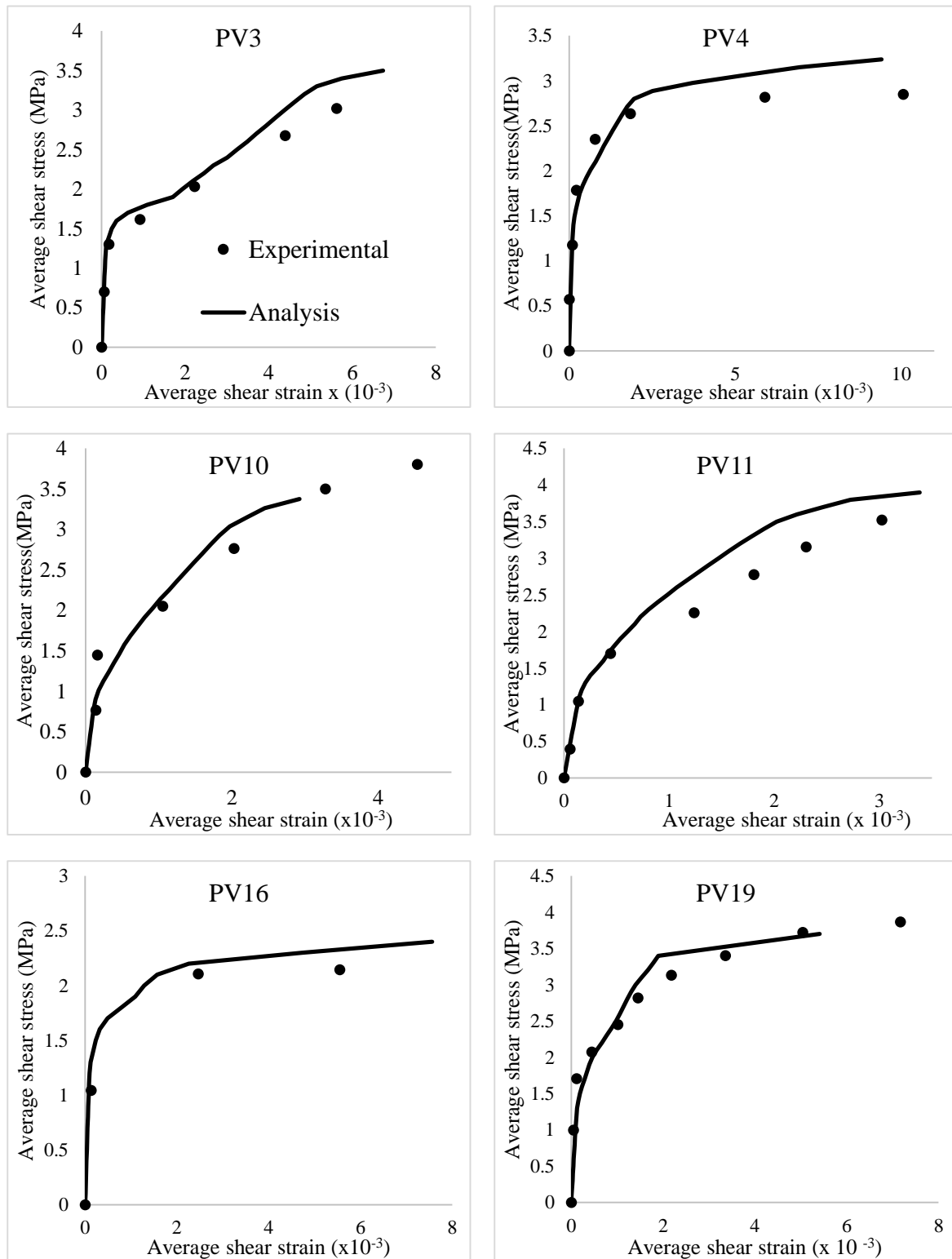


Figure 4.22– Comparison of experimental and analytical results for concrete panel specimens I

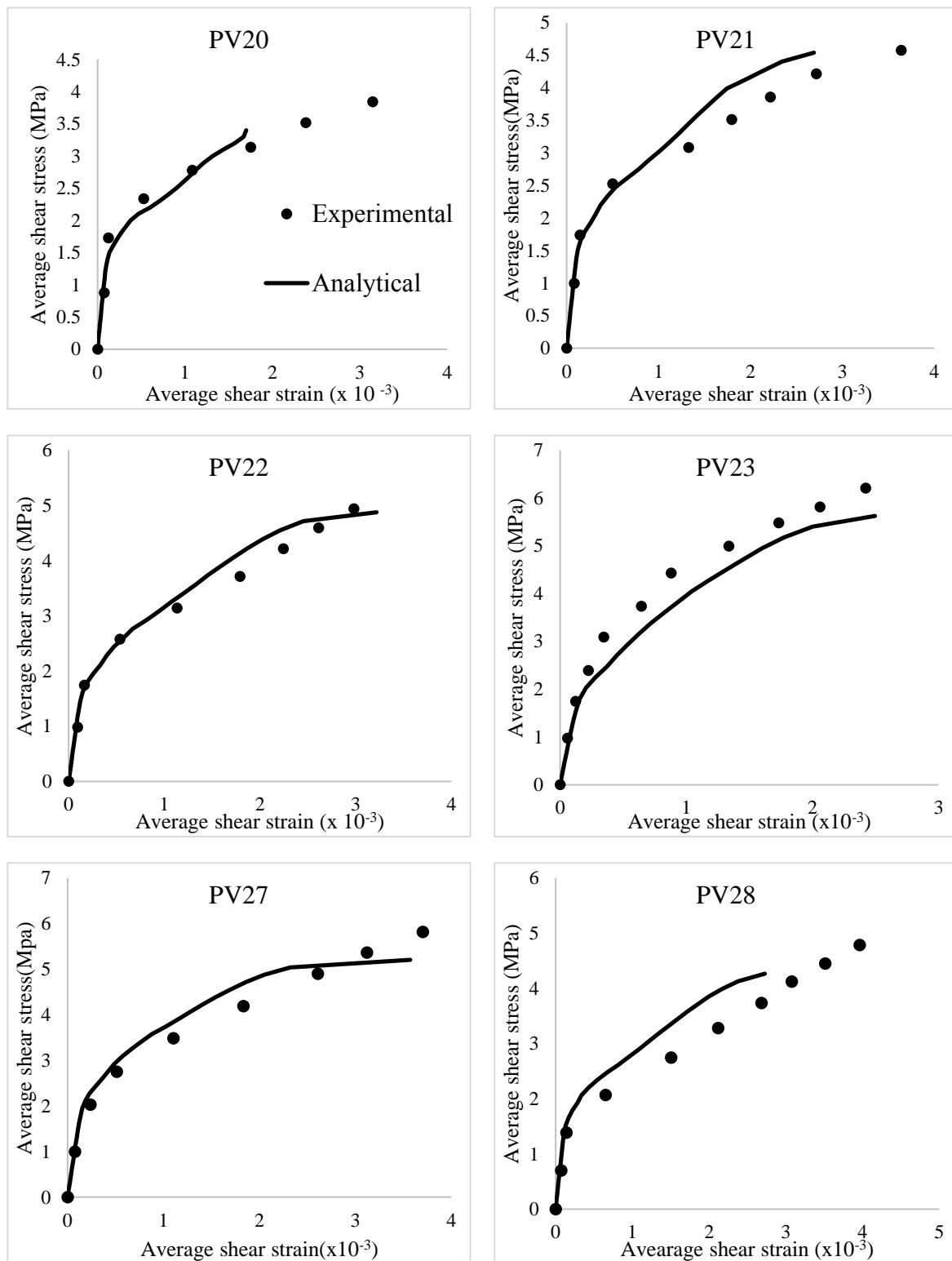


Figure 4.23– Comparison of experimental and analytical results for concrete panel specimens II

In the cases, where there was isotropic arrangement of steel and when steel yielding dominated the failure mode good correlation were observed with the experimental data. In two cases, PV 10 and PV 20 where the spring network became unstable due to excessive springs failing in shear, the analysis stopped before the specimen could reach its shear capacity. When the reinforcing ratio was not isotropic, shear slipping occurs between the cracks, hence it can be used to check the shear contact models. When there was a large change in reinforcement ratio, the results deviated from the experimental data (PV12). These specimens were sensitive to the shear model and also the Mohr–Coulomb parameters. Therefore there is a requirement to study the shear failure criteria in detail in order to appropriately model shear behaviour of concrete.

4.5 Conclusion

Certain points have to be kept in mind regarding the assumptions made in the non-linear analysis of reinforced concrete. The usage of spatially averaged softening models, has a negative tangential stiffness, which leads to a negative wave propagation velocity, which tends to change the type of the governing partial differential equation of the system, which lead to pathological mesh sensitivities (de Borst 2001).

Though element size objectivity of results is obtained within a particular range of element size. The objectivity of results due to mesh heterogeneity may not be possible, due to the simplification of the calculation of element stress/strain along the orientation of the springs. The spring network selection is based on the element size and location in the EDEM phase. So in the case of disordered orientation of the spring network (random meshing), the spring network discretization is dictated by the radius of the randomly sized circular element shapes used.

Simplified 1-D spatially averaged material models are used for concrete compression and tension. These models work effectively to analyse simple RC domains like frames. But these models cannot be used to represent a complex state of stresses especially in 3D. Therefore as long as the domain is kept simple (RC frames) and the state of stress are also simple, these models work fine.

A simplified steel model is used to model the reinforcement. Therefore complicated behavior of steel reinforcement in concrete like pullout, buckling, bond stress/slip, dowel action etc. are not being currently considered. Mesh size objectivity due to failure in compression is also not being considered, as fracture energy due to shear and tension failure are only being considered. To incorporate these behaviors of reinforced concrete appropriate modification have to be made.

In conclusion, a simplified method to perform nonlinear analysis of simple RC structural members has been proposed. The CST spring network can effectively follow the non-linear behaviour of simple RC members like beams and frames. By using the Quad spring network, shear models can also be incorporated in the spring network. The spring network can be used over a wide range of element sizes with objectivity in mesh size and density. An averaged cracking pattern is obtained. At this point, the spring network can effectively follow linear elastic, small deformation nonlinearity and cracking of RC frames, while using relatively large elements.

Chapter 5 **EDEM Phase**

Once the structure has been subjected to significant damage the analysis shifts to Phase II: EDEM phase. This chapter explores the validity of the spring network in the EDEM model. Section 2.3 gives a brief introduction to this method. This method essentially modifies the conventional distinct element method, by the introduction of springs between element centres, to model a continuous medium. Detailed formulation of the Extended Distinct Element Method (Meguro 1991) and the Distinct Element Method (Cundall and Strack 1979) can be found in the relevant literature.

5.1 Transition

In the spring network model the frame is assumed to be a continuum, and in the EDEM phase the frame is modelled as a dis-continuum. A brief description of the differences between the two phases can be found below (Table 5.1). The following changes are made between the two transitions (Figure 5.1):-

5.1.1 Contact springs

The contact springs are introduced between the elements at the point of contact. The contact springs are assumed to be parallel to the joint springs along the direction of the displaced joint spring. The effective stiffness is the sum of the joint and contact stiffness. The joint stiffness correspond to the earlier derived spring stiffness of the spring network.

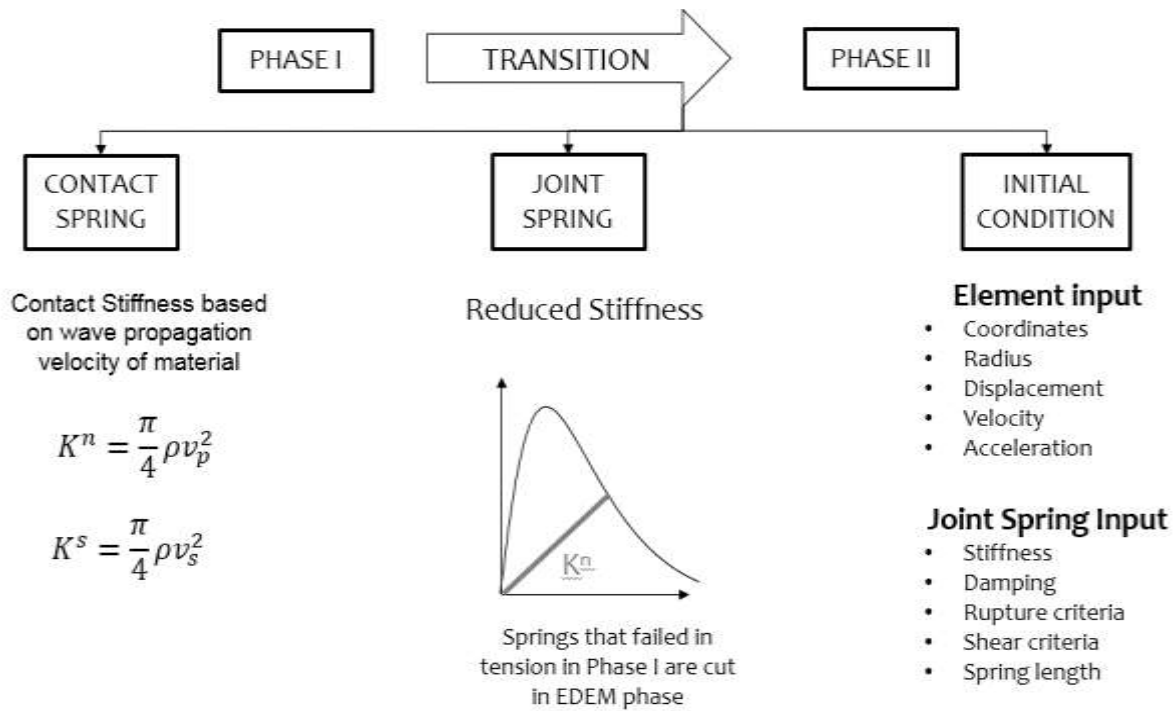


Figure 5.1– Transition between the two phases

Table 5.1 – Dimensions of the beams used in numerical analysis

Spring Network Phase	EDEM Phase
All springs are connected	Springs get ruptured
Springs soften once failed	Soften springs represent failed/ ruptured spring
No contact springs	Contact springs are introduced
Element shape has no physical meaning	Element shape play an important role in material behaviour, contact detection, collision and collapse
Non-linear springs that undergo material (stiffness) degradation	Linear springs with reduced stiffness
Larger time step	Smaller time step

The spring contact spring stiffness is calculated by the stiffness of the material based on the materials natural wave propagation velocity. It is calculated as follows:-

Lame's constant,

$$\mu = G = \frac{E}{2(1 + \nu)} \quad \text{.....(5.1)}$$

$$\lambda = \frac{E \nu}{(1 + \nu)(1 - 2\nu)} \quad \text{.....(5.2)}$$

The P-wave and S-wave velocity,

$$V_s = \sqrt{\frac{G}{\rho}} \quad \text{.....(5.3)}$$

$$V_p = \sqrt{\frac{\lambda + 2G}{\rho}} \quad \text{.....(5.4)}$$

The effective normal and shear stiffness,

$$K_{eff}^n = \frac{\pi \rho V_p^2}{4} \quad \text{.....(5.5)}$$

$$K_{eff}^s = \frac{\pi \rho V_s^2}{4} \quad \text{.....(5.6)}$$

The contact stiffness is obtained by

$$K_{contact}^n = K_{eff}^n - K_{joint}^n \quad \text{.....(5.7)}$$

$$K_{contact}^s = K_{eff}^s - K_{joint}^s \quad \text{.....(5.8)}$$

5.1.2 Joint springs

In the spring network phase, the springs gets deformed and undergoes nonlinear stiffness reduction. As a secant stiffness approach is used, at the instant when the transition occurs the linear stiffness used in EDEM corresponds to the reduced secant stiffness of the spring from the spring network model. The failed springs in tension are cut in the EDEM phase. This ensures that a more realistic damage is induced in the EDEM phase, hence a better correlation to the actual physical collapse of the building is obtained. The tensile spring failure criteria is expressed in terms of the failure tensile strain (ϵ_t). The shear failure criteria is based on the Mohr-Coulomb's criteria with friction angle, $\phi=37^\circ$ and critical shear force $V_{cr} = 0.2f_c(\text{radius})$ (Section 4.2.3).

5.1.3 Element details

The element details that are transferred between the two phases include the element radius, element centre coordinates, initial displacement, velocity and acceleration.

5.1.4 Time step

In explicit analysis, time step plays a very important role to ensure the stability of the analysis. As per the Courant-Friedrichs-Lewy condition, while using finite difference for integration, with spatial discretization increment Δx and time discretization increment Δt , the condition the minimum time increment required for stability can be computed from:-

$$\Delta t \leq \frac{\Delta x}{V} \quad \dots\dots(5.9)$$

In the case of EDEM, Δx is the sum of the radii of two connecting elements. For a safe estimate, it is assumed to be the diameter of the smaller connecting element (D_{min}). V is the wave propagation velocity.

$$\Delta t \leq \frac{D_{min}}{V} \quad \dots\dots(5.10)$$

$$\Delta t \leq 2 \sqrt{\frac{m}{k_{eff}}} \quad \text{.....(5.11)}$$

5.1.5 Damping

Damping is applied through dashpots placed parallel to the spring. The damping force is assumed to be proportional to the relative velocity between the elements. The change in damping force per time increment (ΔF_D)

$$\Delta F_D = \frac{\eta \Delta u}{\Delta t} \quad \text{.....(5.12)}$$

Where η is the damping coefficient given by

$$\eta = \zeta 2 \sqrt{m k_{eff}} \quad \text{.....(5.13)}$$

Where ζ is the damping ratio

5.2 1-storey frame analysis

The RC frame used in Section 4.4.2 is used for analysis. To check the stability of the joint spring and contact springs, the frame is subjected to only gravity loading first (acceleration in the Z direction). The input parameters are given below (Figure 5.2).

Table 5.2 – 1-storey frame EDEM input parameters

Element radius	42.5 mm	Time increment (Δt)	1×10^{-6} sec
Normal Contact stiffness k^n_{contact}	1×10^{10} N/m	Shear Contact stiffness k^s_{contact}	5×10^9 N/m
Joint damping ζ_{joint}	0.1	Contact damping ζ_{contact}	0.1
Density	2400 kg/m ³	Rupture tensile strain	0.4%
Friction angle	37°	Cohesion	7.5×10^5 N
Fundamental frequency (ω)	100 rad/sec	Input Amplitude	0.01 m

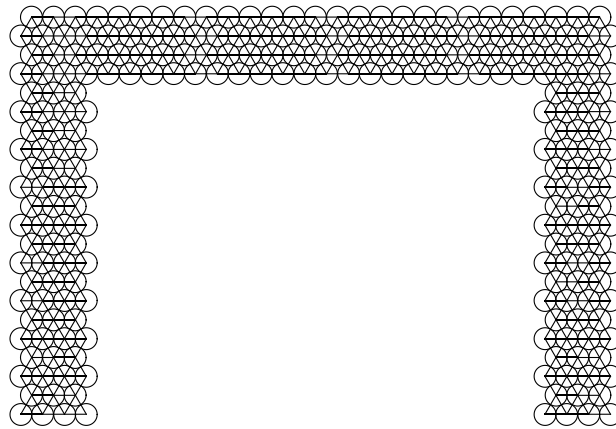


Figure 5.2– EDEM model of the RC Frame

The EDEM model of the frame can be seen above (Figure 5.2). When subjected to gravity loading, the elements initially vibrate and then damp out to the stable deformation state given below (Figure 5.3). A stable and symmetric deformation profile, shows the stability of the spring network obtained from the first phase of analysis.

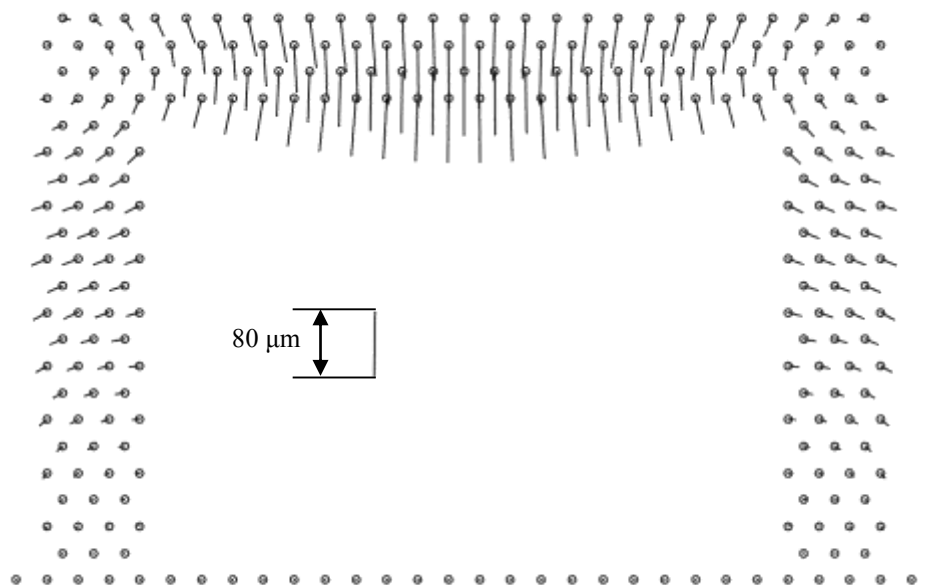


Figure 5.3– Damped deformation profile of undamaged frame under gravity loading

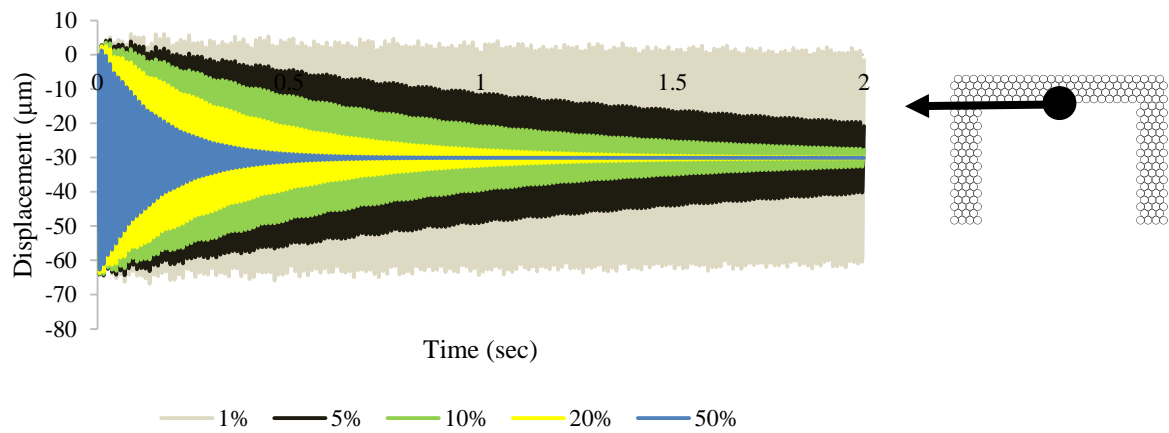


Figure 5.4– Damping of element under gravity loading with varying damping ratios

The variation of the vibration with varying damping ratios can be found above (Figure 5.4). A damping ratio such that vibration under gravity load dampens in around 2 second (10% damping ratio) is chosen (Figure 5.5). The undamaged frame is then subjected to a sinusoidal input displacement motion.

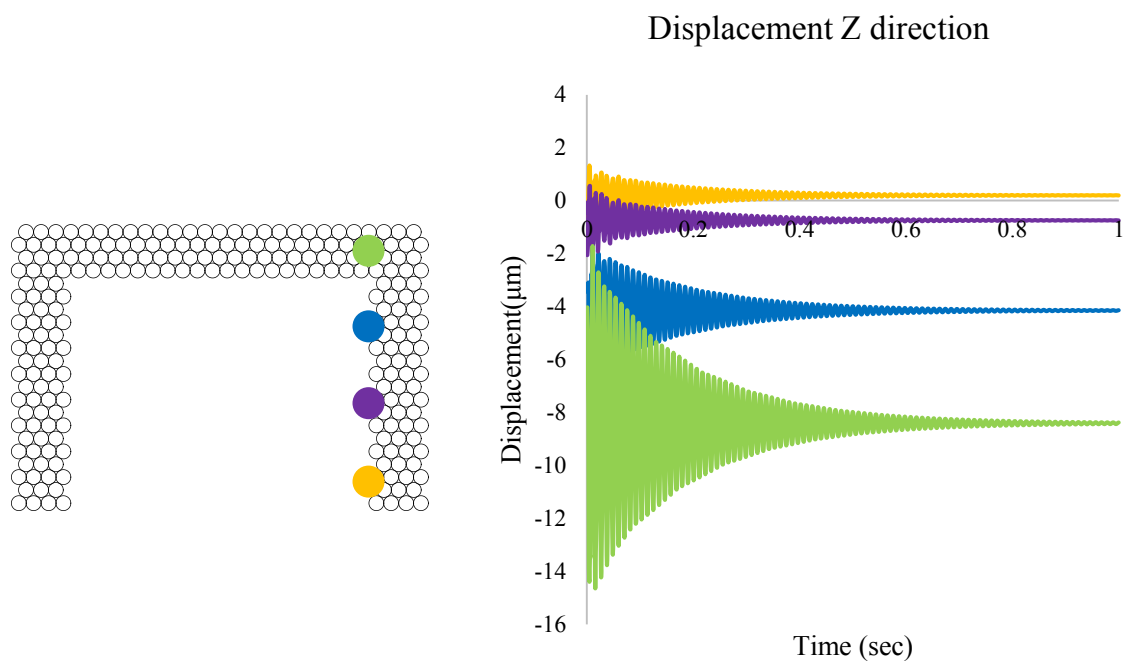


Figure 5.5– Z displacement time history under gravity loading

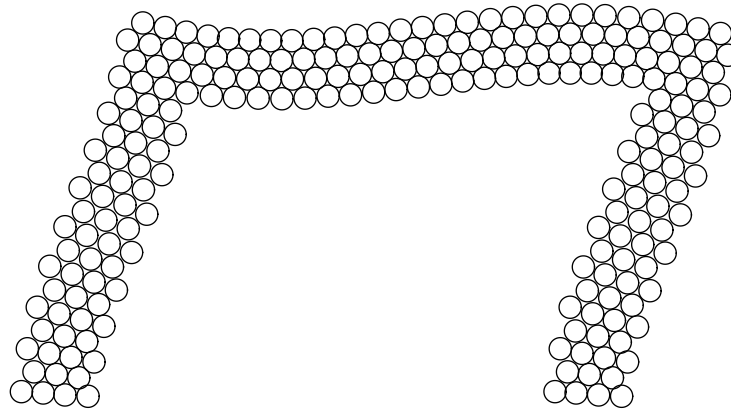


Figure 5.6– Fundamental Mode Shape of the Frame

The frequency of the input motion corresponds to the circular natural frequency of the first mode of shaking of the frame (Figure 5.6), which is computed through the vector shifted iteration technique using the global stiffness and mass matrix. The frame is subjected to an input displacement based loading. The frequency of the input loading corresponds to the frequency of its fundamental mode shape, which is equal to . The amplitude is linearly varied initially as shown below (Figure 5.7). The X direction displacement history along the height of the frame can be seen below (Figure 5.8).

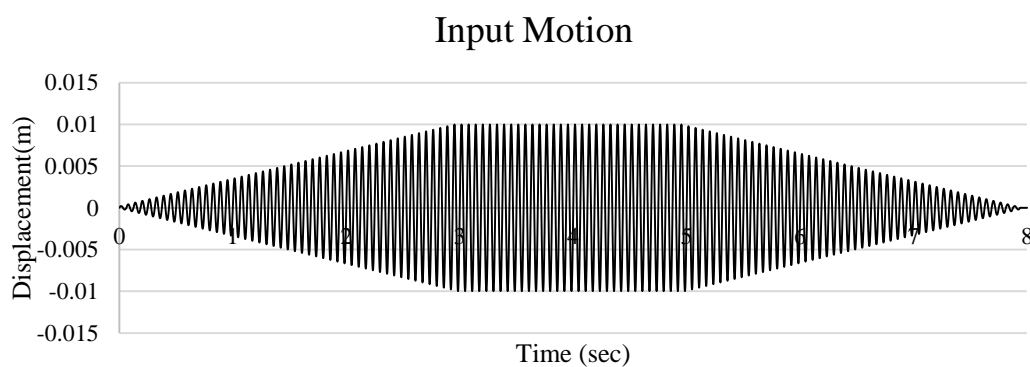


Figure 5.7– Input motion time history

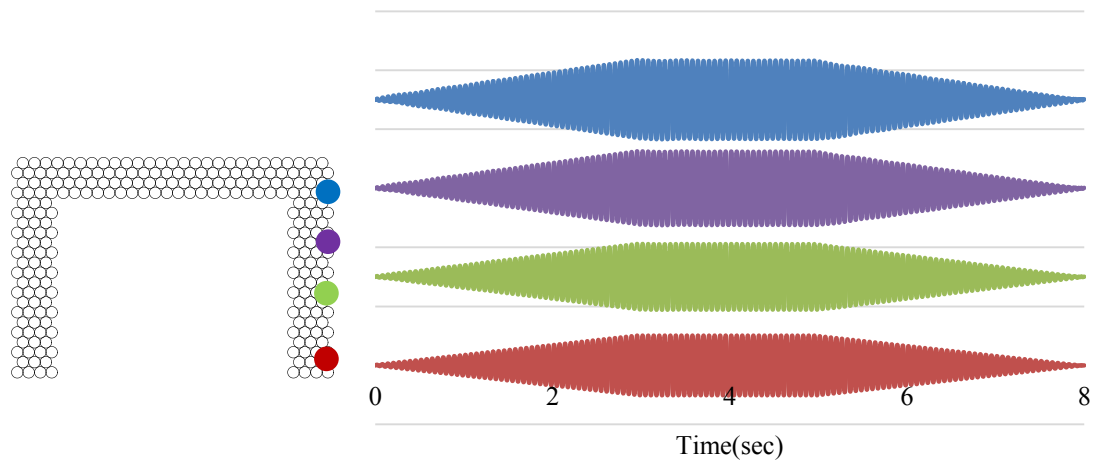


Figure 5.8– Displacement time history of undamaged frame under input motion

The frame is observed to be rigidly deforming under the input motion (Figure 5.6). The next part of the analysis involves damaging the frame by applying lateral load beyond peak (Figure 5.9). The damaged frame can be seen below (Figure 5.9). The cracked springs are represented through the red lines. The stability of the EDEM with the new damaged spring network is checked under gravity loading till the system vibration dampens. The deformation profile of the damaged frame under gravity loading can be observed below (Figure 5.10).

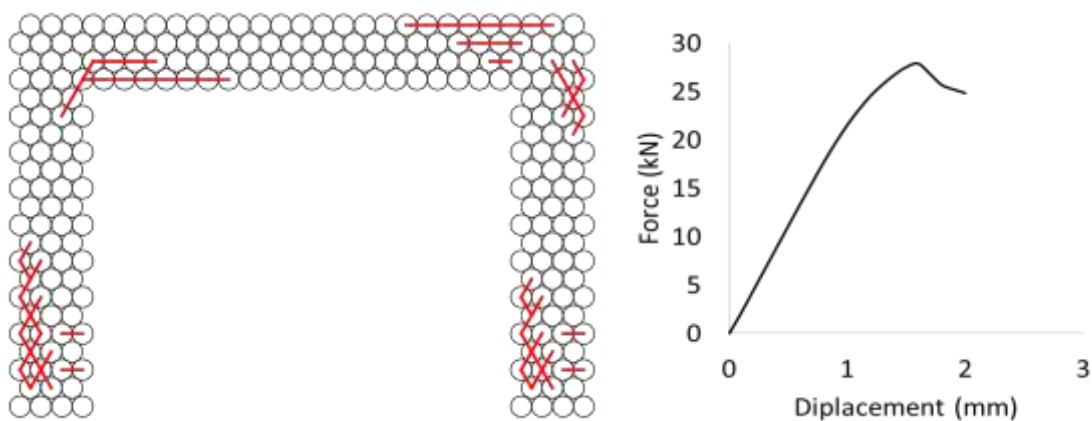


Figure 5.9– Damage induced in the frame due to lateral loading

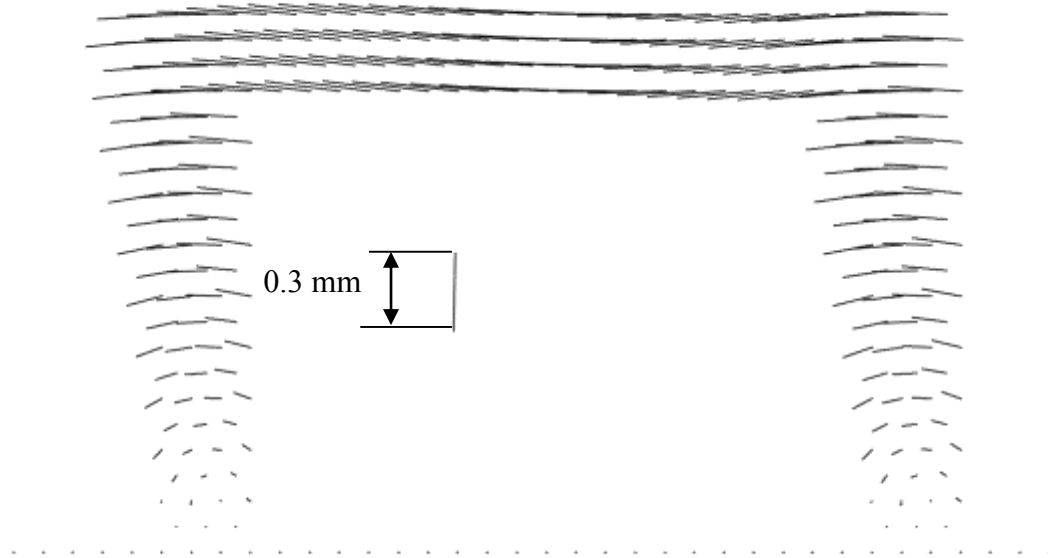


Figure 5.10– Stable (Damped) deformation profile of damaged frame under gravity loading

A slight drift towards the left side can be observed due to the higher number of failed springs on the left column. The damaged frame is then subjected to the same displacement input mentioned above (Figure 5.7). The damaged frame undergoes collapse due to the input loading (Figure 5.11). Initially the beam separated from the right column. The springs at the base of the columns then fail, causing an overall collapse of the frame.

5.3 11-storey frame analysis

A 11-storey experimentally tested (1/15 scale) RC frame (Okada et al. 1989) is simulated using the EDEM. The cross sectional details and the corresponding EDEM model of the frame can be seen below (Figure 5.12).

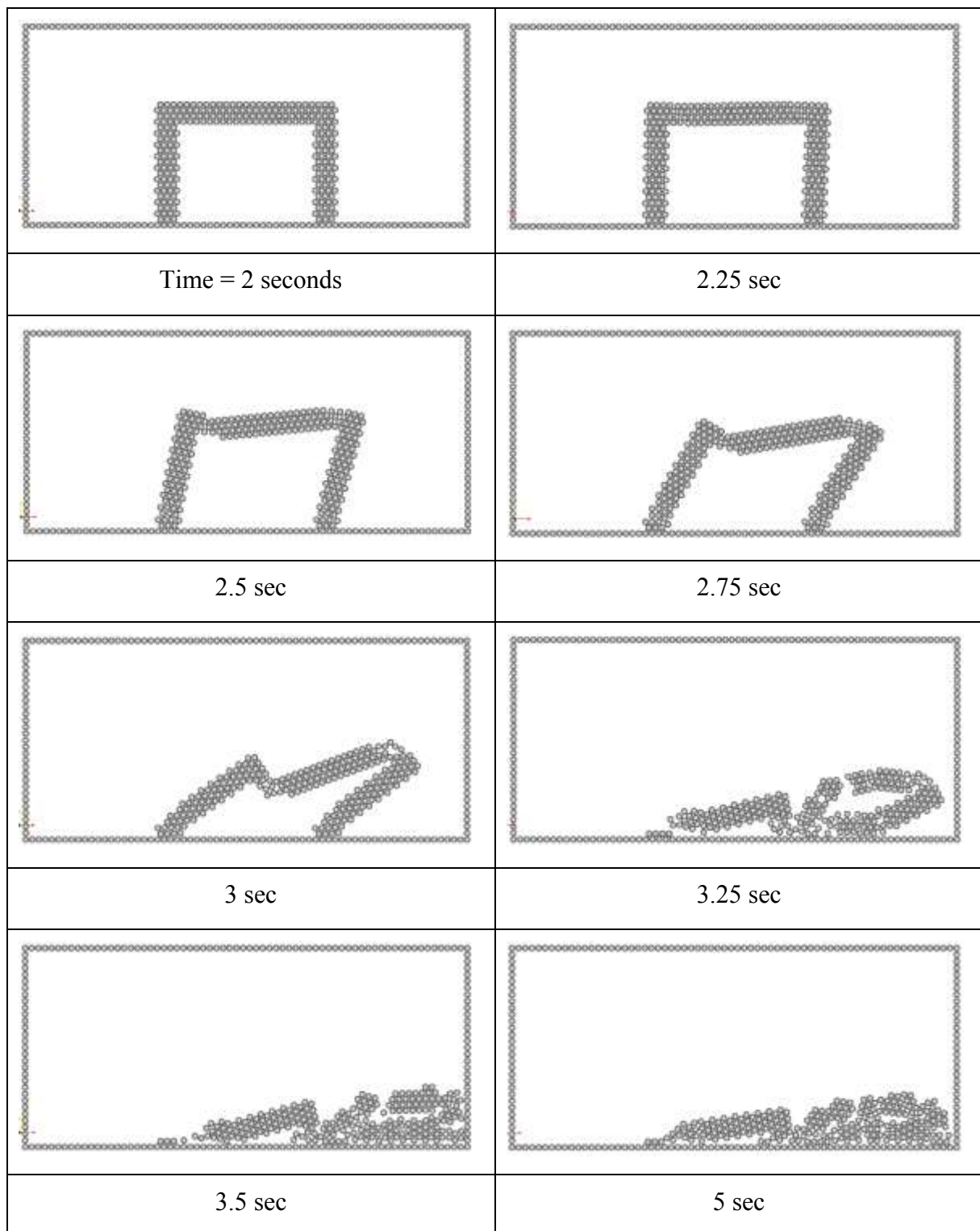


Figure 5.11– Collapse of 1 storey frame

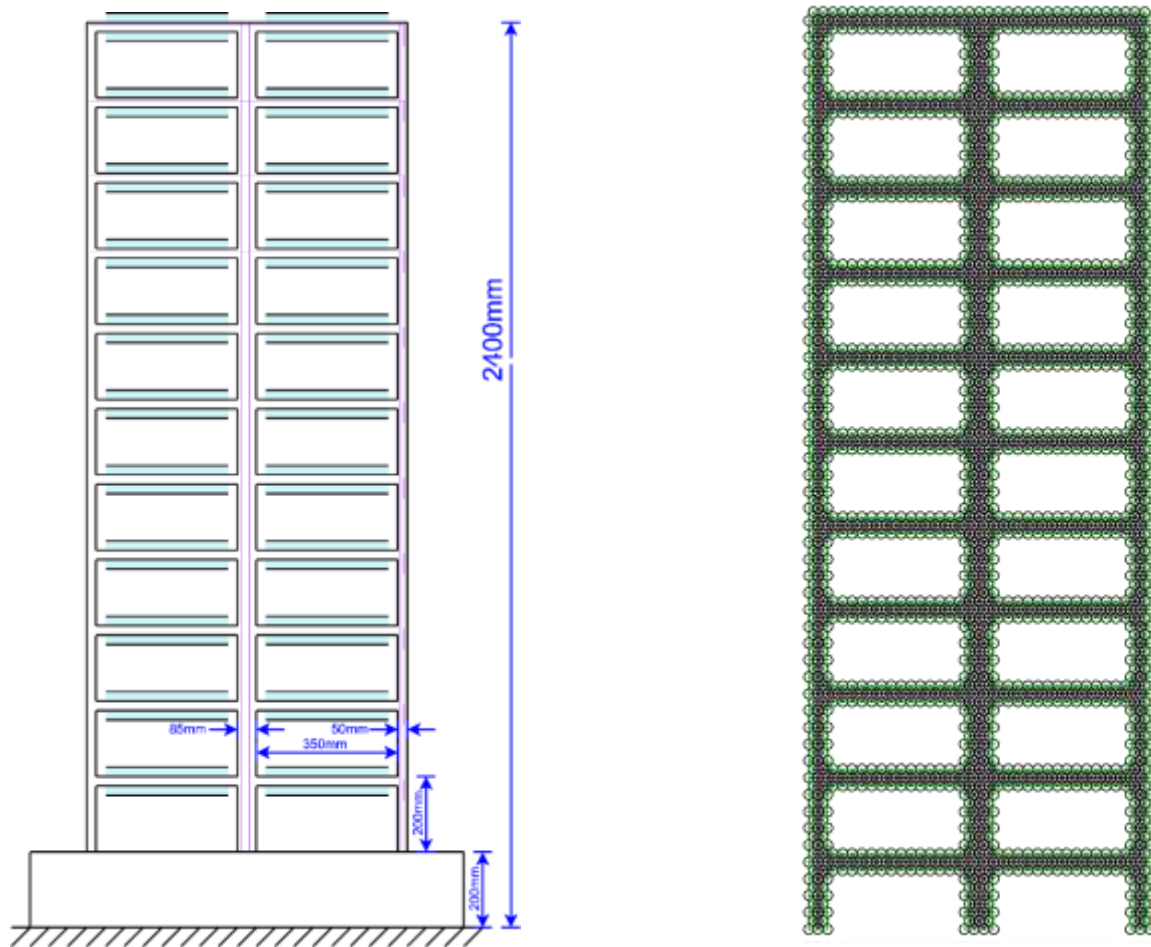


Figure 5.12– Details of the 11 storey frame

Table 5.3 – 11-storey frame EDEM input parameters

Element radius	12.5 mm	Time increment (Δt)	1×10^{-6} sec
Normal Contact stiffness k_{contact}^n	1×10^{10} N/m	Shear Contact stiffness k_{contact}^s	5×10^9 N/m
Joint damping ζ_{joint}	0.1	Contact damping ζ_{contact}	0.1
Density	2400 kg/m^3	Rupture tensile strain	0.4%
Friction angle	37°	Cohesion	7.5×10^5 N
Fundamental frequency (ω)	86 rad/sec	Input Amplitude	0.01 m

Two frames are considered namely, the undamaged frame and the frame that has been damaged due to loading. The stable deformation profile of the two frames under gravity loading can be seen below (Figure 5.14 (a) and (b)). The springs that have failed due to lateral loading can also be seen (Figure 5.14 (c)). The frames are subjected a sinusoidal displacement input (Figure 5.15). The displacement and velocity time history of the various elements along the height of the frame can be seen below (Figure 5.16). The damping of the displacements/velocity under gravity loading can be seen in the first 2 seconds of the input loading. When the damaged frame is subjected to the input loading it undergoes collapse. The collapse pattern of the frame can be seen below (Figure 5.20 and Figure 5.21).

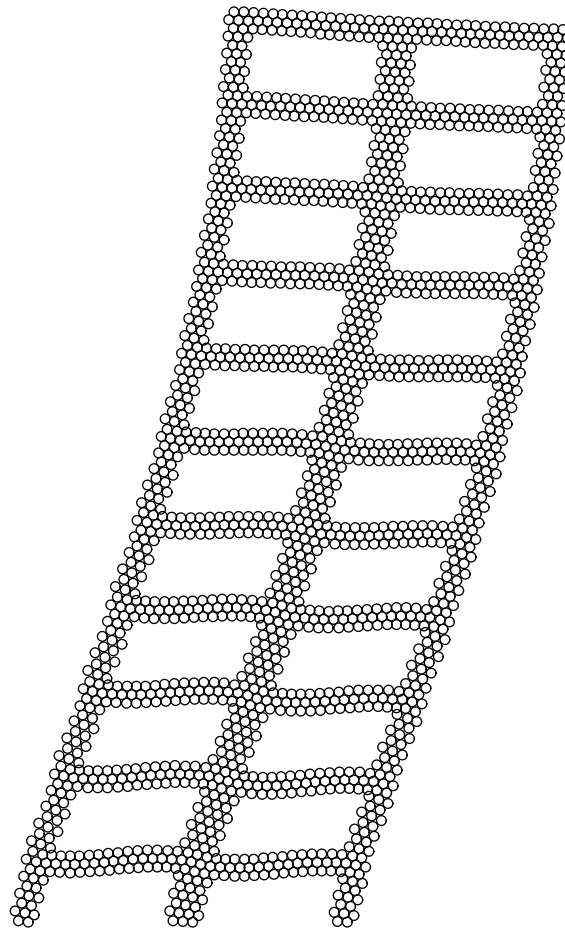


Figure 5.13– Fundamental mode shape of the 11 storey building

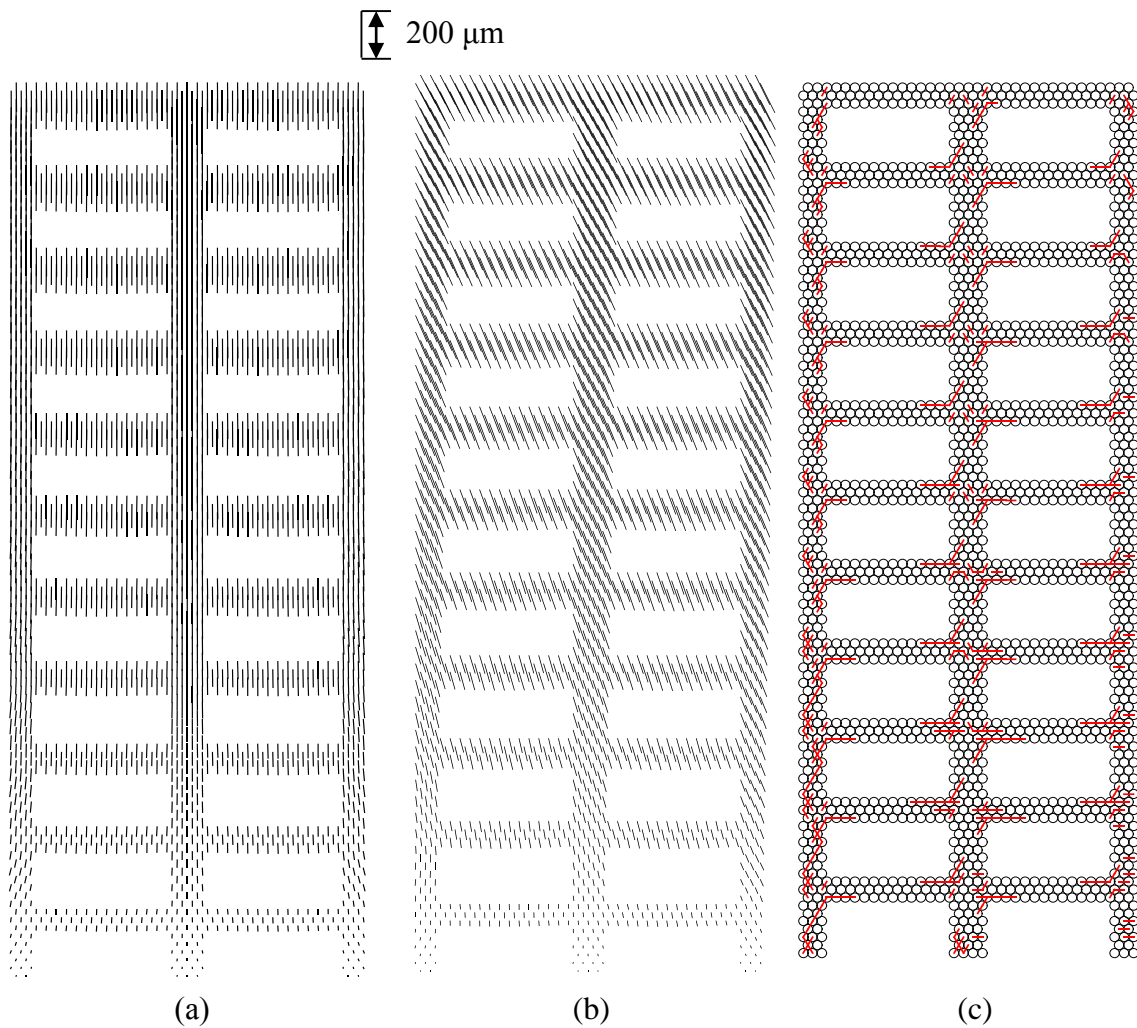


Figure 5.14– Deformation profile of the (a) undamaged and (b) damaged frame under gravity loading (c) Failed spring in the damaged model

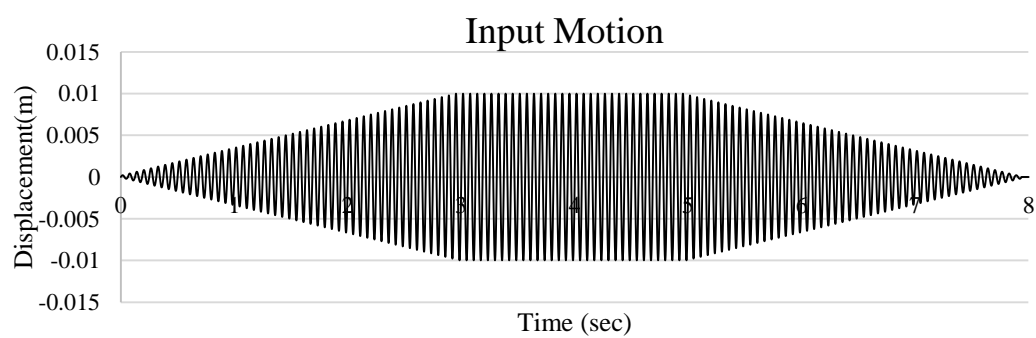


Figure 5.15– Input Ground Motion

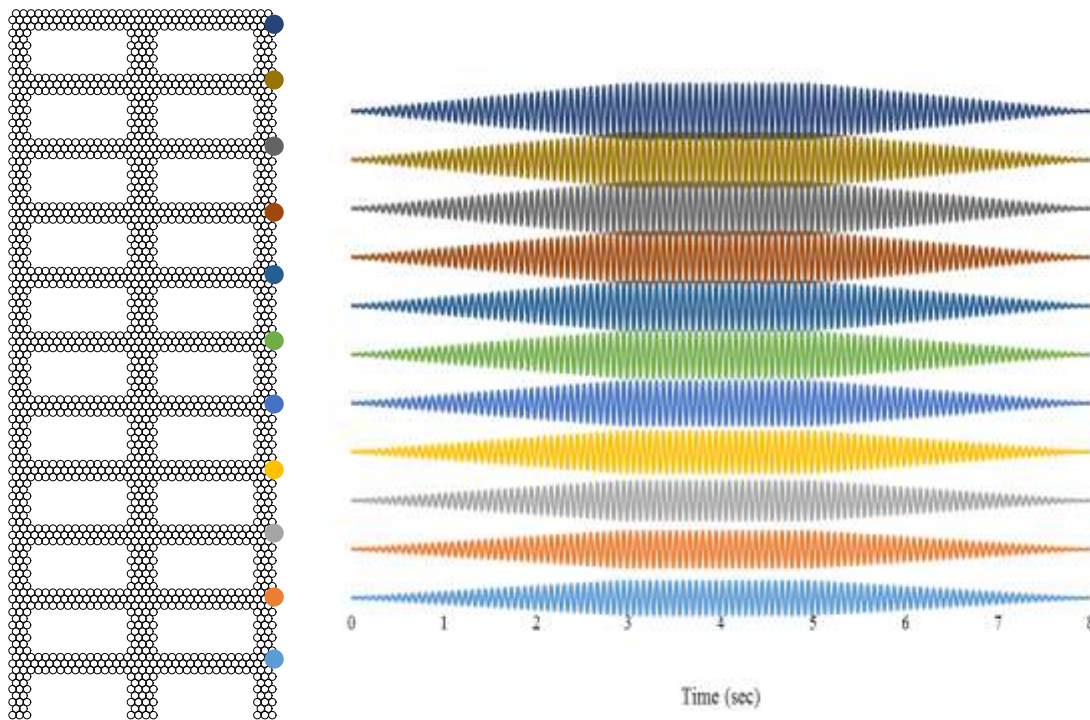


Figure 5.16–X direction Displacement time history along its height

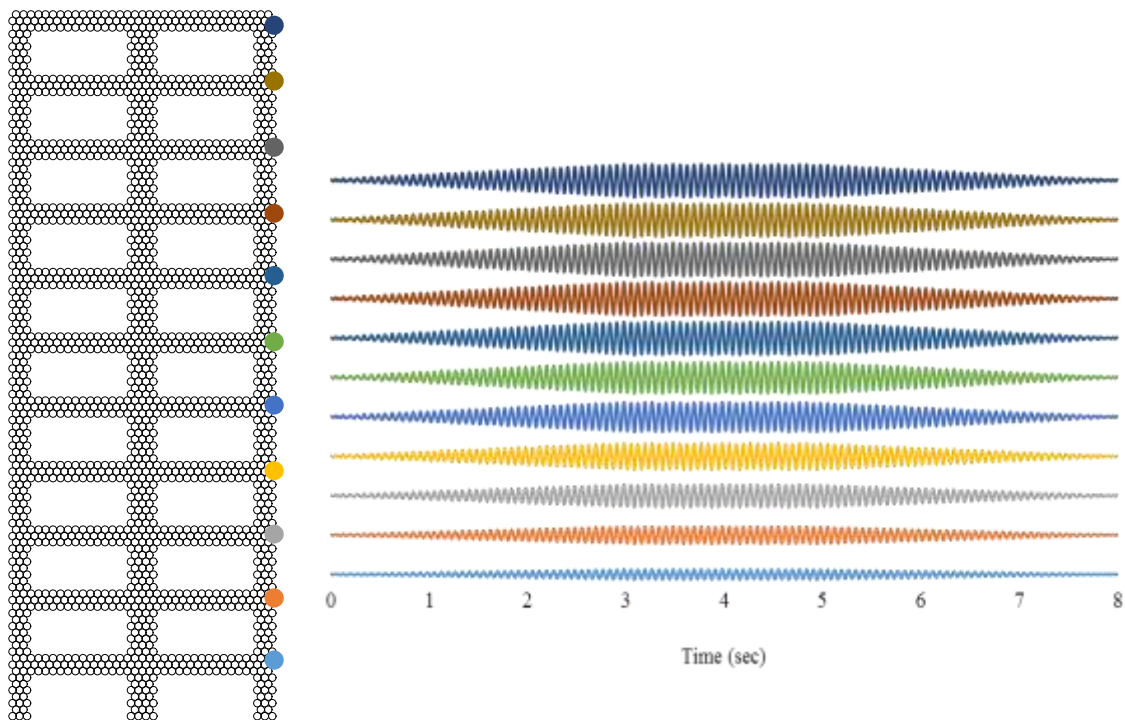


Figure 5.17–Z direction Displacement time history along its height

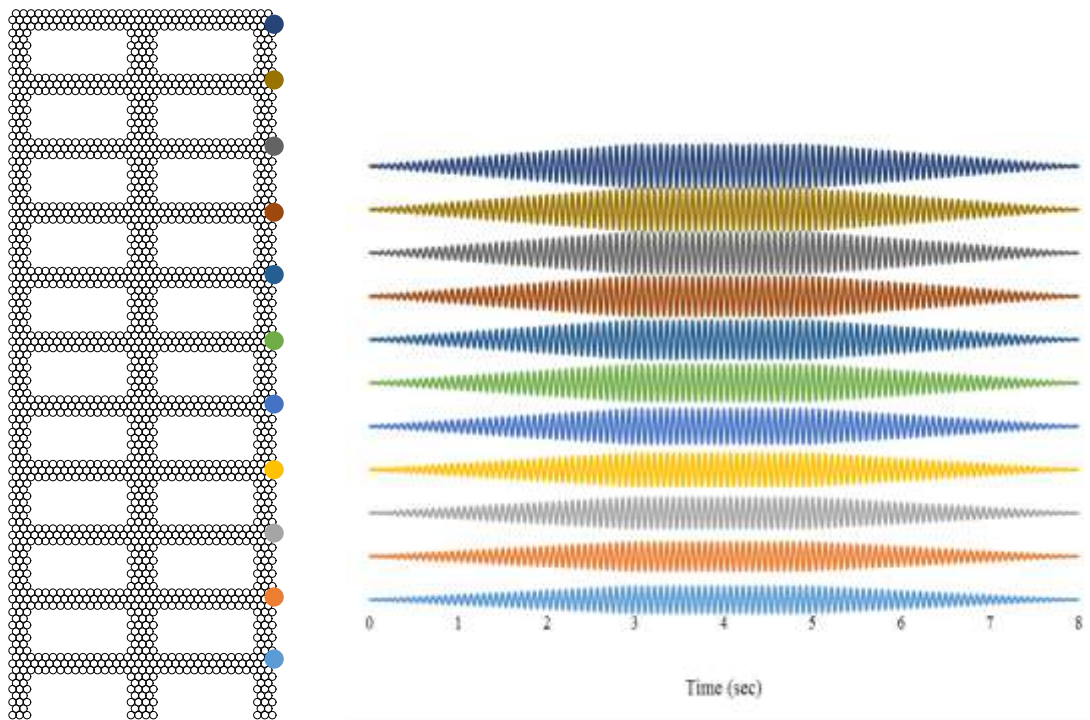


Figure 5.18–X direction Velocity time history along its height

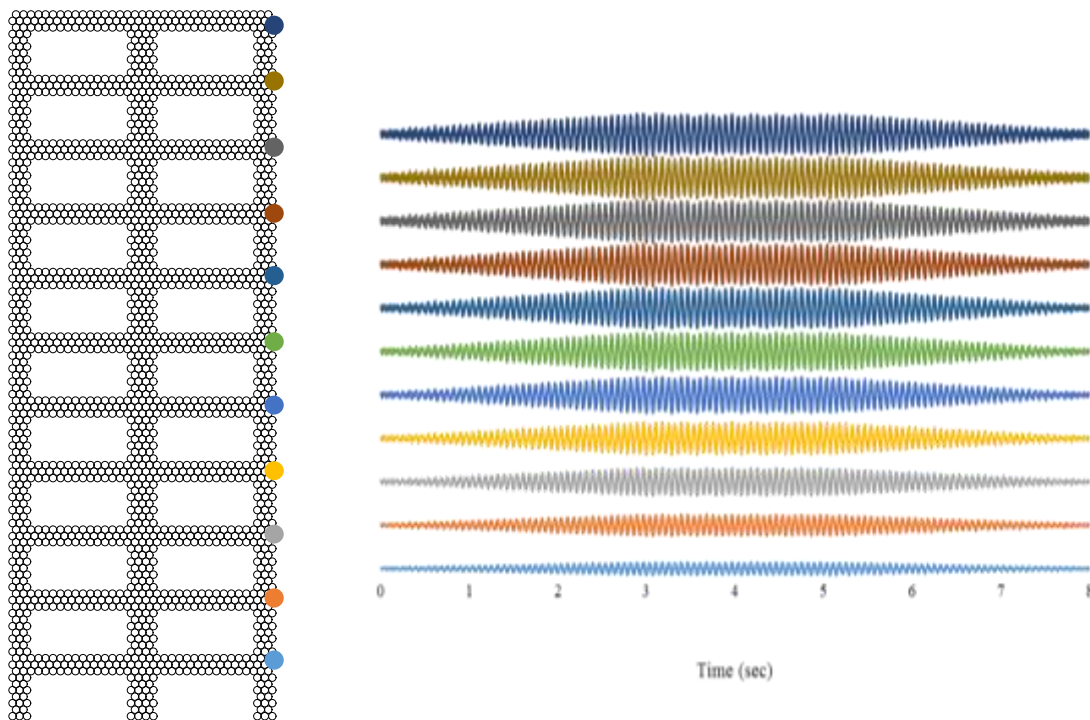


Figure 5.19–Z direction velocity time history along its height

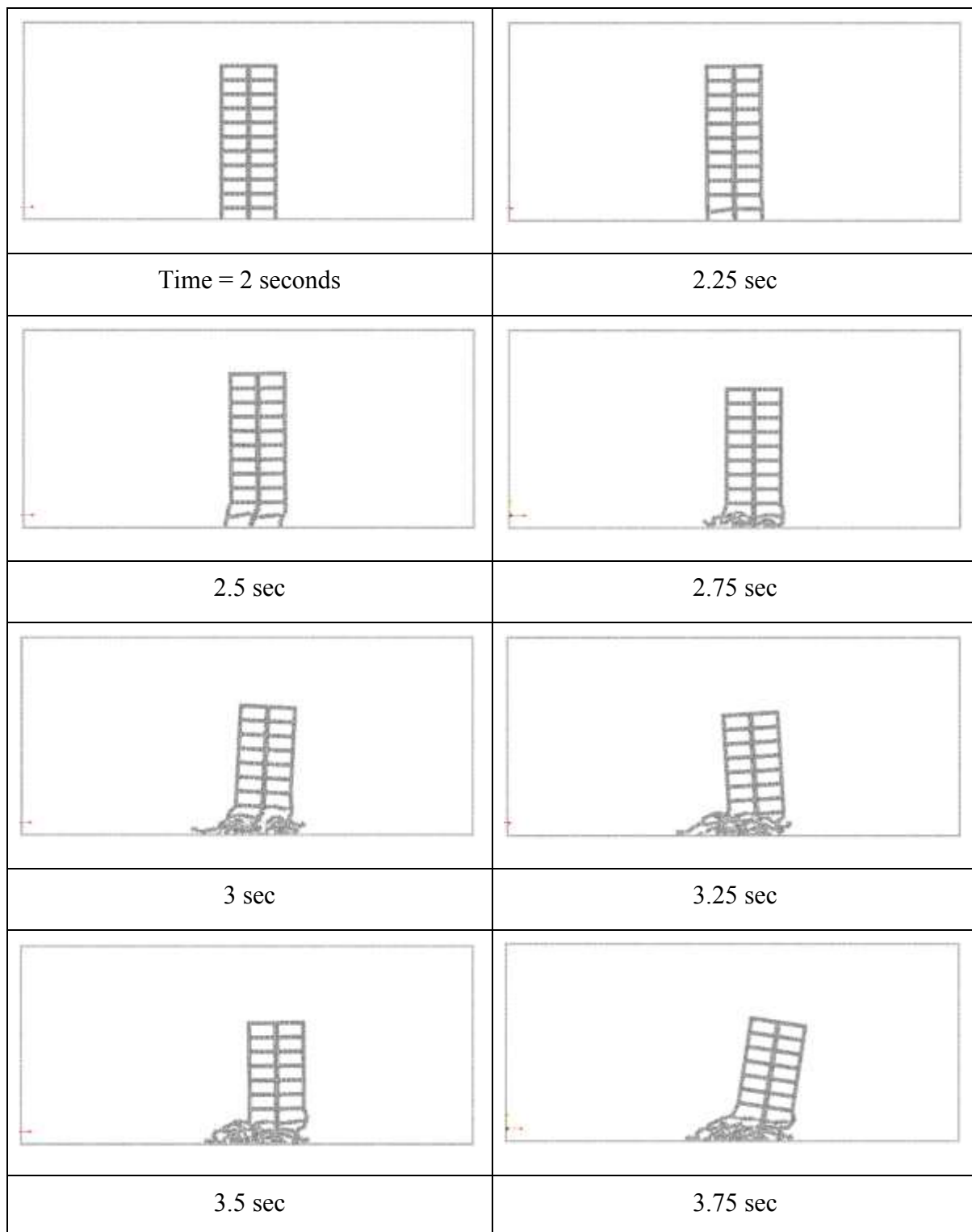


Figure 5.20– Collapse of 11-storey frame I

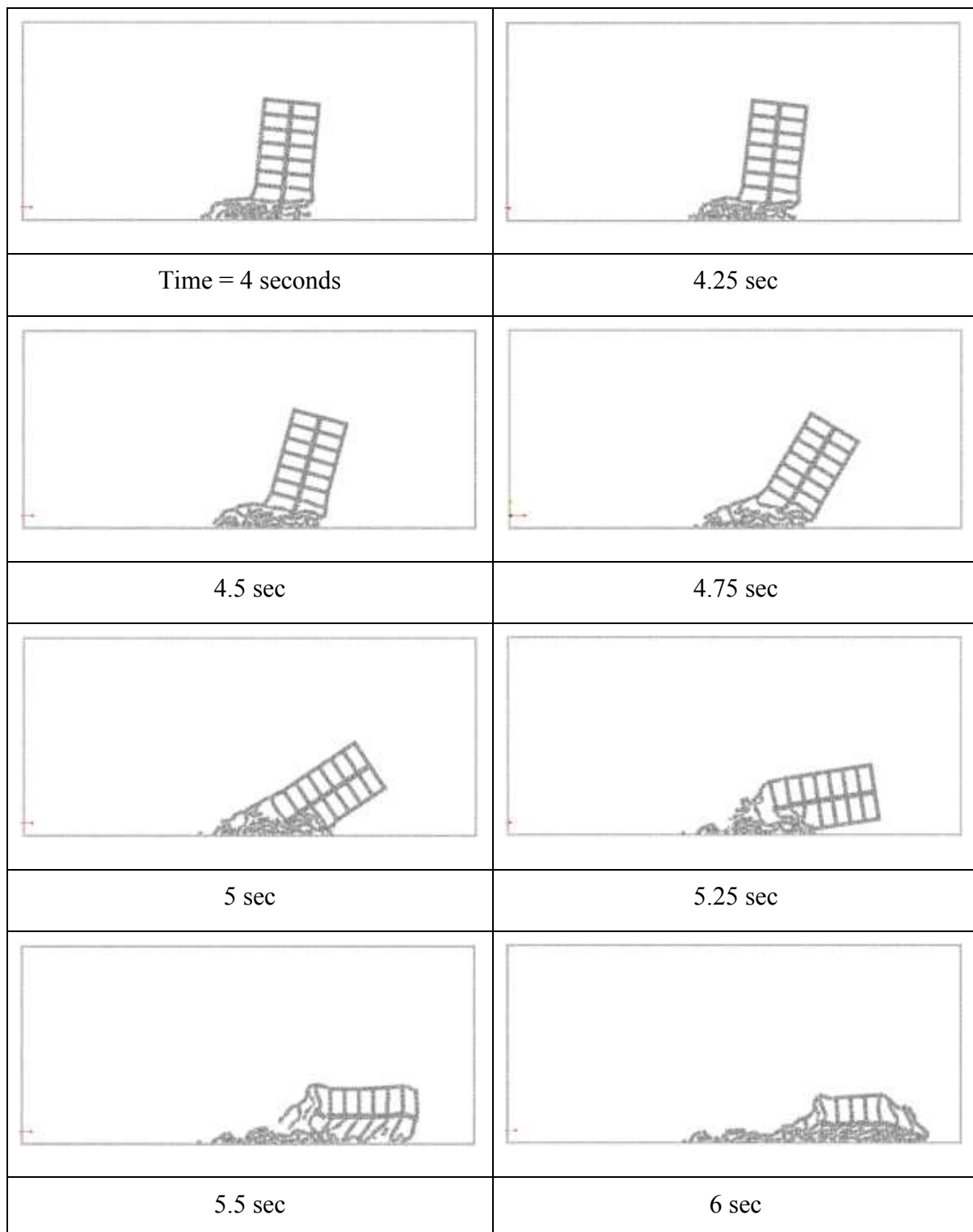


Figure 5.21– Collapse of 12-storey frame II

5.4 Conclusion

The capability of the spring network to be used in the Extended Distinct Element Method has been verified. Initially, the EDEM used linear elastic force-deformation relationships with homogenous strength distribution. Good results can be obtained in fracture analysis of material when using small element sizes and simpler material models. But as the element size increases, more complex material models, that capture the corresponding representative volume of the material the element represents, must be used. Though element sizes used are large and elastic force-deformation relationships are used, the damaged spring network from the first phase of analysis, given a better representation of the actual damaged condition of the structure, through the ruptured spring and reduced stiffness of springs. Hence a more realistic collapse pattern of the structure can be obtained. The damaged spring network is shown to be stable (no spurious oscillations) under loading. The collapse pattern of a multi-storey building was seen to be followed, without much computation effort required, due to the reduced number of elements used. The EDEM method provides a platform to effectively follow the collapse modes of large buildings, like soft storey collapse, pancake collapse, pounding of structures etc., under extreme seismic loading.

Chapter 6 Conclusion

A simplified two phase seismic collapse simulation method for RC frame has been developed. A spring network is used in the first phase for linear and non-linear analysis of the RC frame. The Extended Distinct Element Method is used in the second phase for large deformation analysis, until collapse. The following are the summary/conclusions of the results of the thesis:-

6.1 Linear Analysis

- i. A generalised method, viz. the Finite Element Mapping scheme is used for deriving the spring stiffness. This method which was earlier used for an infinite domain has been adopted to model the finite RC frame domain.
- ii. The accuracy and convergence of the spring network with the derived stiffness is similar to that of the parent finite element discretization.
- iii. Poisson's ratio is implicitly considered.
- iv. An accurate elastic analysis is possible with simple square and triangular spring network arrangement
- v. Because of the discrete lumping of mass at the nodes, mass matrix inversion is trivial

6.2 Non-Linear RC Analysis

- i. Spatially average concrete and steel models are used, which enables the use of larger element sizes.
- ii. With simple concrete compression/tension model and steel model. The nonlinear behaviour of an RC frame can be effectively followed.

- iii. With the secant stiffness formulation approach, the post peak response of RC frames can be followed with numerical stability.
- iv. By varying the tension softening curve accordingly, the element size dependency is reduced, as the spring network dissipates a constant fracture energy per unit area.
- v. Shear models can be easily incorporated into the spring network to model frames with shear dominance.

6.3 EDEM phase

- i. The usage of circular elements makes dynamic contact detection very fast, reducing the overall computation requirement of the model.
- ii. The spring network from the first phase shows stability and can be used in tandem with the contact springs between the rigid elements.
- iii. The failed springs and softened springs induce damage and help to follow the collapse mode of the frame more accurately.

6.4 Future Work

- The usage of improved basic elements or inclusion of rotational degree of freedom at every node, which makes the model invariant under rotation has to be investigated.
- Parametric study of the shear models used for analysis has to be performed. Proper models for shear stress transfer in cracks has to be used.
- Steel models that include pull out, dowel action, bond slip etc. have to be included.
- Cyclic material models that capture opening and closing of cracks properly has to be investigated and incorporated.
- Simplified RC frame analysis using a 3D model
- Modelling of masonry infill, which poses a challenge due to the loss of continuity of media due to spalling of masonry.

6.5 Overall Conclusion

A numerical model has been developed for reinforced concrete frames which can:-

- i. model elastic behaviour accurately.
- ii. model RC non-linearity, cracking, stiffness degradation, and can also predict ultimate load.
- iii. simulate large deformation, separation, collision and complete collapse
- iv. reduce the overall computational effort required due to the large, circular and rigid elements being used
- v. be used to model a large number of building stock, especially in developing countries
- vi. be used to perform a large number of simulation, to obtain a reliable vulnerability assessment of an RC framed building, considering material and geometric randomness of the RC frame.

References

- Ashurst, W. T., and Hoover, W. G. (1976). "Microscopic fracture studies in 2-dimensional triangular lattice." *Phys. Rev. B*, 14(4), 1465–1473.
- Barbosa, R. E., and Ghaboussi, J. (1990). "Discrete finite element method for multiple deformable bodies." *Finite Elements in Analysis and Design*, 7(2), 145–158.
- Bazant, Z., and Oh, B. (1983). "Crack band theory of concrete." *Materials and Structures*, 16, 155.
- Bolander, J. E., and Saito, S. (1998). "Fracture analyses using spring networks with random geometry." *Engineering Fracture Mechanics*, 61(5-6), 569–591.
- De Borst, R. (2001). "Some recent issues in computational failure mechanics." *International Journal for Numerical Methods in Engineering*, 52(12), 63–95.
- Bresler, B., and Scordelis, A. C. (1963). "Shear strength of reinforced concrete beams." *Journal of American Concrete Institute*, 60(1), 51–72.
- Camborde, F., Mariotti, C., and Donzé, F. V. (2000). "Numerical study of rock and concrete behaviour by discrete element modelling." *Computers and Geotechnics*.
- Chopra, A. K. (2007). *Dynamics of Structures*. Pearson Education.
- Coburn, A., and Spence, R. (2002). *Earthquake Protection*. John Wiley & Sons.
- Courant, R., Friedrichs, K., and Lewy, H. (1967). "On the Partial Difference Equations of Mathematical Physics." *IBM Journal of Research and Development*, 11(2), 215–234.
- Cundall, P. A. (1971). "A Computer model for simulating progressive large scale movement in blocky rock systems." *Proceedings of the Symposium of the International Society of Rock Mechanics*.
- Cundall, P. A., and Hart, R. (1992). "Numerical Modelling of Discontinua." *Engineering Computations*.
- Cundall, P. A., and Strack, O. D. L. (1979). "A discrete numerical model for granular assemblies." *Géotechnique*.

- Donzé, F. V., Richefeu, V., and Magnier, S.-A. (2008). "Advances in Discrete Element Method Applied to Soil, Rock and Concrete Mechanics." *Electronic Journal of Geotechnical Engineering*, Bouquet 08(2008), 1–43.
- Griffiths, D. V., and Mustoe, G. G. W. (2001). "Modelling of elastic continua using a grillage of structural elements based on discrete element concepts." *International Journal for Numerical Methods in Engineering*, 50(7), 1759–1775.
- Gusev, A. a. (2004). "Finite element mapping for spring network representations of the mechanics of solids." *Physical Review Letters*, 93(3), 034302–1.
- Gusev, A. a. (2006). "Gusev reply." *Physical Review Letters*.
- Hakuno, M., and Meguro, K. (1993). "Simulation of Concrete-Frame Collapse due to Dynamic Loading." *Journal of Engineering Mechanics*.
- Hassold, G. N., and Srolovitz, D. J. (1989). "Brittle fracture in materials with random defects." *Physical Review B*, 39(13), 9273–9281.
- Hentz, S., Daudeville, L., and Donzé, F. V. (2004). "Identification and Validation of a Discrete Element Model for Concrete." *J. Engrg. Mech.*, 130(June), 709–719.
- Hrennikoff, A. (1941). "Solution of Problems of Elasticity by the Frame-Work Method." *Applied Scientific Research*, A8, 169–175.
- Isobe, D., and Tsuda, M. (2003). "Seismic collapse analysis of reinforced concrete framed structures using the finite element method." *Earthquake Engineering & Structural Dynamics*, 32(13), 2027–2046.
- Iwashita, K., and Hakuno, M. (1990). "Modified distinct element method simulation of dynamic cliff collapse." *Structural Eng./Earthquake Eng., JSCE*, 7(1), 133s–142s.
- Jagota, A., and Bennison, S. (1994). "Spring-network and finite-element models for elasticity and fracture." *Non-linearity and Breakdown in Soft Condensed Matter*, K. K. Bardhan, B. K. Chakrabarti, and A. Hansen, eds., Springer Berlin, 186–201.
- Jagota, A., and Bennison, S. J. (1999). "Element breaking rules in computational models for brittle fracture." *Modelling and Simulation in Materials Science and Engineering*, 3(4), 485–501.
- Japan Society of Civil Engineers. (2007). "STANDARD SPECIFICATIONS FOR CONCRETE STRUCTURES - 2007 'Design.'" *Concrete*.
- Jing, L. (1998). "Formulation of discontinuous deformation analysis (DDA) - an implicit discrete element model for block systems." *Engineering Geology*, 49(3-4), 371–381.
- Kawai, T. (1977). "A New Discrete Model for Analysis of Solid Mechanics Problems." *Journal of Seisan Kenkyu, Inst. Ind. Sci. University Tokyo*.

- Kawai, T., Ueda, M., Takeuchi, N., Watanabe, M., Higuchi, H., and Kei, T. (1986). "Discrete Limit Analysis of Reinforced Concrete Structures (I) - Formulation of Rigid Body Spring Model for R/C Element." *Journal of Seisan Kenkyu, Inst. Ind. Sci. University of Tokyo*, 38(4), 181–184.
- Keating, P. N. (1966). "Effect of invariance requirements on the elastic strain energy of crystals with application to the diamond structure." *Physical Review*, 145(2), 637–645.
- Kikuchi, A., Kawai, T., and Suzuki, N. (1992). "The rigid bodies—spring models and their applications to three-dimensional crack problems." *Computers & Structures*.
- Krawinkler, H., Medina, R., and Alavi, B. (2003). "Seismic drift and ductility demands and their dependence on ground motions." *Engineering Structures*, 25(5), 637–653.
- Krawinkler, H., and Seneviratna, G. D. P. K. (1998). "Pros and cons of a pushover analysis for seismic performance evaluation." *Engineering Structures*, 20(4-6), 452–464.
- Lemos, J. V. (2007). "Discrete Element Modeling of Masonry Structures." *International Journal of Architectural Heritage*.
- Liu, K., Gao, L., and Tanimura, S. (2004). "Application of discrete element method in impact problems." *JSME International Journal Series A*, 47(2), 138–145.
- Lu, X., Lu, X., Guan, H., and Ye, L. (2013). "Collapse simulation of reinforced concrete high-rise building induced by extreme earthquakes." *Earthquake Engineering and Structural Dynamics*, 42(5), 705–723.
- Maekawa, K., Pimanmas, A., and Okamura, H. (2003). *Nonlinear Mechanics of Reinforced Concrete*. Spon Press.
- Meguro, K. (1991). "Study on Dynamic Fracture Analyses by Distinct Element Method (in Japanese)." The University of Tokyo.
- Meguro, K., and Hakuno, M. (1989). "Fracture analyses of concrete structures by the modified distinct element method." *Structural Eng./Earthquake Eng., JSCE*, 6(2), 283s–294s.
- Meguro, K., and Hakuno, M. (1994). "Application of the Extended Distinct Element Method for Collapse Simulation of a Doubledeck Bridge." *Structural Eng./Earthquake Eng., JSCE*, 10(4), 175s–185s.
- Munjiza, A. (2004). *The Combined Finite-Discrete Element Method*. John Wiley & Sons.
- Murty, C. V. R., Brzev, S., Faison, H., Comartin, C. D., and Irfanoglu, A. (2006). *At Risk: The Seismic Performance of Reinforced Concrete Frame Buildings with Masonry Infill Walls* | Shelter Centre. October.
- Muto, K. (1965). *Strength and Deformation of Structures*. Maruzen, Tokyo.

- Nagai, K., Sato, Y., and Ueda, T. (2004). "Mesoscopic Simulation of Failure of Mortar and Concrete by 2D RBSM." *Journal of Advanced Concrete Technology*.
- Nakagawa, T., Narafu, T., Imai, H., Hanazato, T., Ali, Q., and Minowa, C. (2012). "Collapse behavior of a brick masonry house using a shaking table and numerical simulation based on the extended distinct element method." *Bulletin of Earthquake Engineering*, 10(1), 269–283.
- Nukala, P. K. V. V., and Šimunović, S. (2006). "Comment on 'Finite Element Mapping for Spring Network Representations of the Mechanics of Solids.'" *Physical Review Letters*, 96(19), 199401.
- Okada, T., Kumazawa, F., Horiuchi, S., Yamamoto, M., Fujioka, A., Shinozaki, K., and Yoshiaki, N. (1989). "Shaking Table Tests of Reinforced Concrete Small Scaled Model Structure." *Bulletin of Earthquake Resistant Structures*, 22, 13–40.
- Okamura, H., and Maekawa, K. (1991). *Nonlinear Analysis and Constitutive Models of Reinforced Concrete*. Gihodo-Shuppan Co. Tokyo.
- Ostoja-Starzewski, M. (2002). "Lattice models in micromechanics." *Applied Mechanics Reviews*.
- Ostoja-Starzewski, M., Sheng, P. Y., and Alzebdeh, K. (1996). "Spring network models in elasticity and fracture of composites and polycrystals." *Computational Materials Science*, 7(1-2), 82–93.
- Pearce, C. J., Thavalingam, a., Liao, Z., and Bićanić, N. (2000). "Computational aspects of the discontinuous deformation analysis framework for modelling concrete fracture." *Engineering Fracture Mechanics*, 65(2-3), 283–298.
- Ren, W.-X., Tan, X., and Zheng, Z. (1999). "Nonlinear analysis of plane frames using rigid body-spring discrete element method." *Computers & Structures*, 71(1), 105–119.
- Sasani, M., and Kropelnicki, J. (2008). "Progressive collapse analysis of an RC STRUCTURE." *Structural Design of Tall and Special Buildings*, 17(4), 757–771.
- Sawamoto, Y., Tsubota, H., Kasai, Y., Koshika, N., and Morikawa, H. (1998). "Analytical studies on local damage to reinforced concrete structures under impact loading by discrete element method." *Nuclear Engineering and Design*.
- Shi, G., and Goodman, R. (1985). "Two dimensional discontinuous deformation analysis." *International Journal for Numerical and ...*, 9(April 1984), 541–556.
- Sivaselvan, M. V., and Reinhorn, A. M. (2002). "Collapse Analysis: Large Inelastic Deformations Analysis of Planar Frames." *Journal of Structural Engineering*.

- Sun, L., Zhou, C., Qin, D., and Fan, L. (2003). "Application of extended distinct element method with lattice model to collapse analysis of RC bridges." *Earthquake Engineering & Structural Dynamics*, 32(8), 1217–1236.
- Tagel-Din, H. (1998). "A new efficient method for nonlinear, large deformation and collapse analysis of structures." *Ph. D. thesis, Civil Eng. Dept., The University of Tokyo*.
- Vamvatsikos, D., and Fragiadakis, M. (2010). "Incremental dynamic analysis for estimating seismic performance sensitivity and uncertainty." *Earthquake engineering & ...*, 39(2), 141–163.
- Vecchio, F. J. (1989). "Nonlinear Finite Element Analysis of Reinforced Concrete Membranes." *ACI Structural Journal*, 86(1), 26–35.
- Vecchio, F. J., and Collins, M. P. (1982). *Response of reinforced concrete to in-plane shear and normal stresses, Technical report*.
- Villaverde, R. (2007). "Methods to Assess the Seismic Collapse Capacity of Building Structures: State of the Art." *Journal of Structural Engineering*, 133(1), 57–66.
- Wei, H., Yi, D., Li, S., Liu, X., and Zhao, M. (2006). "Study on spring properties of continuum-based discrete element method (in Chinese)." *Chinese Journal of Rock Mechanics and Engineering*, 25(973).
- Williams, J. R., and O'Connor, R. (1999). "Discrete element simulation and the contact problem." *Archives of Computational Methods in Engineering*.
- Xuehui, A. N., Maekawa, K., and Okamura, H. (1998). "Numerical Simulation of Size Effect in Shear Strength of RC Beams." *Concrete Library of JSCE*, (564), 297–316.
- Yan, H., G, L., and Sander, L. M. (2007). "Fracture Growth in 2d Elastic Networks with Born Model." *Europhysics Letters (EPL)*, 10(1), 7–13.
- Zareian, F., Krawinkler, H., Ibarra, L., and Lignos, D. (2010). "Basic Concepts and Performance Measures in Prediction of Collapse of Buildings Under Earthquake Ground Motions." *The Structural Design of Tall and Special Buildings*, 181(October 2009), 167–181.
- Zhao, G. F., Fang, J., and Zhao, J. (2010). "A 3D distinct lattice spring model for elasticity and dynamic failure." *International Journal for Numerical and Analytical Methods in Geomechanics*, 35(8), 859–885.
- Zienkiewicz, O. C., and Taylor, R. L. (2000). *The Finite Element Method Vol 1: The Basis*. (5th, ed.), Butterworth-Heinemann.

